INFORMATION TO USERS

This material was produced from a microfilm copy of the original document. While the most advanced technological means to photograph and reproduce this document have been used, the quality is heavily dependent upon the quality of the original submitted.

The following explanation of techniques is provided to help you understand markings or patterns which may appear on this reproduction.

1. The sign or "target" for pages apparently lacking from the document photographed is "Missing Page(s)". If it was possible to obtain the missing page(s) or section, they are spliced into the film along with adjacent pages. This may have necessitated cutting thru an image and duplicating adjacent pages to insure you complete continuity.

2. When an image on the film is obliterated with a large round black mark, it is an indication that the photographer suspected that the copy may have moved during exposure and thus cause a blurred image. You will find a good image of the page in the adjacent frame.

3. When a map, drawing or chart, etc., was part of the material being photographed the photographer followed a definite method in "sectioning" the material. It is customary to begin photoing at the upper left hand corner of a large sheet and to continue photoing from left to right in equal sections with a small overlap. If necessary, sectioning is continued again — beginning below the first row and continuing on until complete.

4. The majority of users indicate that the textual content is of greatest value, however, a somewhat higher quality reproduction could be made from "photographs" if essential to the understanding of the dissertation. Silver prints of "photographs" may be ordered at additional charge by writing the Order Department, giving the catalog number, title, author and specific pages you wish reproduced.

5. PLEASE NOTE: Some pages may have indistinct print. Filmed as received.

University Microfilms International
300 North Zeeb Road
Ann Arbor, Michigan 48106 USA
St. John's Road, Tyler's Green
High Wycombe, Bucks, England HP10 8HR

PALEOHYDROLOGY, PALEOMORPHOLOGY AND DEPOSITIONAL ENVIRONMENTS OF SOME FLUVIAL SANDSTONES OF PENNSYLVANIAN AGE IN EASTERN KENTUCKY

A dissertation submitted to the

Division of Graduate Studies
of the University of Cincinnati

in partial fulfillment of the
requirements for the degree of

DOCTOR OF PHILOSOPHY

in the Department of Geology
of the Graduate School of Arts and Sciences

1977

by

Thomas William Gardner

B.A. Franklin and Marshall College, 1971
M.S. Colorado State University, 1973

UNIVERSITY OF CINCINNATI

October 21 19 77

I hereby recommend that the thesis prepared under my supervision by Thomas William Gardner

entitled Paleohydrology, Paleomorphology and Depositional Environments of Some Fluvial Sandstones of Pennsylvanian Age in Eastern Kentucky

be accepted as fulfilling this part of the requirements for the degree of Doctor of Philosophy

Approved by:

Wayne A. Pryor

J. Barry Maynard

Warren D. Huff

Form 668—Grad. School—1M—12-69

TABLE OF CONTENTS

LIST OF FIGURES

LIST OF TABLES

ABSTRACT

KEY WORDS: Pennsylvanian, Fluvio-deltaic Depositional Environments, Paleohydrology, Paleomorphology, Paleogeography

An integrated stratigraphic, sedimentologic and petrologic investigation of fluvio-deltaic sandstones of Pennsylvanian age in eastern Kentucky 1) developed criteria for distinguishing facies of fluvio-deltaic environments, 2) developed a method for estimating velocity of flow in ancient fluvial sandstones, 3) reconstructed quantitative hydraulic and morphologic characteristics of Breathitt age fluvial systems and 4) developed a general paleogeographic and depositional model for fluvio-deltaic sediments in the middle Pennsylvanian of eastern Kentucky.

Five depositional environments were recognized from the lower delta plain sediments in the Breathitt formation. These are 1) interchannel bay, 2) channel mouth bar, 3) fluvial, 4) crevasse splay and subaerial levee and 5) marine and tidal channel. Initial environmental assignments were based on 1) vertical and lateral stratigraphic relationships as depicted in sixteen vertical and lateral profiles, 2) nature of bounding surfaces 3) bedding style and distribution and 4) grain size distribution.

The shape of log-probability plots, derived textural parameters, petrology and clay mineralogy were used to test initial assigments. The shape of log-probability plots of grain size distribution was not environmentally sensitive. Cross-plots of skewness and standard deviation had limited success in separating fluvial from nonfluvial

samples. Fluvial samples tended to be finely skewed and more poorly sorted than nonfluvial samples. Deposits from channel mouth bars, marine sheet sandstones, tidal channels and fluvial channels are protoquartzites, whereas bay fill sandstones and sandstone from the upper part of fluvial channels are subgraywackes. Fluvial samples have more authigenic kaolinite and nonfluvial samples have more total carbonate. This can be related to leaching from coal swamps and the position of the paleowater table. The dominant clay minerals are illite and kaolinite with subordinate amounts of chlorite and mixed layered clays. Cross-plotting of kaolinite (001) peak height and illite (001) peak height showed excellent separation of fluvial from nonfluvial samples. None of these additional tools were sensitive enough to discriminate precisely among depositional environments, but when used in conjunction with basic stratigraphic data are valuable tools to aid in environmental identification.

Recognition of abandoned meander channels permitted accurate determination of fluvial channel dimensions; namely width, depth and cross-sectional area. This allowed critical evaluation of the methodology that is used by most workers for paleomorphologic calculations. Channel depth for both the Harold and Allen Sandstones is 10 ± 0.5 meters and is equal to the thickness of point bar surfaces. Channel width is 140 meters and 130 meters for the Harold and Allen Sandstones, respectively. Channel width is equal to 1.4 times the horizontal extent of point bar surfaces, not the arbitrary value of 1.5 used in previous publications. Channel cross-sectional shape more closely approximates a trapezoid, not the commonly assumed rectangular shape.

A new and more accurate method for estimating velocity of flow in ancient fluvial systems has been developed. The equation $\bar{V} = V^* \sqrt{8/f}$, based on hydraulic theory was combined with Middleton's criterion for suspension, $\omega / V^* = 1$, based on experimental studies. From the resulting equation $V = \omega\sqrt{8/f}$, velocity of flow was estimated for ancient fluvial systems. Data from this study support the underlying assumptions in Middleton's criterion for suspension; that the "breaks" in straight line segments of log-probability plots are hydraulically controlled and that the T-Junction does, in fact, indicate the coarsest particles that can be taken into suspension. Velocity in the Harold Sandstone was 45 ± 7.5 cm./sec. near the channel center, but decreased to 25 ± 5 cm./sec. near the inner bank. These velocity values fall within the range of velocity values that are based on experimental data. They are also very close to values estimated from initiation of sediment motion curves, indicating that the velocity during deposition is probably similar to the critical erosion velocity.

Discharge is an important paleohydraulic parameter, but methods for calculating it are limited. By using the continuity equation, discharge was estimated from cross-sectional area of abandoned meanders and the previously calculated velocity. Average discharge was 400 ± 180 m^3/sec. and 375 ± 110 m^3/sec. for the Harold and Allen Sandstones, respectively. Close agreement exists among values of discharge calculated from several independent regression equations and the continuity equation. However, the error of estimating discharge is significantly less by using the continuity

equation. When a rectangular cross-sectional shape, instead of the actual cross-sectional shape, was used to calculate discharge, the discharge was in error by a factor of 50 percent. Mean annual flood ranged from 500 to 1900 m^3/sec. for both channels.

Although the sediment load parameter, weighted percent silt-clay in the channel alluvium, is difficult to estimate for ancient fluvial sandstone, it can still be used in paleomorphologic and paleohydraulic calculations with reliability. Meander amplitude was approximately 600 meters. Meanderbelt width was approximately 3300 meters and stream length ranged from 100 to 600 kilometers. Calculated values of meander amplitude, meanderbelt width and stream length agree with available outcrop evidence. Values of meander wavelength, drainage basin area, sinuosity and slope could not be verified from outcrop data, but independent regression equations gave consistent results. Meander wavelength ranged from 1000 to 2200 meters. Channel sinuosity ranged from 1.6 to 2.2. Channel slope was approximately one foot per mile. Drainage basin area was between 6400 and 100,000 square miles.

Petrologic and paleocurrent data indicate that the source for the Harold and Allen Sandstones was in low to moderate grade metamorphic rocks to the south and southeast. Volcanic rock fragments are present, but rare, indicating minor volcanism. Sericitized feldspars and a mature heavy mineral suite suggest a wet, warm climate in the source. The Breathitt fluvial system had small localized drainage basins (probably much less than the upper estimate

of 100,000 km^2) that fed small elongate, highly constructive deltas. These deltas prograded over shallow seas and had frictionally dominated effluent. Channel mouth bars developed pronounced middle grounds and fluvial channels bifurcated in distributaries. Distributaries were short and occuppied only the distal part of the delta. The fluvial systems meandered nearly to the end of the deltas as does the modern Rio Grande. Abandonment of fluvial channels on the delta occurred in two ways: 1) rapid abandonment by upstream avulsion and 2) gradual constriction by siltation. Tectonism was contemporaneous with sedimentation and faulting deflected major fluvial systems. Carboniferous shallow water deltas had processes of delta building that are similar to modern delta processes.

ACKNOWLEDGEMENTS

I would like to take this opportunity to express my deepest gratitude to Dr. Wayne A. Pryor, my advisor, for his advise and consultations. He initially suggested the problem of paleohydraulics and pointed me in the direction of eastern Kentucky. His critical discussions during all phases of the study were invaluable. I am also indebted to Drs. Warren Huff, J. Barry Maynard and Paul E. Potter for fruitful discussions during various phases of the research. My sincere thanks go to several associates in the department of geology. Michael Ray Short gave unselfishly of his time while in the field in eastern Kentucky. Jim Harrell provided many of the computer programs for grain size and cluster analyses. Bob Garrison and Michael Lewan engaged the author in numerous discussions concerning depositional environments in the study area. Bob Lenhart's photographic skills were most valuable. Pete Litz produced excellent thin sections for which I am especially thankful. I would also like to thank Dr. John C. Horn and Bruce Baganz of the University of South Carolina for their valuable assistance in stratigraphic correlations. Last, but not least, I want to especially thank my wife, Susan, who devoted much of her time and effort to this project. She sacrificed herself to the ticks and snakes in eastern Kentucky for me.

The research was supported by grants from Sigma Xi, the Ohio Academy of Science, the Sedimentology Fund of the University of Cincinnati and a Penrose Bequest from the Geological Society of America.

INTRODUCTION

General Statement

Recent construction of interstate and other four lane, divided highways in eastern Kentucky provides excellent and accessible exposures of fluvio-deltaic sediments of Carboniferous age. These outcrops are undoubtedly some of the best exposures of fluvio-deltaic sediments in the eastern United States and permit detailed reconstructions of deltaic environments in general and fluvial environments in particular. Within the past thirty years experimental data from laboratory flumes and detailed examinations of modern fluvial environments have significantly expanded our quantitative understanding of fluvial depositional systems. This recent data from flume studies and modern fluvial environments, together with data assembled from Carboniferous outcrops in eastern Kentucky provides a basis for a quantitative analysis of ancient fluvio-deltaic systems.

Purpose and Objectives

The purpose of this research is to: 1) develop meaningful criteria for distinguishing facies of fluvio-deltaic environments, namely, fluvial channel, channel mouth bar, crevasse splay, subaerial levee, interchannel bay, and marine, 2) develop a method for estimating velocity of flow in ancient fluvial sandstones, 3) reconstruct quantitative hydraulic and morphologic characteristics of Carboniferous meandering, fluvial systems in the Appalachian Basin, using empiric relationships developed from modern fluvial environments and flume experiments and 4) develop a paleogeographic and depositional

model for fluvio-deltaic systems in the Middle Pennsylvanian of eastern Kentucky. To achieve these objectives a detailed stratigraphic, sedimentologic, petrologic and petrographic investigation of several laterally traceable units was undertaken over a two year period.

Location

The study area is located in the Appalachian Plateau physiographic province, which in eastern Kentucky is termed the Kanawha Plateau. Mature topography is characteristic of the area. Most of the land surface slopes moderately to steeply. Flood plains and terraces of moderate size have formed on resistant sandstones along some of the major streams. Local relief of the Kanawha Plateau increases from three hundred or four hundred feet in the north near the Ohio River to about two thousand five hundred feet in the south near Cumberland Mountain. The Kanawha Plateau is dissected by tributaries of the Ohio River, namely, Big Sandy and its tributary Levisa Fork.

Outcrops described in the study are located in the Prestonsburg-Pikeville area along the valley of Levisa Fork in Floyd County, Kentucky (Figure 1). Middle Pennsylvanian fluvio-deltaic sediments are exposed along U.S. 460 and 23 south of Prestonsburg. Outcrops are up to three hundred feet high, terraced every thirty feet and exposed for nearly sixty percent of the thirty miles from Prestonsburg to Pikevile. Moreover, due to the sinuous pattern of the road as it follows the valley of Levisa Fork, the exposures provide a three dimensional view rarely observed in most outcrops. Additional outcrops are located on U.S. 114, one to five miles west

FIGURE 1. Location map of study area. Outcrops are located along U.S. Highway 460 and 23 between Prestonsburg and Pikeville in the valley of Levisa Fork. Additional outcrops are located on Rte. 114, 3 and 979.

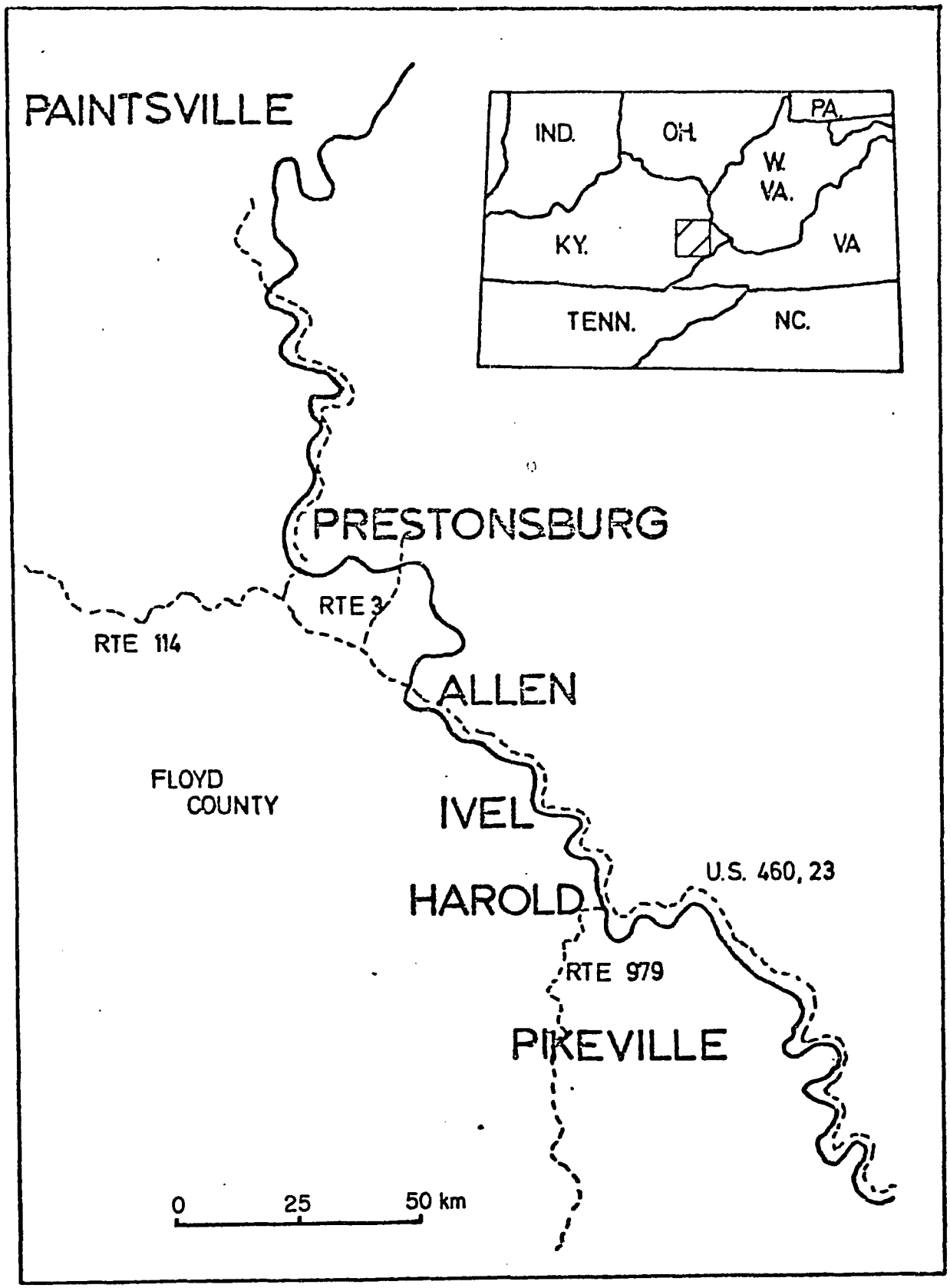

of Prestonsburg, Kentucky, route 3, three miles south of Prestonsburg, U.S. 80, west of Allen, Kentucky and Kentucky 979 at Harold, Kentucky.

General Stratigraphy

The Pennsylvanian System in the eastern Kentucky coal field is divided into three formations (Table I), the basal Lee composed of mostly orthoquartzitic sandstones and conglomerates, the Breathitt formation containing mineable coal seams and the Conemaugh formation characterized by varigated shales and several marine limestones.

Stratigraphic units studied in this report are within the Breathitt formation. First named by Campbell (1898) for rocks overlying the Lee formation in Breathitt County, the Breathitt formation consists of cyclic deposits of shales, siltstones, sandstones, discontinuous limestones and coal. Most of the commercial coal of eastern Kentucky is in this formation. The shale and siltstone beds are light to dark gray, attain a maximum thickness of twenty-five meters, contain numerous fossil plants and siderite which ranges from separate concretions to nearly continuous beds. Thin, discontinuous calcareous zones make up a very small part of the formation. Marine invertebrate fossils are present in the calcareous zones at many places and brackish water and marine fossils occur in some non-calcareous rocks that contain plant fossils.

Sandstones in the study area attain maximum thicknesses of thirty-five meters, but generally average ten meters. Abundant coal and siderite grains give the sandstone a speckled appearance resulting in the term "salt and pepper sand". Macerated plant fossils and micaeous minerals accentuate bedding planes.

TABLE 1

Carboniferous Stratigraphic Units in Eastern Kentucky and Southern West Virginia

LOCATION		EASTERN KENTUCKY	SOUTHERN WEST VIRGINIA
UPPER CARBONIFEROUS	PENNSYLVANIAN	Conemaugh	Conemaugh
		Breathitt	Allegheny
			Kanawha
		Lee	New River
			Pocahontas
LOWER CARBONIFEROUS	MISSISSIPPIAN	Pennington	Mauch Chunk
		Newman	Greenbriar

A few beds or zones have distinctive properties and are sufficiently widespread to be useful as key marker beds throughout the eastern Kentucky coal fields. These are, in their relative order of importance, the Fire Clay coal, the Magoffin beds (Morse, 1931) and the Kendrick shale (Jillson, 1919).

Much of the later work on the stratigraphy of the Breathitt formation is based on these initial paleontologic studies by Jillson and Morse and is summarized in an excellent paper by Wanless (1946). Later studies by Hunt (1937), Price (1956) and Huddle (1963) dealing with the economic aspects of coal and water resources further refined the stratigraphy. Within the past decade the United States Geological Mapping Program has completed geologic maps for most 7-$\frac{1}{2}$' quadrangles in the eastern Kentucky coal field.

With construction of new interstate highway and coal access roads creating excellent exposures, detailed environmental and stratigraphic studies by Smith, et.al., (1971), Baganz, et.al., (1975) and Horn, et.al., (1976) have assigned stratigraphic units in the study area to environments of the lower and upper delta plain. Donaldson (1974) concluded that the Breathitt consists of a sequence of small, northwardly prograding delta lobes. These works provide the basis for stratigraphic correlations used in this study.

Geologic Setting

The study area is located in the Pocahontas Basin (Figure 2), an elongate basin bounded on the west by the Cincinnati Arch and on the east by the folded Appalachian Basin. On the north it is confined

FIGURE 2. Location of study area in relationship to major structural features. The study area is located in the Pocahontas Basin in the southern part of the North-South cross-section. Details of this cross-section are shown in figure 3 (after Horn, et.al., figure 1, 1976).

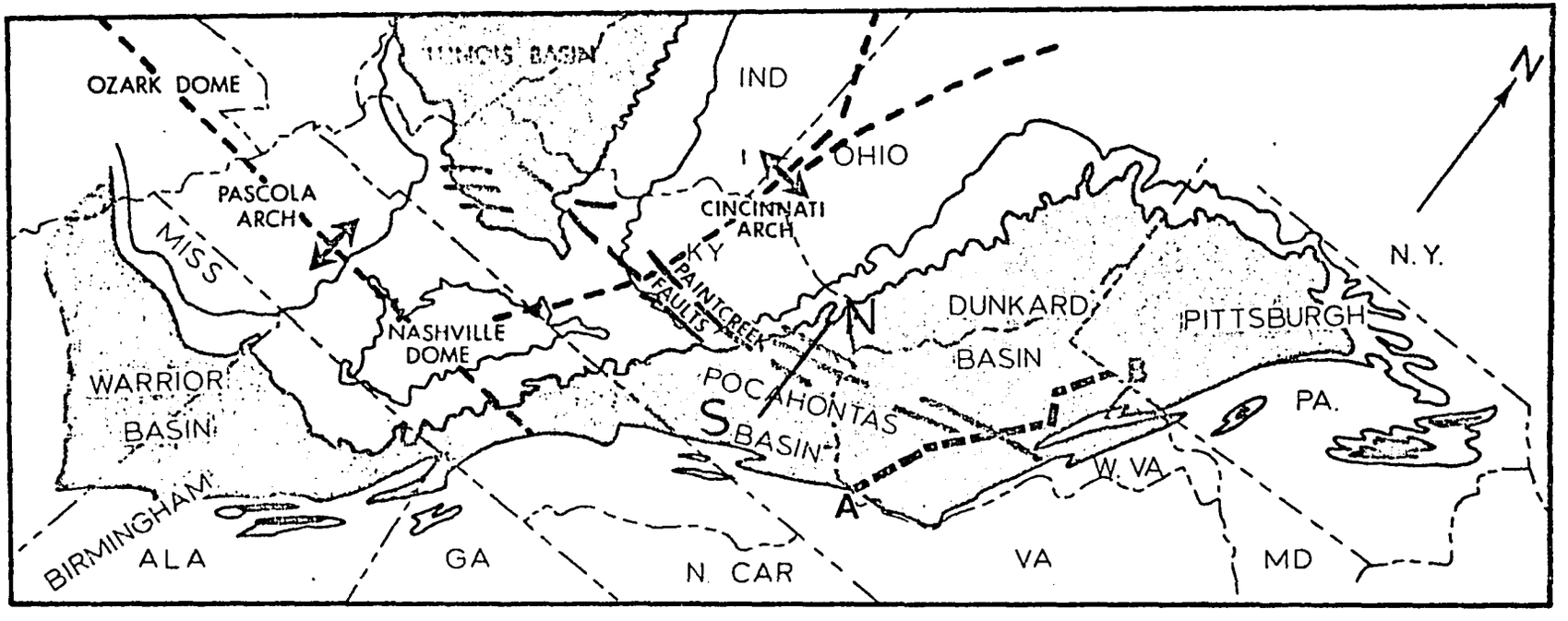

☐ LOWER CARBONIFEROUS, MOSTLY MARINE LIMESTONE & RED & GREEN SHALE

☐ UPPER CARBONIFEROUS, COAL BEARING SHALE & SANDSTONE

by the Paint Creek-Irvine Fault Zone. A north-south cross-section (Figure 3) through the Pocahontas Basin shows the generalized stratigraphic relationships in the Breathitt formation. The interval between the Lower Elkhorn Coal and the Kendrick beds in the southern third of figure 3, extending from Prestonsburg to Pikeville along U.S. Highway 23, lies within the study area. From the northern end of figure 3, near the Blaine-Walbridge Fault, south through the study area, the interval from the lower Elkhorn Coal to the Kendrick Marine Zone thickens from fifty to five hundred feet. The study area is located slightly south of a hinge zone separating the subsiding Appalachian Basin on the south from the stable cratonic platform to the north, as evidenced by the thickening sedimentary sequence. As seen in figure 3 this hinge is composed of a series of southeast dipping down-to-the-basin faults.

FIGURE 3. North-South cross-section through the Pocahontas Basin. The study area is located in the southern third of the cross-section. The hinge zone that separated the subsiding Appalachian Basin from the stable interior platform is represented by a series of down-to-the basin growth faults. The unnamed fault, labeled A, is located in the northern part of Floyd County in the study area (after Horn, et.al., figure 4, 1976).

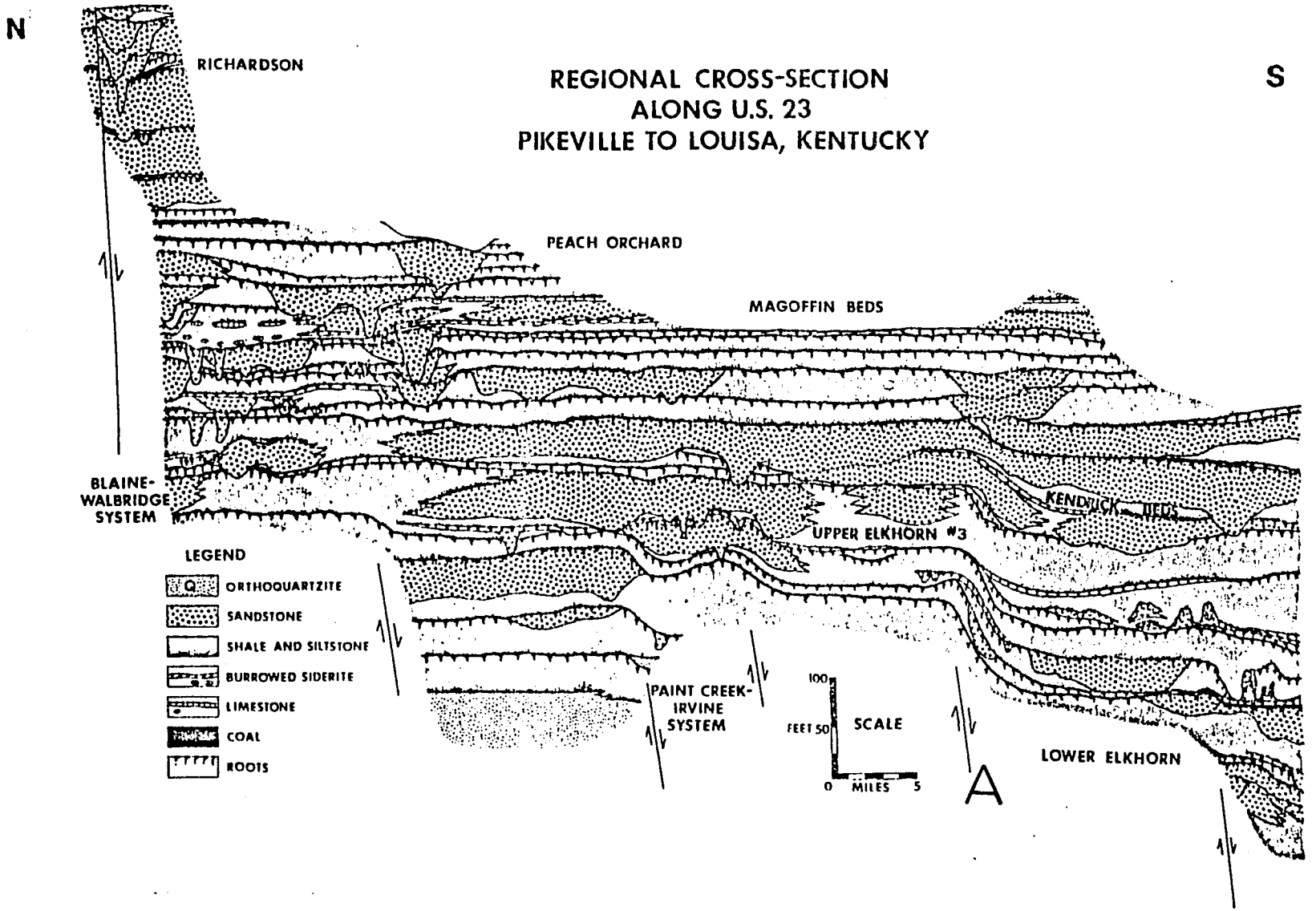

METHODOLOGY

Field Procedure

Units selected for study in the report are based on detailed stratigraphic correlations of Horn (1976), Baganz (1975) and the author's field reconnaissance. Criteria used in selecting particular intervals were lateral traceability where facies relationships in the fluvio-deltaic environment could be observed in detail, diagnostic upper and lower boundary units and sandstones with particularly well developed fluvial characteristics.

Entire outcrops, some nearly one mile long, were photographed in sections using a thirty-five mm., wide angle lense. Photographs were overlapped to form a mosaic of the entire outcrop length; some photo mosaics reached eight feet in length. Dimensions of each outcrop were measured by a pace and Brunton method and transferred to composite outcrop photographs at the appropriate scale. Error produced by this method in the estimate of outcrop geometry is approximately five percent. Composite outcrop photographs were then used in the field to record the location of paleocurrent data, thin section sample, vertical profiles, distribution of bedding styles, major erosional surface and other pertinent outcrop data.

Data collected in the field included detailed geometry of thirty-two outcrops, with emphasis on fluvial channel dimensions, sixteen vertical and lateral profiles containing detailed information on distribution of bedding types, grain size and derived textural parameters, clay mineralogy, petrology and paleocurrent directions. Over six hundred paleocurrent directions were measured. (See Appendix I for the method of analysis of paleocurrent data.)

Laboratory Procedure

One hundred ten thin sections were prepared for grain size analysis. Sixty-one of these were used in petrographic analysis. All thin sections were stained for plagioclase and orthoclase feldspar and carbonate using the methods adopted by Friedman (1971, p. 523) and Carver (1971, p. 515) respectively. Point counting included two hundred counts per slide for size analysis and two hundred different counts per slide of petrologic analysis. Grain sizes were classed in quarter phi intervals and plotted as cumulative percent finer on log-probability paper. Moment measures and various derived textural parameters were calculated from these curves. After transformation to equivalent sieve sizes by the method of Harrell and Erickson (in preparation, see Appendix II), these parameters were used in paleohydraulic calculations and in distinguishing depositional environments.

The use of Harrell's method in this study is justified by comparison of data in Table II. Two carbonate cemented sandstones, HA-2-23 and HA-23-23, were disaggregated in dilute hydrochloric acid, sieved at quarter phi intervals and the resulting distributions plotted on log-probability paper. Values of derived textural parameters from sieved samples compare well with converted parameters from thin section point counts of the same sample.

Fifty-one samples from various depositional environments were collected and analyzed for clay mineral content and cation exchange capacity (Ulmschneider, in preparation). The procedure for clay mineral preparation and data analysis is described in Appendix III.

TABLE II

COMPARISON OF TEXTURAL PARAMETERS FROM TRANSFORMED THIN SECTION SAMPLES AND IDENTICAL SIEVED SAMPLES*

Sample	Maximum Diameter (ø)	Median (ø)	Standard Deviation	Skewness
$HA\text{-}2\text{-}23_{sieve}$	1.50 - 1.75	3.5	0.40	0.03
$HA\text{-}2\text{-}23_{TS}$ after transformation	1.60±	3.40 ± 0.09	0.53 ± .04	0.09 ± .04
$HA\text{-}23\text{-}23_{sieve}$	1.50 - 1.75	3.30	0.42	0.05
$HA\text{-}23\text{-}23_{TS}$ after transformation	1.75	3.31 ± .08	0.46 ± .04	0.10 ± .04

*Sieved data were obtained by disaggregating carbonate cemented samples. Error estimated from 95% confidence interval.

These data were used to develop criteria for delineating environments of deposition in a fluvio-deltaic environment and for quantitatively reconstructing the hydrology and morphology of fluvial systems in the Breathitt formation in eastern Kentucky.

GENERAL STRATIGRAPHY

General Statement

A generalized cross section (Figure 4) along U.S. Highway 460 and 23 between Prestonsburg and Pikeville shows the stratigraphic relationships of the Breathitt formation in the study area. Three distinct stratigraphic intervals in the Breathitt from the lower and upper delta plain environment (Baganz, et.al., 1975) were studied in detail in this report. The lowest interval occurs immediately below the Upper Elkhorn No. 1, 2 coal in the southern third of figure 4. The middle interval occurs as a split in the Upper Elkhorn No. 1, 2 coal in the central part of figure 4. The upper interval occupies a position in the Upper Elkhorn No. 3 coal zone. The total average stratigraphic thickness is seventy meters. The lowest interval is approximately sixty meters above the base of the Breathitt formation.

Stratigraphic Units

The sandstone immediately below the Upper Elkhorn No. 1, 2 coal is, in this study, termed the Harold Sandstone because of excellent exposures at Harold, Kentucky. Outcrops of the Harold Sandstone are located on figure 5. The sandstone unit is approximately ten meters thick and has eroded into interdistributary bay silts and silty-shales (Baganz, et.al., 1975). In places, however, the sandstone is absent and the Upper Elkhorn No. 1, 2 coal rests directly upon the interdistributary bay sediments. The Harold Sandstone displays prominent fluviatile features that will be described in the next chapter. To the north, beyond HA-2b, the sandstone drops into the subsurface. To the south, beyond BB-4 the sandstone rises to the tops of the hills and is eroded or not exposed.

FIGURE 4. Generalized cross-section along U.S. Highway 460 and 23 in the study area. Stratigraphic relationships of the three intervals studied in this report; the Harold Sandstone, the Allen Sandstone and the Upper Elkhorn No. 3 coal zone are clearly depicted (after Baganz, et.al., figure 2, 1975).

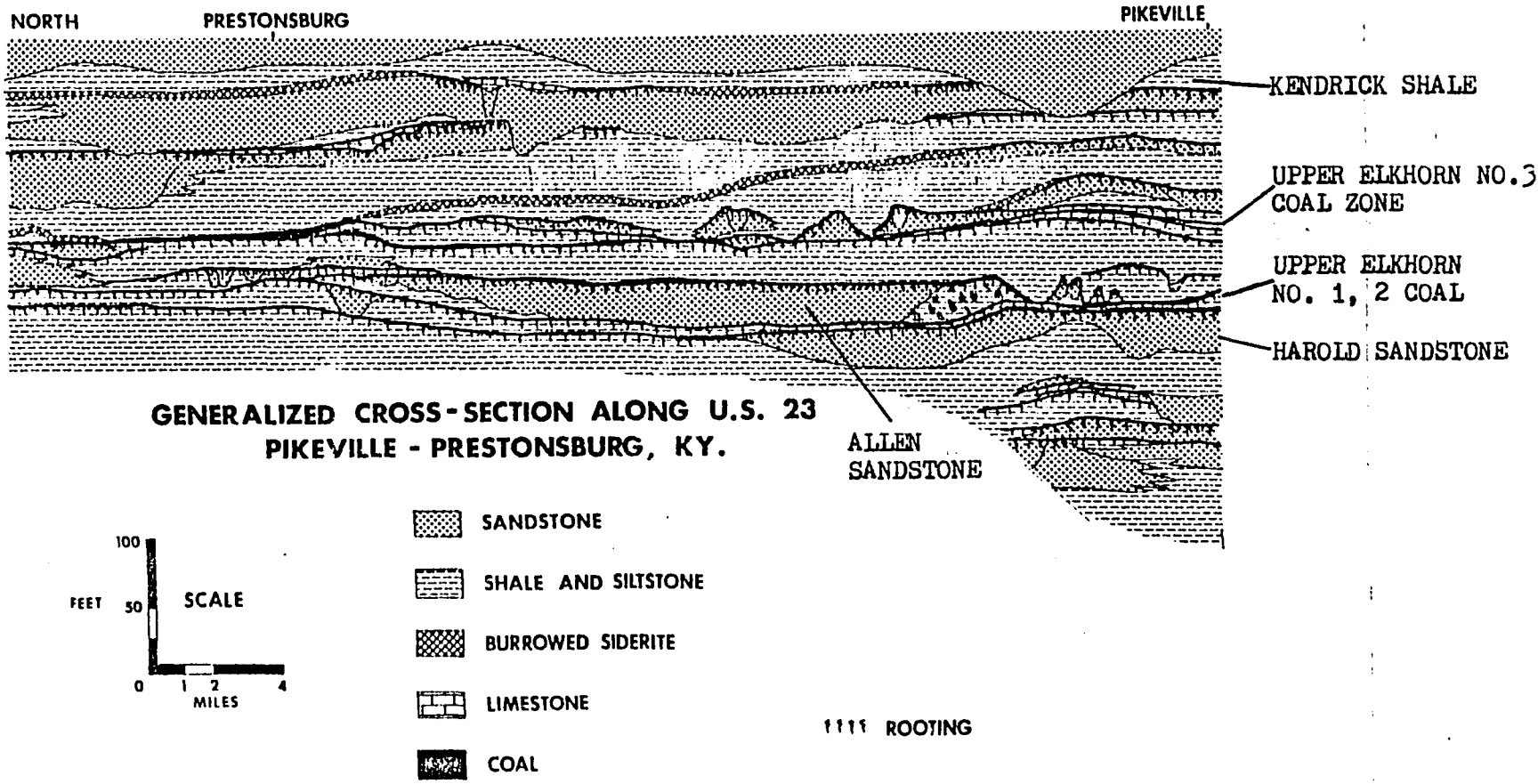

GENERALIZED CROSS-SECTION ALONG U.S. 23
PIKEVILLE - PRESTONSBURG, KY.

FIGURE 5. Location map of outcrops of the Harold Sandstone. Location numbers are used as reference to each outcrop. Location BB-3 is the only outcrop of the Blairtown Sandstone.

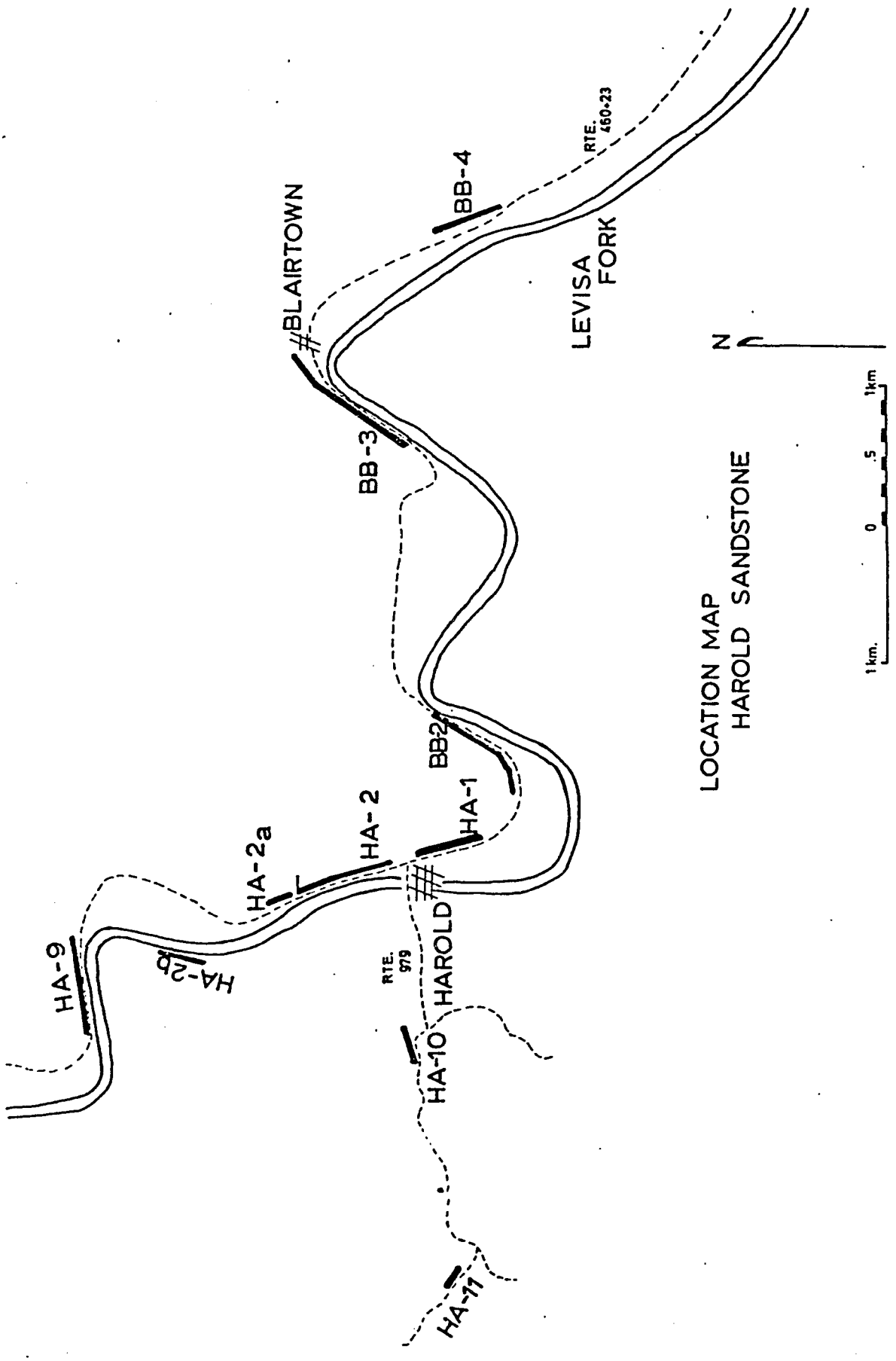

LOCATION MAP
HAROLD SANDSTONE

Invariably, the Harold Sandstone is capped by the Upper Elkhorn No. 1, 2 coal which is easily recognized in the vicinity of Harold and provides a good marker bed for correlation of the Harold Sandstone between outcrops. It is approximately 1.6 meters thick, by far the thickest coal in the area. Extensive strip mining provides a good marker bench for correlation purposes.

North of the outcrops of the Harold Sandstone the Upper Elkhorn No. 1, 2 split into the Upper Elkhorn No. 1 and Upper Elkhorn No. 2 (Figure 4). This interval is occupied by a fluvial sandstone system, here termed the Allen Sandstone, from superb outcrops at Allen, Kentucky. Outcrops of the Allen Sandstone are located on figure 6. The Allen Sandstone is approximately 10 meters thick, but thickens to 12 meters in places and is completely absent locally. Subfacies of the fluvial environment are present in this interval and will be described later. To the north, beyond U.S. Highway 114, the Allen Sandstone is absent, the interval being occuppied by interdistributary bay sediments. To the south, beyond HA-9, where the Upper Elkhorn No. 1 and Upper Elkhorn No. 2 join, the interval is absent.

The Upper Elkhorn No. 1 is a good marker bed at the base of the Allen Sandstone. It is a cannel coal approximately 15 cm. thick. In places, it occurs several meters below the Allen Sandstone, with intervening siltstones that contain brackish water pelycopods. At several localities the sandstone has eroded through the cannel coal and large mats of coal are preserved within the lower two meters of the sandstone. The Upper Elkhorn No. 2 coal caps the Allen Sandstone at all observed localities.

FIGURE 6. Location map of outcrops of the Allen Sandstone. Location numbers are used as reference to each outcrop. Location HA-22 is an outcrop in the Upper Elkhorn No. 3 coal zone which may correspond to the Blairtown Sandstone.

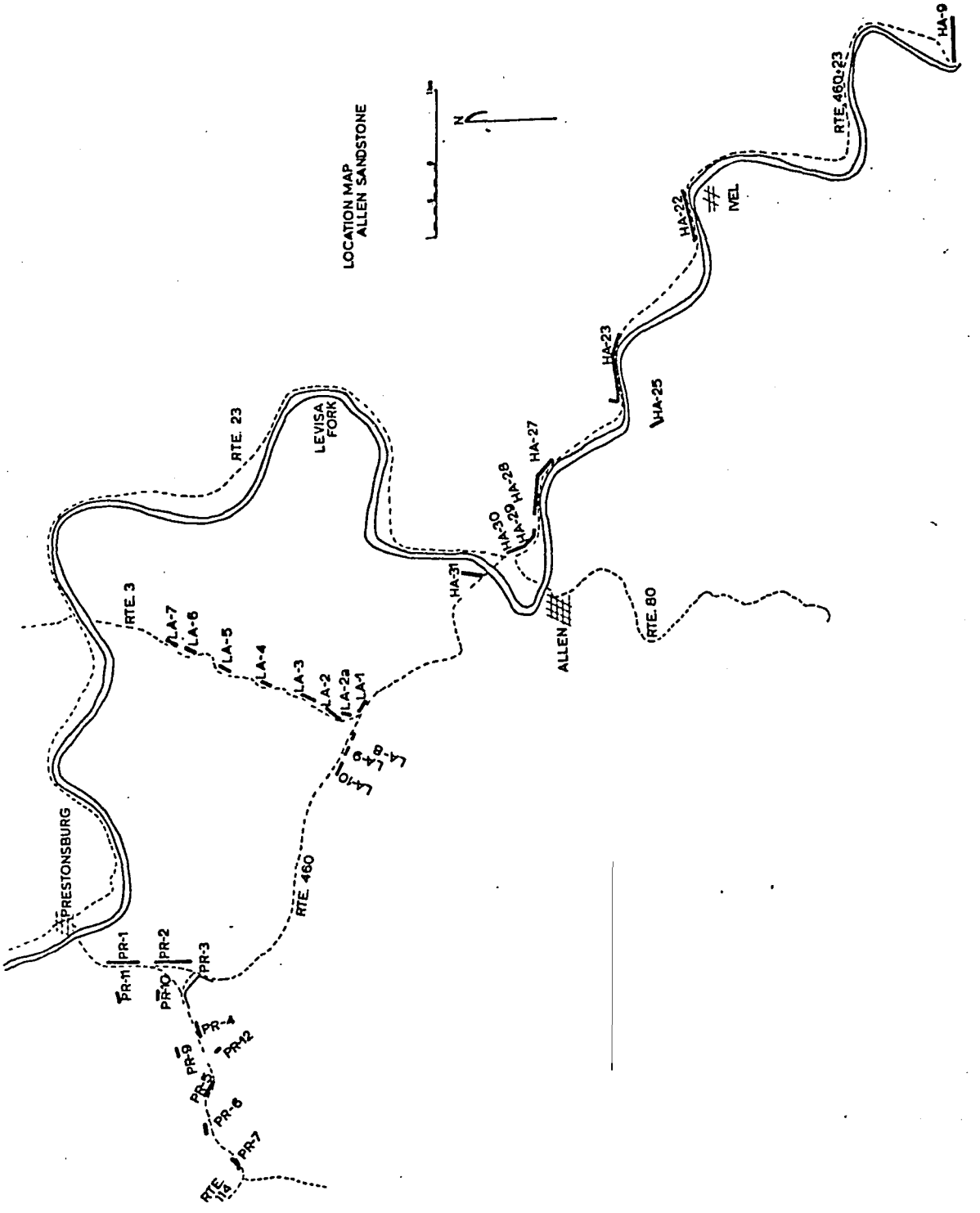

The highest stratigraphic interval studied in this report occurs in the Upper Elkhorn No. 3 coal zone. This interval is characterized by splitting and rejoining of numerous Upper Elkhorn No. 3 coal seams (Figure 4). Exact correlation from outcrop to outcrop is exceedingly difficult. Excellent exposures of fluvio-deltaic environments are present in the Upper Elkhorn No. 3 zone at Blairtown, Kentucky (location BB-3, figure 5). The sandstone exposed there is termed the Blairtown Sandstone.

Stratigraphically below the Blairtown Sandstones, but within the Upper Elkhorn No. 3 coal zone, at BB-3, an extensively bioturbated tidal channel will be compared with the characteristics of fluvial channel sands.

At locality HA-22, near Ivel, Kentucky (Figure 6), a superbly developed isolated, abandoned channel is completely exposed in the Upper Elkhorn No. 3 coal zone. Although this channel cannot be directly correlated to any sandstones in other outcrops, it will be used in the construction of a paleogeographic and depositional model.

DEPOSITIONAL ENVIRONMENTS

General Statement

In the preceding chapter the stratigraphy of the Breathitt formation was described in general terms. A cursory examination of the lithologic units revealed several distinct types in this lower and upper delta plain environment. The purpose here is to delineate the different lithologic units as to depositional facies in the deltaic environment in general and describe characteristics of the fluvial sandstone facies in particular. The criteria used are 1) vertical and lateral stratigraphic relationships as depicted in measured sections, 2) nature of bounding surfaces, 3) bedding style and distribution, 4) grain size distribution plots and derived textural parameters, 5) petrology and 6) clay mineralogy. Lithologic units were first assigned to depositional environments on the basis of vertical and lateral stratigraphic relationships, nature of the bounding surfaces and bedding style and distribution. Grain size distribution curves and the derived textural parameters, petrology and clay mineralogy were used to test, verify and refine those initial environmental interpretations.

Previous Works

Modern studies of deltaic sedimentation, initiated by H.N. Fisk, contributed significantly to knowledge of depositional and environmental aspects of recent deltaic sediments. Detailed studies of the Mississippi Delta by Fisk, et.al., (1954), Fisk (1961), Coleman and Gagliano (1967) and Frazier (1967) have led to the development of a deltaic model applicable to ancient deltaic sediments. Similarly, Fulton (1975) has developed a deltaic model from subsurface studies of the Rio Grande.

Most work on deltaic sedimentation is summarized in volumes such as Deltas in Their Geologic Framework, (Shirley and Ragsdale, eds., 1966), Delta Systems in the Exploration for Oil and Gas, (Fisher, Brown, Scott and McGowen, eds., 1969), Deltaic Sedimentation, Modern and Ancient, Morgan and Shaver, eds., 1970), Deltas, Models for Exploration, (Broussard, ed., 1975) and most recently, Deltas: Processes of Deposition and Models for Exploration, (Coleman, ed., 1976). An excellent summary arranged by facies in a deltaic setting is provided in Clastic Depositional Systems - A Genetic Approach to Facies Analysis: Annotated Outline and Bibliography, (Fisher and Brown, eds., 1972).

Publications concerned with Pennsylvanian age fluvio-deltaic systems are numerous. The search for oil and gas prompted much work, mostly in the subsurface, in Texas, such as Pennsylvanian Depositional Systems in North Central Texas, (Brown, Cleaves and Erxleben, 1973), Geometry and Distribution of Fluvial and Deltaic Sandstones, Pennsylvanian and Permian, North Central Texas (Brown, 1969) and Recent and Ancient Deltaic Sediments: A Comparison, (Coleman, Ferm and Gagliano, 1969). Deltaic deposits of late Paleozoic age from the Interior Basin are summarized by Wanless, et.al., (1970). Several studies by Hopkins, (1958), Potter, (1962a, 1962b, 1963, 1967), and Friedman, (1957, 1959, 1960) deal specifically with fluvio-deltaic sandstones of Pennsylvanian age in the Interior Basin, Indiana and Illinois.

Publications describing Pennsylvanian age deltaic sediments in Kentucky, Ohio, Pennsylvania and West Virginia by Ferm, (1970, 1974), Ferm and Cavaroc, (1968), Donaldson, (1970, 1974), Baganz, et.al., (1975) and Horn and Ferm, (1976) are used extensively in this study.

Environments of Deposition

Lower and upper delta plain sediments in the study area can be classified into five general depositional environments. These are 1) interchannel bay, 2) channel mouth bar, 3) fluvial channel, 4) crevasse splay and subaerial levee and 5) marine. The characteristics of these five environments are described below.

Interchannel Bays: Interchannel bays are represented by sequences of shales, silty shales and siltstones that gradationally coarsen upward and laterally into sandstones of channel mouth bars and crevasse splays. Locality BB-3 (see Figure 5 for location) is an excellent exposure showing the vertical and lateral stratigraphic relationship (Plate I).

Bay fill sediments are approximately ten to twenty meters thick and coarsen up from a median value of 5ϕ at the base to a median value of 3ϕ at the top (Figure 7). Maximum grain diameter also coarsens up from 3.2ϕ near the base to 1.7ϕ. The base is commonly parallel bedded shales containing few invertebrate fossils, mostly Lingula. Parallel to wavy bedded, silty shales commonly occur above the basal shale. Concentrations of mica and finely divided plant material occur on bedding planes. "Frozen" current ripples and wavy laminations (Coleman, 1965, p. 136) are common (Figure 8). Maximum ripple height is two centimeters. Bioturbation is present, but rare, in the lower sequence of bay sediments. It is absent in the coarser upper part.

Current and oscillatory ripples (Figure 9 and 10), microscour and fill structures and microtrough cross-lamination occur in fine sands and coarse silts above the lower bay fill. Cross-laminations

FIGURE 7. Vertical profile through bay fill at location BB-3 in the Blairtown Sandstone. See plate I for the general stratigraphic relationship between the bay fill and fluvial system. The legend that accompanies the figure refers to all other vertical profiles as well.

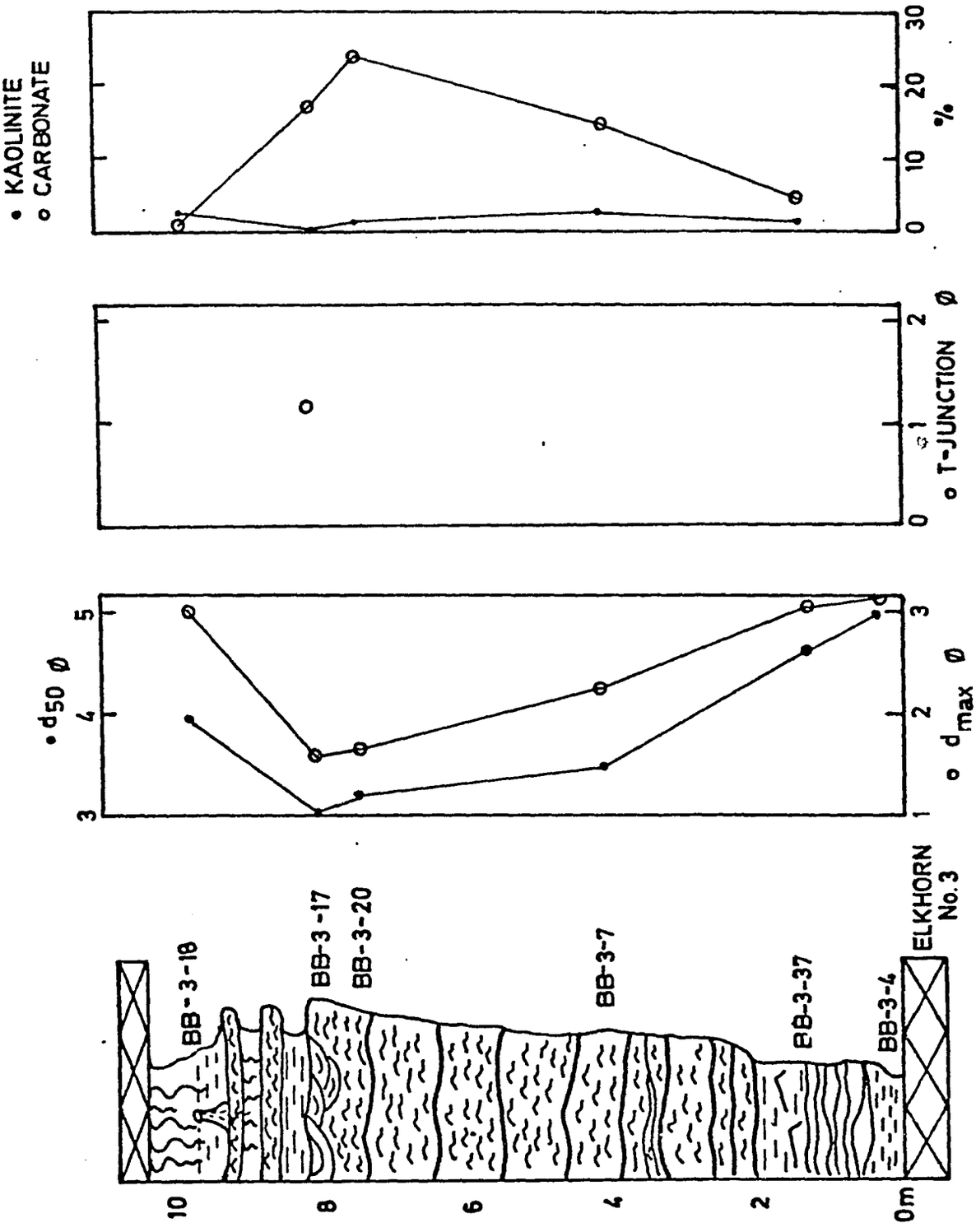

LEGEND

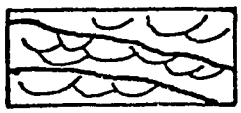
PRIMARY BEDDING PLANES

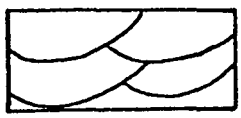
LARGE TROUGH BEDS .5-1.0m

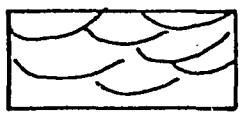
SMALL TO MEDIUM TROUGH BEDS .1-.5m

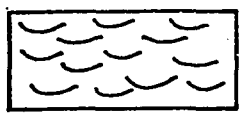
MICROTROUGH BEDS .02-.1m

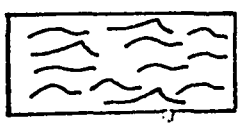
RIPPLES

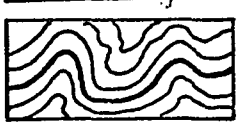
CONVOLUTED LAMINATIONS

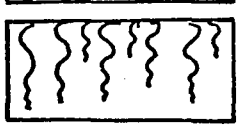
ROOTING

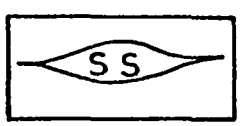

SIDERITE

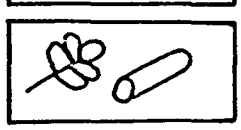
FOSSIL PLANTS

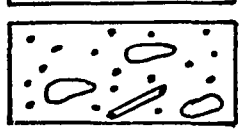
CONGLOMERATE

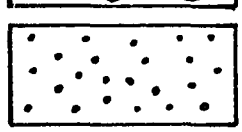
SANDSTONE

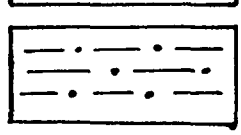
SILTSTONE

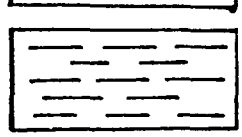
SHALE

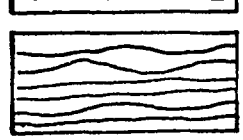
HORIZONTAL TO WAVY LAMINATIONS

FIGURE 8. Photograph of horizontal and wavy beds typical of bay fill sediments. "Frozen" ripples are occasionally well developed. Sediments are shales with interbedded silts and fine sands.

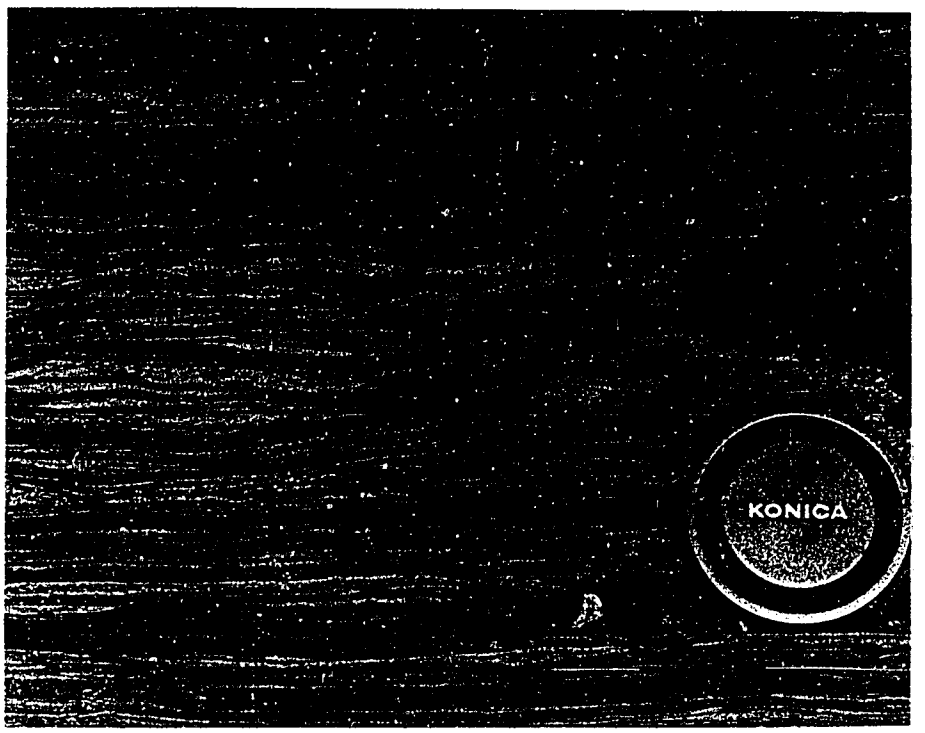

FIGURE 9. Photograph of well developed oscillatory ripples in bay fill sediments. Ripples are composed of coarse silt.

FIGURE 10. Close up of oscillatory ripples in figure 9. Ripple crests are five centimeters apart. View is down onto bedding plane.

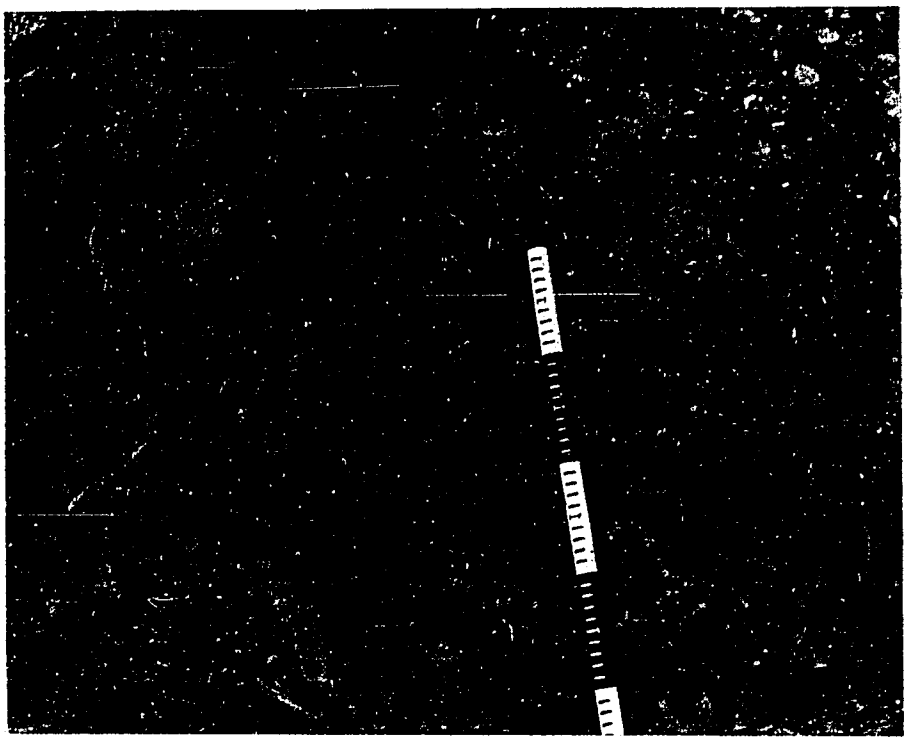

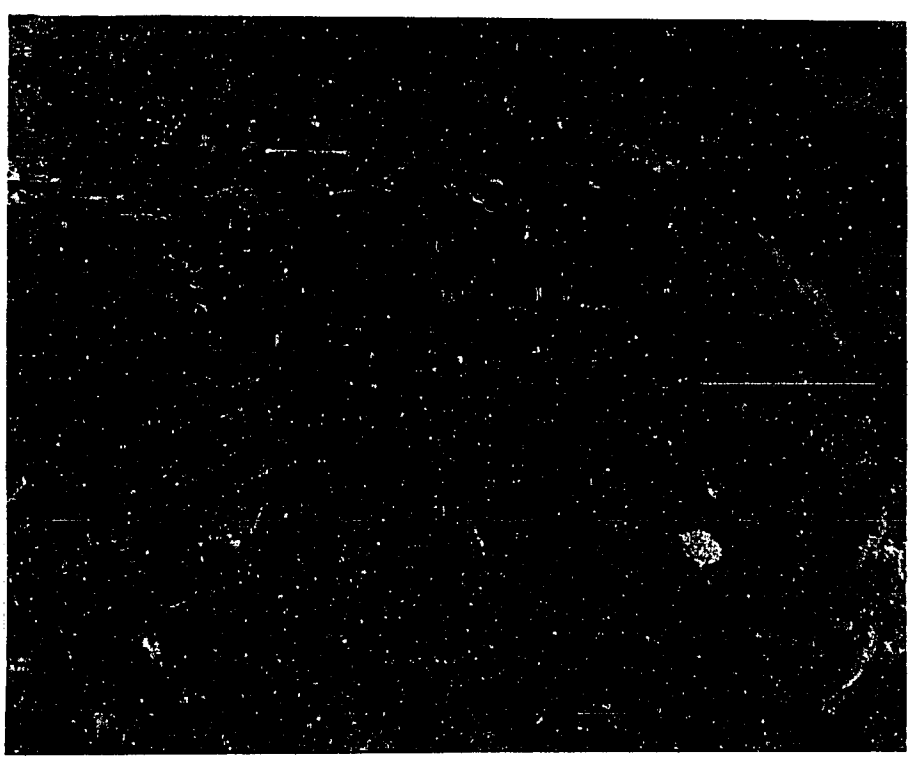

average three centimeters thick, but troughs up to seven centimeters are common. These structures indicate that currents from waves, tides and fluvial flooding were active during deposition of the middle sequence of bay sediments. Small scale trough cross-bedding, up to twenty centimeters thick, is prevalent near the top of the fine sand unit.

Above this unit extensively rooted, fine silts and silty shales are abundant. Fossil plants in growth position are common. Vegetation established itself when bays filled sufficiently to form a surface upon which plants could root (Baganz, et.al., 1975). Discontinuous lenses of fine sand are commonly interbedded with silty shales, indicating periodic innudation of the coal swamp by fluvial or marine currents.

Lateral relationships in the interchannel bay environment are similar to vertical relationships (Figure 11). Sediments grade from parallel to wavy bedded silty shales (4.5ϕ) in the bay to rippled and microtrough cross-bedded fine sands (3ϕ) in the channel mouth bar. Maximum grain diameter similarly coarsens from 3ϕ to 1.2ϕ in the direction of the channel mouth bar.

Primary bedding surfaces are pronounced, sub-horizontal and laterally continuous (Plate I) in the bay environment. They commonly exhibit clay drapes and concentrated accumulations of fossil plant debris. These bedding surfaces probably correspond to periods of low sediment influx. Chemically precipitated siderite commonly occurs as persistant bands or concretions along bedding surfaces. Both siderite and bioturbation disappear towards the source of fresh water influx.

FIGURE 11. Lateral profile of bay fill at location BB-3 in the Blairtown Sandstone. See plate I for the general stratigraphic relationship between bay fill and fluvial system.

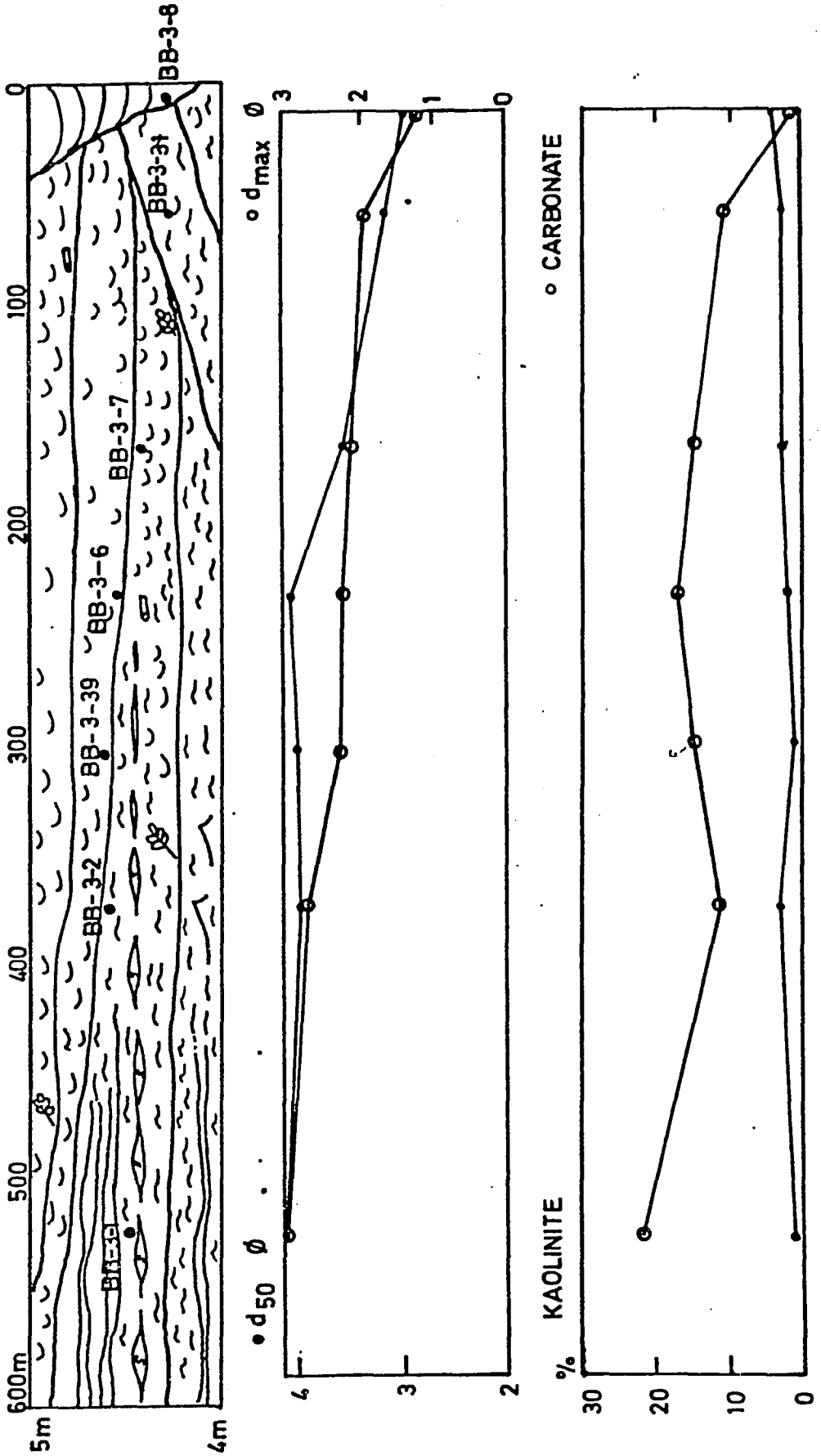

Channel Mouth Bars: Channel mouth bars are areas of shoaling associated with the terminus of a channel mouth. Deposition results from a decrease in velocity and decline in carrying capacity of streams as they leave the confines of their channels. These are areas of rapid deposition and constant reworking by marine waves and river currents.

Plates I east end, II and II show the outcrop geometry of three different channel mouth bars. The general position of each outcrop in relation to the fluvial system is depicted in figure 12 taken from Coleman's (1965) study of channel mouth bars on the Mississippi River. The general stratigraphic relations in these plates corresponds well with Coleman's figure 12.

In plate I the exposure of the Blairtown Sandstone is perpendicular to channel orientation, determined from paleocurrents in the channel sandstone (Figure 19). The primary bedding surfaces on the bar flanks are inclined and slope away from the channel center line, in opposite directions. Primary bedding planes are similarly inclined on the bar flanks on the west side of the abandoned channel in plate III, figure 13. Inclined bedding surfaces are also developed in the section parallel to the channel system (Plate II). Thus, flanks of channel mouth bars in the study area form a surface that slopes uniformly away from the center of the channel, consistent with observations from modern environments. Paleocurrent orientations (Figure 19 and 20, Table III) indicate that currents moved down the dip of the inclined, primary bedding surfaces.

Channel mouth bar sediments thin rapidly away from the channel. Concentrations of muscovite, finely divided plant material and clay

FIGURE 12. Orientation and location of channel mouth bar outcrops with respect to the fluvial channel. Section AA' corresponds to outcrop BB-3 and Plate I of the Blairtown Sandstone. Section BB' corresponds to outcrop HA-22 and Plate III in the Upper Elkhorn coal zone and may be correlated with BB-3. Section CC' corresponds to outcrop LA-9 and Plate II of the Allen Sandstone. (Modified from Coleman, figure 9, 1965).

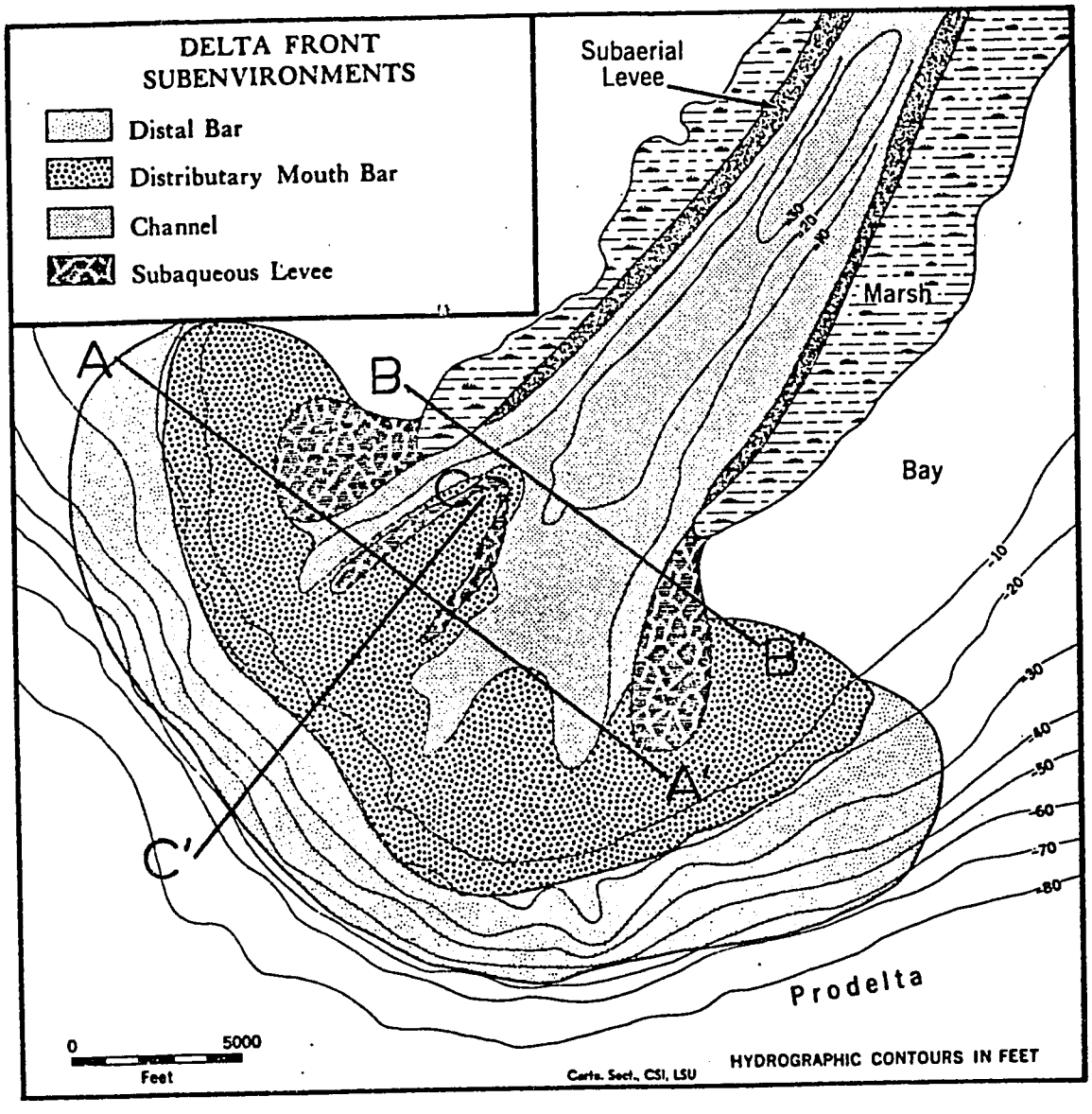

FIGURE 13. Photograph of abandoned channel at HA-22. Corresponds to Plate III. Flanks of channel mouth bar deposit slope gently away from the channel on the west side.

chips up to five centimeters long commonly occur on bedding planes. Development of these bedding surfaces is caused by fluctuations in sediment input and probably related to variation in river discharge, with clay chips eroding during high flows and mica and plant material settling out during low flows. The spatial association of primary bedding planes on the northeast side of Plate I indicates that the channel mouth bar was fully developed prior to infilling of the bay sediments. Bay fill sediments overlap those of the channel mouth bar.

Details of the internal stratigraphy can be seen in vertical profiles (Figure 14). Figure 14 is a section through the axial portion of the channel mouth bar. The fluvial channel has eroded into the upper portion of the bar at 2.4 meters.

A basal prodelta clay occuppies the interval from 0 to 0.6 meters. It is parallel bedded, unfossiliferous and contains some silty laminations. A sharp, but nonerosive contact separates this from 1.2 meters of the overlying coarse silts and fine sands of the bar flank deposits. Current ripples, oscillatory ripples and micro-trough cross-laminations (3 centimeters maximum) predominate in this unit (Figures 15 and 16). Occasionally graded bedding is developed in the bar flanks. Grain size is very uniform along the length of bar flanks. Samples BB-3-27, BB-3-28 and BB-3-29 which extend from the central portion of the bar to the distal bar flanks (Plate I) have median values of 3.73ϕ, 3.82ϕ and 3.76ϕ respectively.

A sharp, erosive contact separates the bar flanks from the coarser, fine sands (3.2ϕ) of the central portion of the bar. Multi-

FIGURE 14. Vertical profile through channel mouth bar and overlying channel deposits at BB-3 in the Blairtown Sandstone. See Plate I for location of section. Channel is filled with horizontally bedded clays.

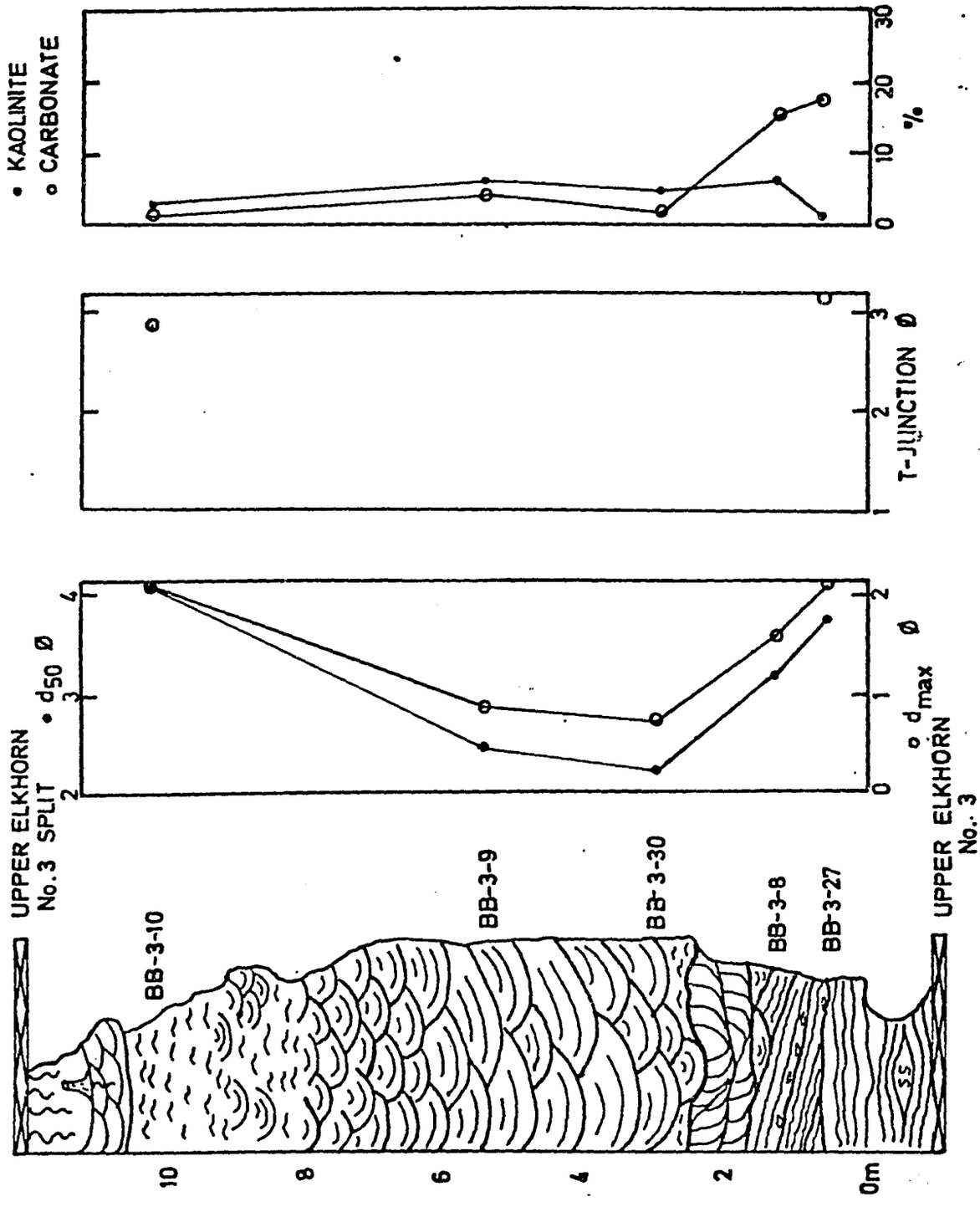

FIGURE 15. Photograph of straight, round crested, oscillatory ripples on a primary bedding surface of the channel mouth bar, LA-9.

FIGURE 16. Photograph of sharp, straight crested, oscillatory ripples which occur in the micro-trough cross-lamination of the central portion of the bar, BB-3.

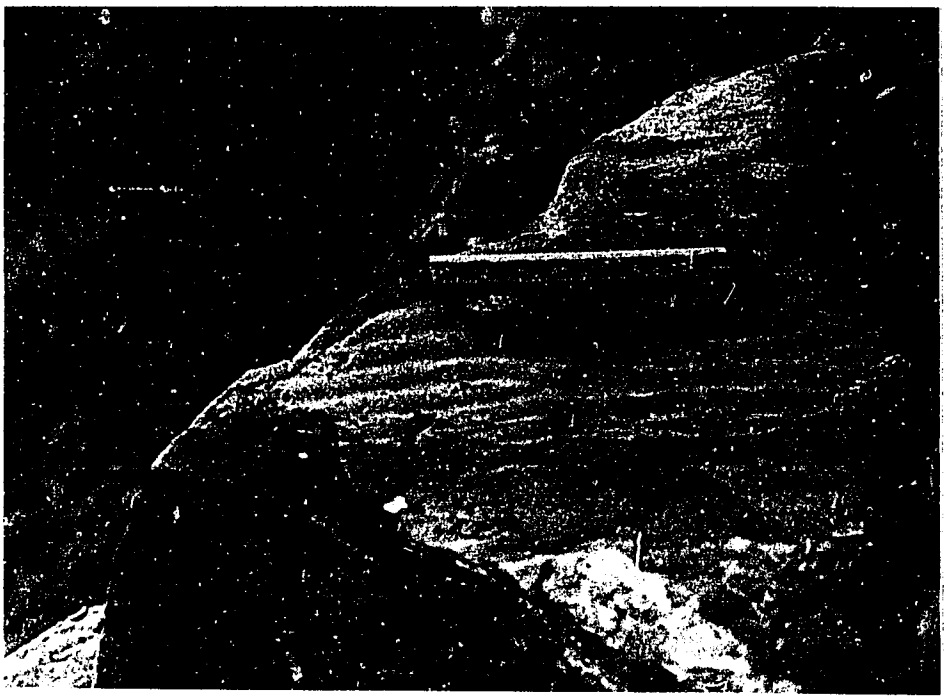

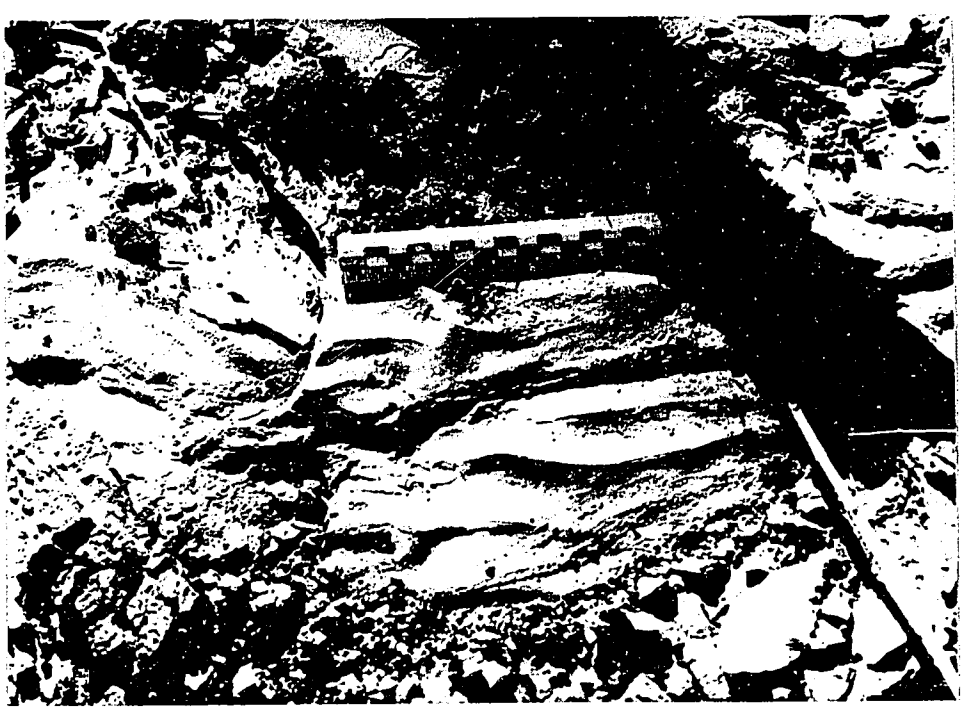

directional, trough cross-bedding, up to 50 centimeters thick, is predominant in the central portion of the bar. Primary, inclined bedding surfaces are not developed. There is little lateral continuity of bedding in the central portion of the bar. Microfaulting is well developed locally (Plate III). Bioturbation is absent from any portion of the bar. Gas heave structures, well developed on Mississippi River mouth bars (Coleman, 1965), are also absent.

Channel mouth bars may coarsen upward (Figure 13, samples BB-3-27 and BB-3-8) or fine upward (Figure 17) depending upon location of exposed section and the relationship of the channel bar system. In figure 17 the channel has not prograded over or eroded into the channel mouth bar sediments. The completely preserved channel mouth bar grades from medium sand (2.0ϕ) at the base to very fine sand and coarse silt at the top. Medium scale, multi-directional trough cross-beds (50 centimeters) at the base grade upward into a thick (6 meter) interval of small trough beds (10 centimeters), microtrough cross-laminations, current and oscillatory ripples, convoluted laminations and climbing ripples. This style and distribution of bedding is common on channel mouth bars and subaqueous levees on the Mississippi River (Coleman, 1965, Coleman, et.al., 1964, Fisk, 1961).

A sharp, erosional contact separates the medium scale trough cross-beds from the underlying bay sediments. However, where these cross-bedded sands are absent and bar flank deposits rest directly upon bay or prodelta sediments the contact is sharp, but nonerosive (Plate II north end) and the grain size of channel mouth bar sediments is finer (3.9ϕ), indicating a waning of current velocity away from the central portion of the bar.

FIGURE 17. Vertical profile through channel mouth bar deposit in the Allen Sandstone at LA-9. Note fining upward sequence and distribution of bedforms.

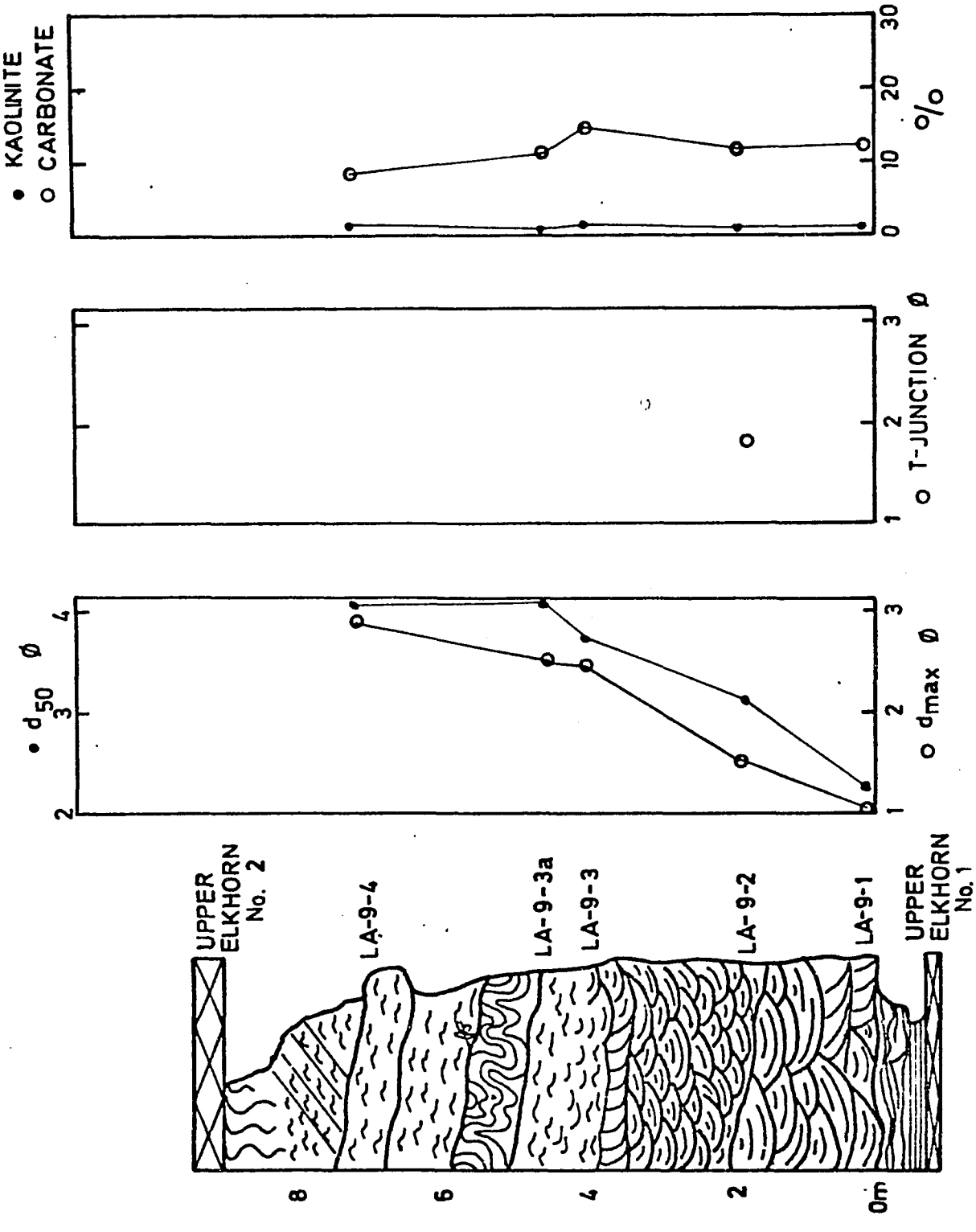

Fluvial Channels: Fluvial channels are natural flumes that accomodate discharge and transport sediment to the delta front. Channel deposits invariably truncate underlying channel mouth bar and interchannel bay sediments.

Fluviatile sandstones, in the study area, exhibit general morphologic features commonly depicted in models for fluvial deposition of meandering streams (Allen, 1970, Visher, 1965, Jackson, 1975). Migration of a meandering fluvial system ideally develops three pronounced morphologic characteristics, 1) point bar (lateral accretion) surfaces, 2) abandoned meander channels, and 3) major erosional truncations, where deposits of one meander cross cut those of a previous meander. Point bar surfaces are inclined surfaces that extend from the channel thalweg to the flood plain deposits (Figure 18). They tend to be erosional, cutting through the small scale trough stratification within the sandstone body. Clay drapes, and concentrations of micaceous mineral and macerated plant material commonly accentuate these surfaces.

Inclination of point bar surfaces increases with decreasing river size, but averages around 12° (Allen, 1970; Leeder, 1973). The apparent dip decreases to 0° as the orientation of the outcrop approaches that of the paleocurrent direction. For this reason detailed accounts of occurrence of point bar surfaces are not numerous. They have been described in detail from Pennsylvanian age sediments (Beutner, et.al., 1968; Allen, 1965, Padgett, 1976 and Sedimentation Seminar, in press) from Devonian sediments (Allen and Friend, 1966; Moody-Stuart, 1966) from Jurassic sediments (Nami, 1976) and Cretaceous age sediments (Cotter, 1971).

FIGURE 18. Model for development of point bar surfaces in meandering delta rivers. As channel migrates from right to left a series of point bar surfaces develop. Seen in vertical profile, the point bar surfaces are moderately inclined and extend from the base of the channel to the overbank deposits. Flow parallels the strike of the point bar surface. (After Horn, et.al., figure 59, 1976).

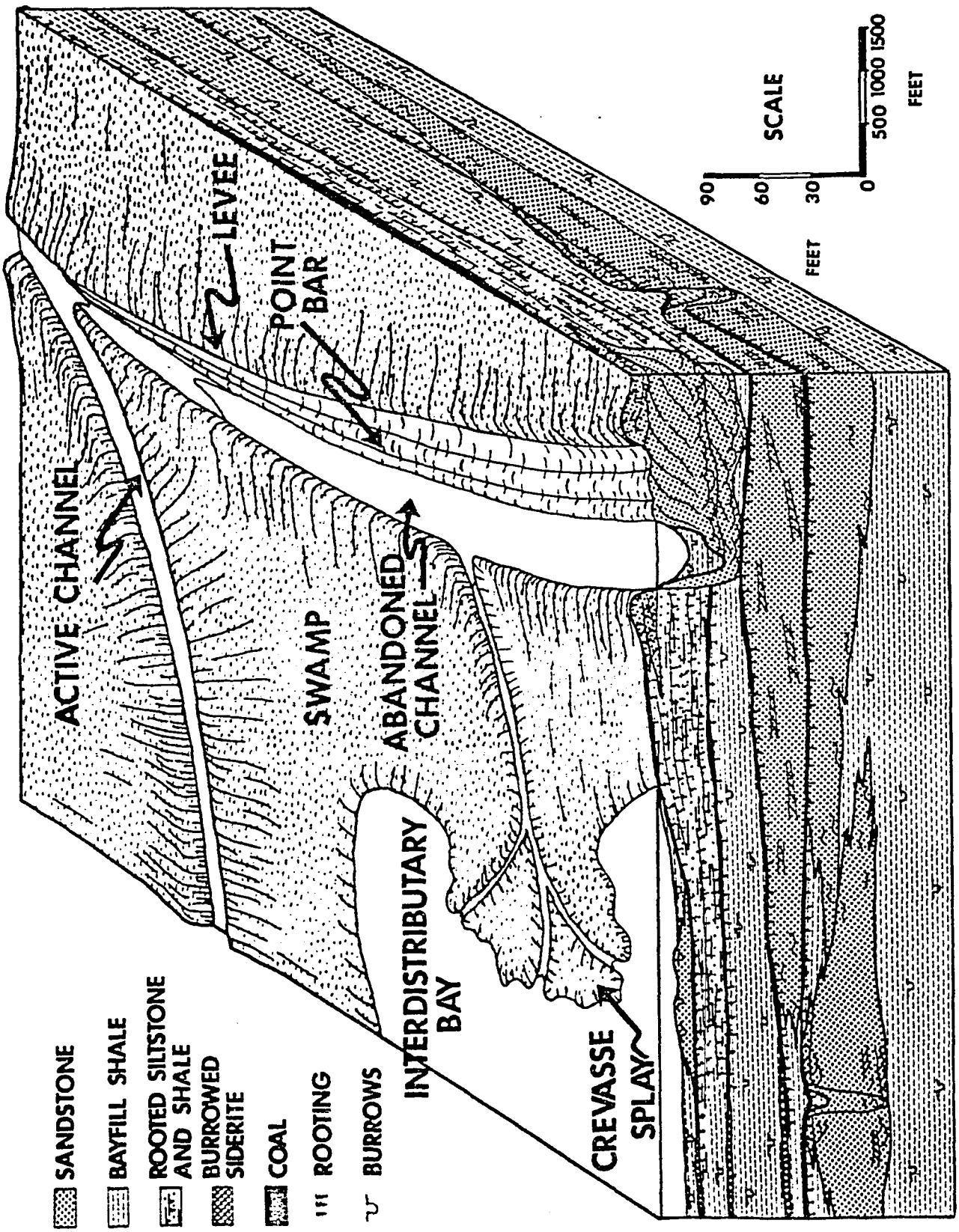

Because of the sinuous nature of outcrops in the study area, several exposures oriented perpendicular to channel flow (Figure 19 and 20) show well developed point bar surfaces (Plate IV, Figure 21, 22 and 23). Paleocurrent orientation data (Table III) indicates that flow was nearly perpendicular to the inclination of the point bar surfaces.

The second morphologic attribute of meandering fluvial systems is the development of abandoned meander channels (Figure 24). Abandoned meander channels have not been previously reported or recognized in outcrops. Two well developed, abandoned meanders were recognized in the study area. In plate IV, point bar accretion surfaces in the Harold Sandstone are well developed on the southwest end where the sandstone is uniformly ten meters thick. Paleocurrent data indicate that current direction was perpendicular to inclination of point bar surfaces. Inclined point bar surfaces indicate that the channel migrated from left to right. The sandstone thins to the right and the interval between the basal scour surface, marked by a siderite pebble lag deposit and the overlying Upper Elkhorn No. 1, 2 coal is occuppied by a clay plug. The clay plug is three meters thick near the channel thalweg, but thins rapidly up the point bar surface. The clay plug is composed of a black to gray organic-rich, fissile shale with minor, discontinuous lenses of fine sand and coarse silt (Figure 25). It is distinct from the underlying reddish-gray, sideritic, silty shale of the interchannel bay environment and is separated from it by an erosional surface marked by a siderite pebble lag deposit. A steep

FIGURE 19. Paleocurrent orientation data for Harold Sandstone. See table III for a summary of data.
NC = North channel
SC = South channel
MC = Main channel
c = Chute-fill from upper part of vertical profile in HA-1 and HA-27

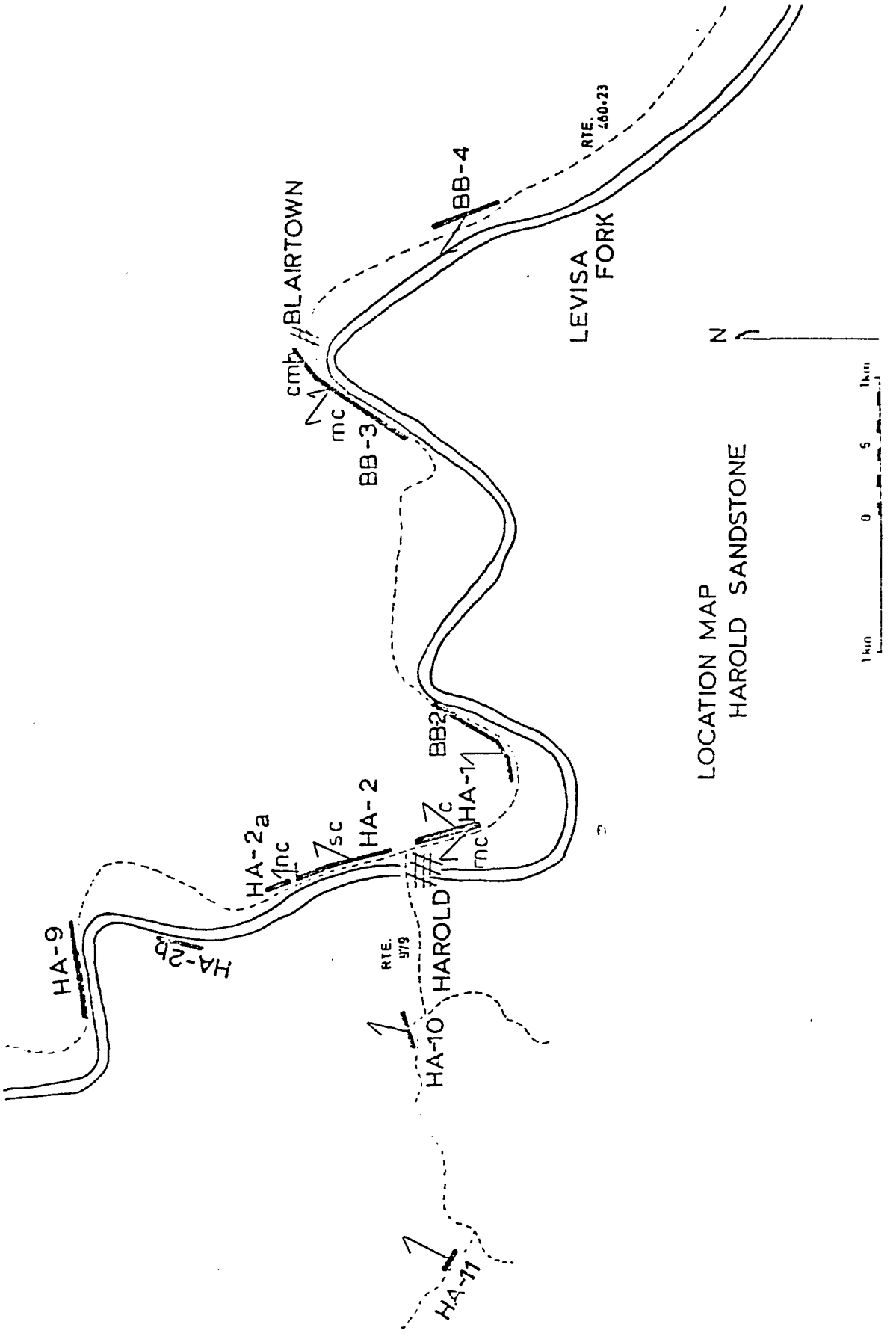

FIGURE 20. Paleocurrent orientation data for Allen Sandstone. See table III for a summary of the data.
LC = Lower channel
UC = Upper channel
NC = North channel
SC = South channel

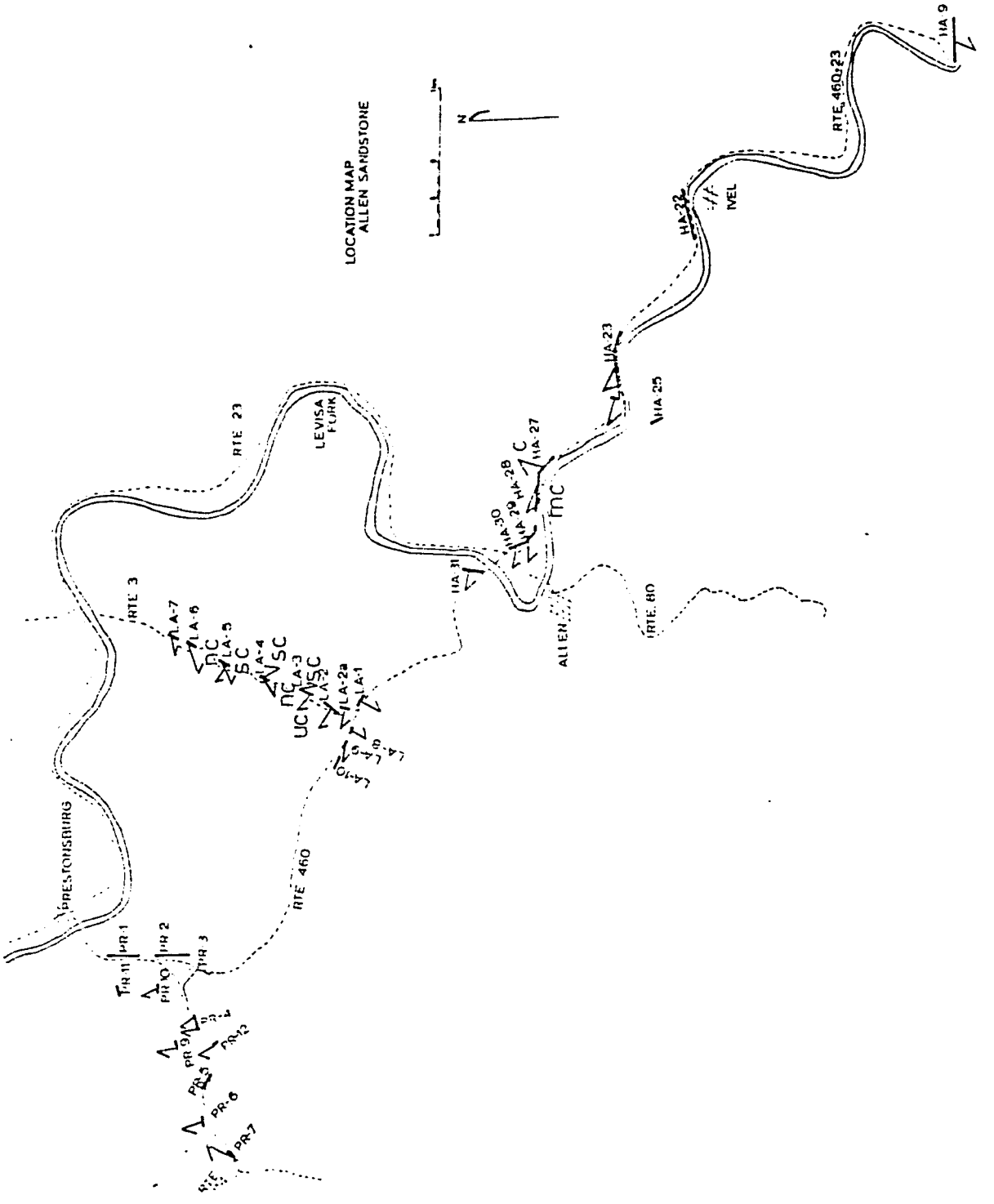

FIGURE 21. Composite photograph of point bar surfaces at HA-1 in the Harold Sandstone. Point bar surfaces extend from channel base to chute fill near top. Paleocurrent orientations indicate that current flowed toward viewer. Channel migrated from right to left. Coal above channel is the Upper Elkhorn No. 1, 2.

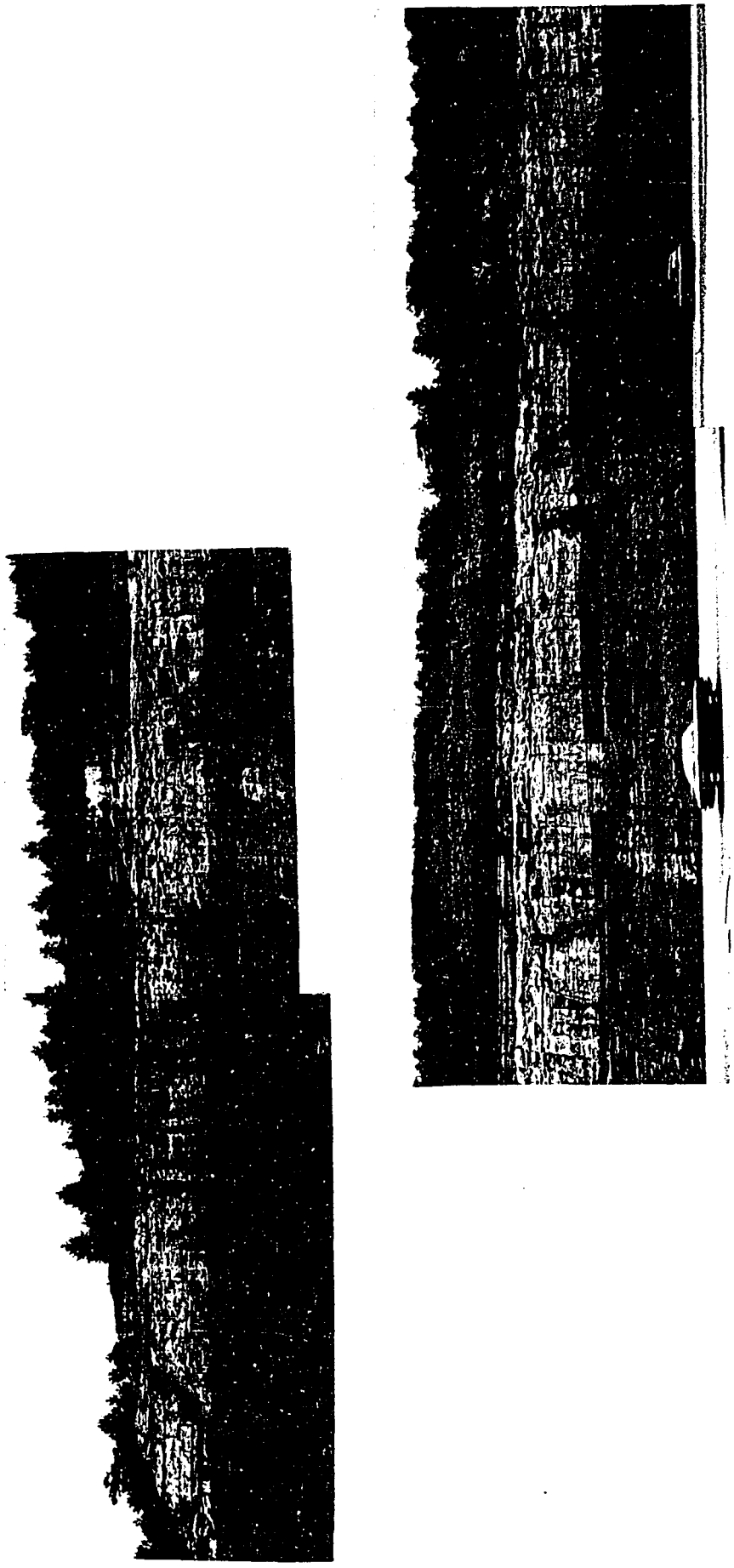

FIGURE 22. Photograph of point bar surfaces at HA-23 in the Allen Sandstone just above road level. Paleocurrent orientations indicate that current flowed out of outcrop. Channel migrated from right to left. View is to north. Car on left gives scale. Coal above channel is the Upper Elkhorn No. 2.

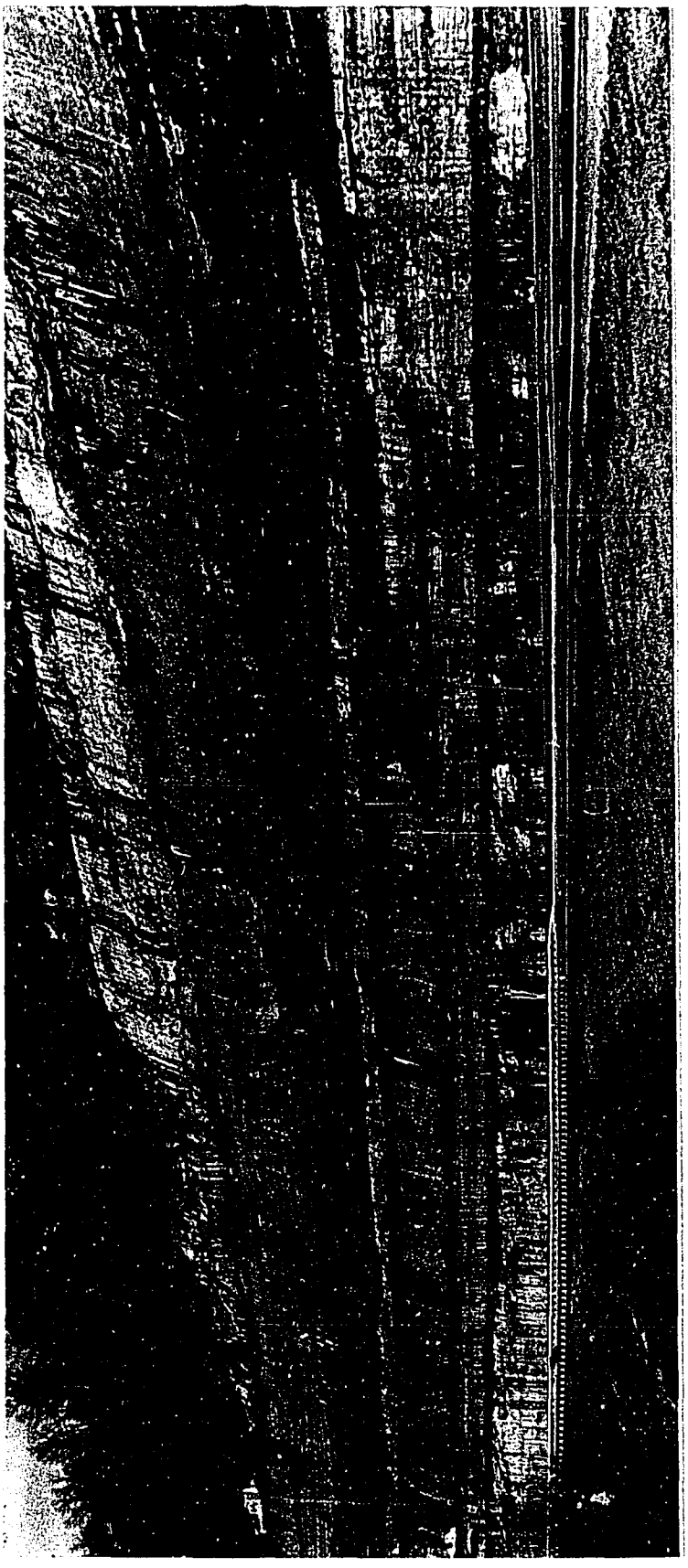

FIGURE 23. Photograph of point bar surfaces at PR-3 in the Allen Sandstone. Paleocurrent orientations indicate that current flowed from left to right. Channel migrated toward viewer. Base of channel not exposed.

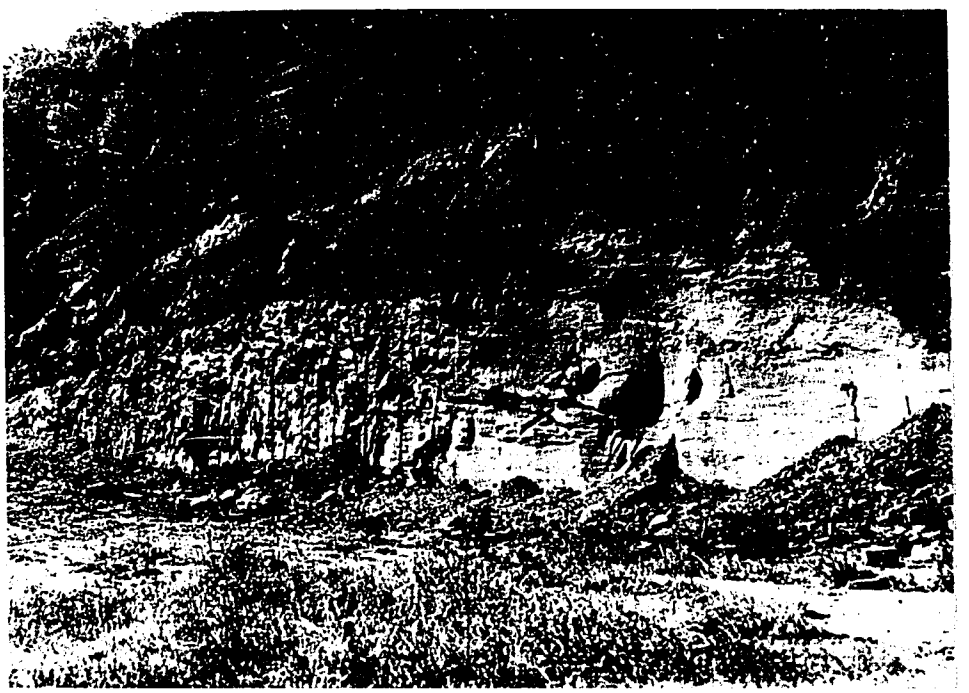

TABLE III

SUMMARY OF PALEOCURRENT ORIENTATION DATA
(See Appendix for methodology and explanation of symbols)*

Sample No.	n	$\bar{x}^{o}$ azimuth	R	L percent
Harold Sandstone				
BB-2	23	8	20.8	90.6
HA-1 grand average	43	307	35.0	80.1
HA-1 main channel	33	300	25.4	77.0
HA-1 chute fill, top	10	31	8.3	83.5
HA-2 south channel	30	23	28.1	93.5
HA-2 north channel	10	5	9.1	91.1
HA-10	10	31	8.7	87.3
HA-11	10	40	6.5	65.2
Allen Sandstone				
HA-23	10	294	9.4	93.0
HA-27 main channel	30	280	24.8	82.7
fossil log	4	280 - 100		
HA-27 chute fill, top	7	9	6.9	98.5
HA-29	15	271	13.3	88.9
HA-30	20	283	16.3	80.8
LA-1	10	198	9.5	94.5
LA-2	20	300	19.4	96.9
LA-2a	14	274	13.6	97.0
LA-3 upper channel	15	185	13.8	92.3
LA-3 lower channel	43	319	37.5	87.2
LA-4 south end	19	155	18.2	96.0

Sample No.	n	x° azimuth	R	L percent
LA-4 north end	10	224	9.4	93.0
LA-5 south channel	10	316	9.8	98.1
LA-5 north channel	37	248	34.8	93.9
LA-6	16	246	15.2	95.1
LA-7	36	254	31.4	87.2
LA-8	15	212	9.7	64.9
LA-9 channel mouth bar	10	300	4.2	42.0
PR-3	10	285	8.1	81.5
PR-4a	15	305	14.1	94.2
PR-4b	15	356	14.2	94.2
PR-6 bottom	12	331	11.6	96.6
fossil log	2	0 - 180		
PR-6 top	12	303	11.4	95.1
PR-7	10	30	9.8	98.3
fossil log	3	20 - 200		
PR-9	10	334	8.8	87.2
PR-10	10	331	8.6	86.1
PR-12	11	330	9.8	89.5

*Sample numbers correspond to outcrop locations as shown in figures 19 and 20.

FIGURE 24. Photograph of abandoned meander channel at BB-2 in the Harold Sandstone. The photograph corresponds to Plate IV. Point bar surfaces are well developed in sandstone on left and indicate channel migrates from left to right. Sandstone thins to right and is replaced by dark organic-rich clay plug. Steep rise of Upper Elkhorn No. 1, 2 coal in right portion of photo marks the position of the cut-bank. Paleocurrent data indicate that currents flowed into outcrop.

FIGURE 25. Close up photograph of clay plug in abandoned meander at BB-2. Pinching out of sandstone is visible on right. The clay plug is a dark organic-rich shale and is separated from the underlying bay fill sediment by a zone of siderite lag pebbles. The cut-bank is clearly visible on the right above the car.

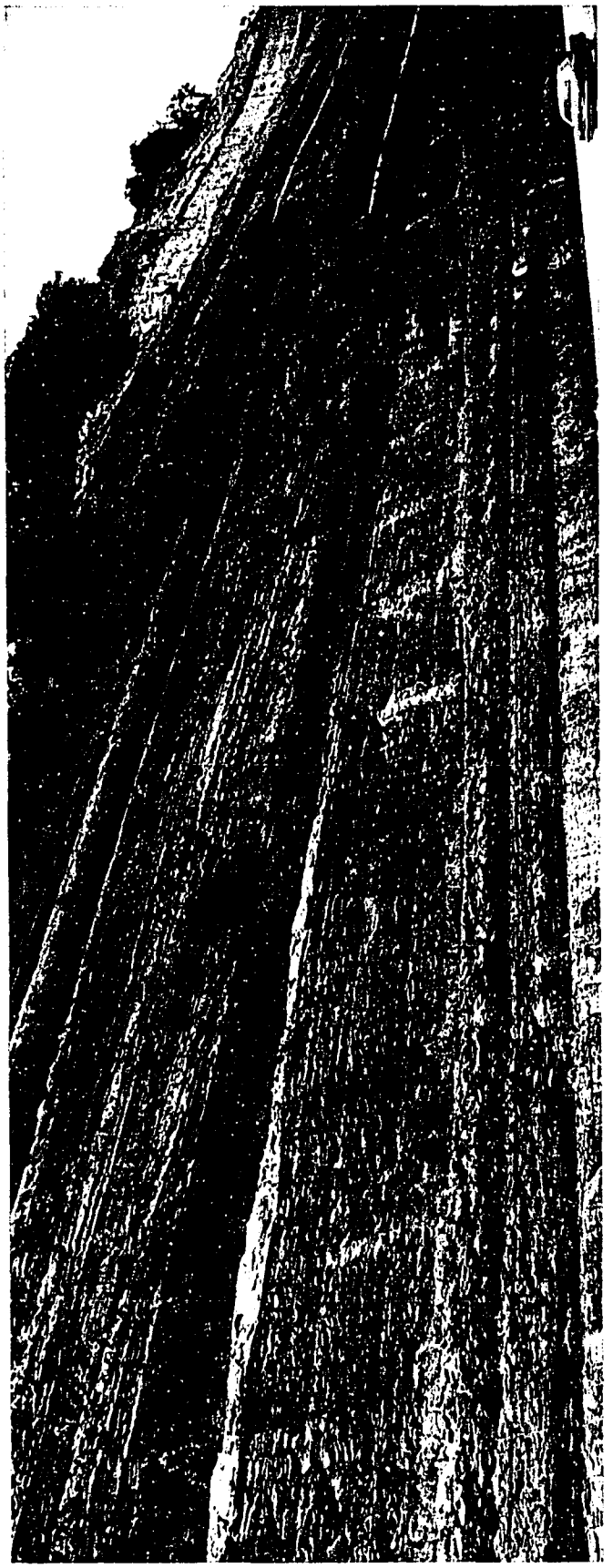

cutbank with minor slumping marks the edge of the abandoned meander channel (Figure 26). The relief on the Upper Elkhorn No. 1, 2 coal as it drops into the abandoned channel probably resulted in part from differential compaction of the sandstone, clay plug and interchannel bay sediments.

The second abandoned meander (see Figure 71 for general shape) occurs in the Allen Sandstone. It is similar in shape to the Harold Sandstone. Paleocurrent orientation is also nearly perpendicular to inclined point bar surfaces. The abandoned channel fill, however, is rippled siltstones with numerous fine sand lenses and scour and fill structures. Fisk (1947) describes this type of sediment as typical of abandoned meander channel fills close to the point of cutoff where river currents are still active during times of high flow.

The third morphologic attribute of migrating, but not necessarily meandering fluvial systems is the development of major erosional truncation surfaces where deposits of the fluvial system cross-cut earlier fluvial deposits. These major truncation surfaces are easily recognized. They extend through the entire thickness of sandstone and contain lags of clay chips, siderite and abundant fossil logs and stems. Paleocurrent orientation data (Table III and Figures 19 and 20) indicate that the two channel deposits separated by this major truncation surface have distinct paleocurrent orientation. These major truncations are well developed in the Allen Sandstone in figure 27.

The internal stratigraphy (bedding and texture) of these fluvial sandstones as portrayed in vertical profiles corresponds well with that established from modern fluvial environments (Jackson, 1975, 1976)

FIGURE 26. Close up photograph of cut-bank in abandoned meander at BB-2. A thin shale separates the horizontally bedded bay fill sediments from the overlying Upper Elkhorn No. 1, 2 coal.

FIGURE 27. Composite photograph of major erosional truncations of LA-5 in the Allen Sandstone. North channel is to the left and south channel is to the right. Current flowed at observer. Paleocurrent data (Table III and Figure 20) indicate that the two channels had distinct orientations. Upper Elkhorn No. 1 coal caps sandstone. Sandstone is 10 meters thick.

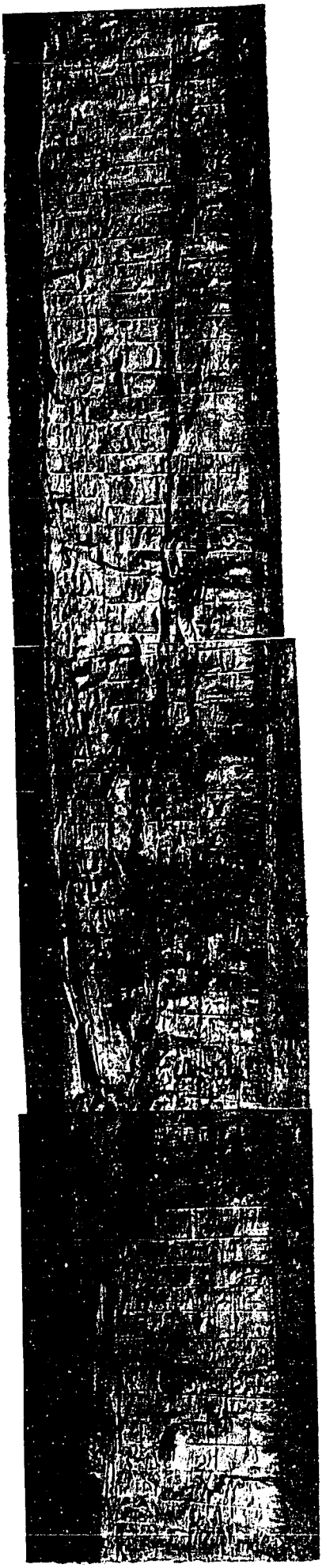

and ancient fluvial deposits (Potter and Glass, 1958; Visher, 1965, 1972 and Allen, 1965, 1970). Eight vertical profiles of fluvial sandstones are presented here; three from the Harold Sandstone (Figures 28, 29 and 30), five from the Allen Sandstone (Figures 31, 32, 33, 34 and 35) and one from the Blairtown Sandstone (Figure 13). In addition, two profiles from individual point bar surfaces in the Harold Sandstone are also presented here for comparison (Figures 36 and 37). Bounding units on the vertical profile are the marker coal beds, where exposed.

In general, sandstones from the fluvial environment are ten meters thick and fine upward from a highly erosive basal conglomerate to rooted, silty shale overbank deposits. Median size at the base averages 1.9ϕ, medium sand and grades upward to a median size of 4ϕ at the top. Maximum grain size also fines upward from 1ϕ at base to 2.5ϕ.

The basal erosional surface has up to two meters of relief, locally. It commonly exhibits oriented flute and sole marks and is usually conglomeratic. Where the channel truncates bay fill sediments the conglomerate is composed of slightly rounded, elongate, platy, often imbricated, siderite clasts up to seven centimeters long (Figure 38) or clay chips of similar dimensions. Where streams have eroded through coal swamps, the siderite conglomerate is replaced by abundant, fish-tailed coal rafts and oriented logs and stems. Bedding in this basal conglomeratic zone is commonly distorted by slumping from cut-banks (Figure 39) and collapse around decaying logs and stems (Figure 40).

FIGURE 28. Vertical profile of fluvial deposits in the Harold Sandstone at BB-2.

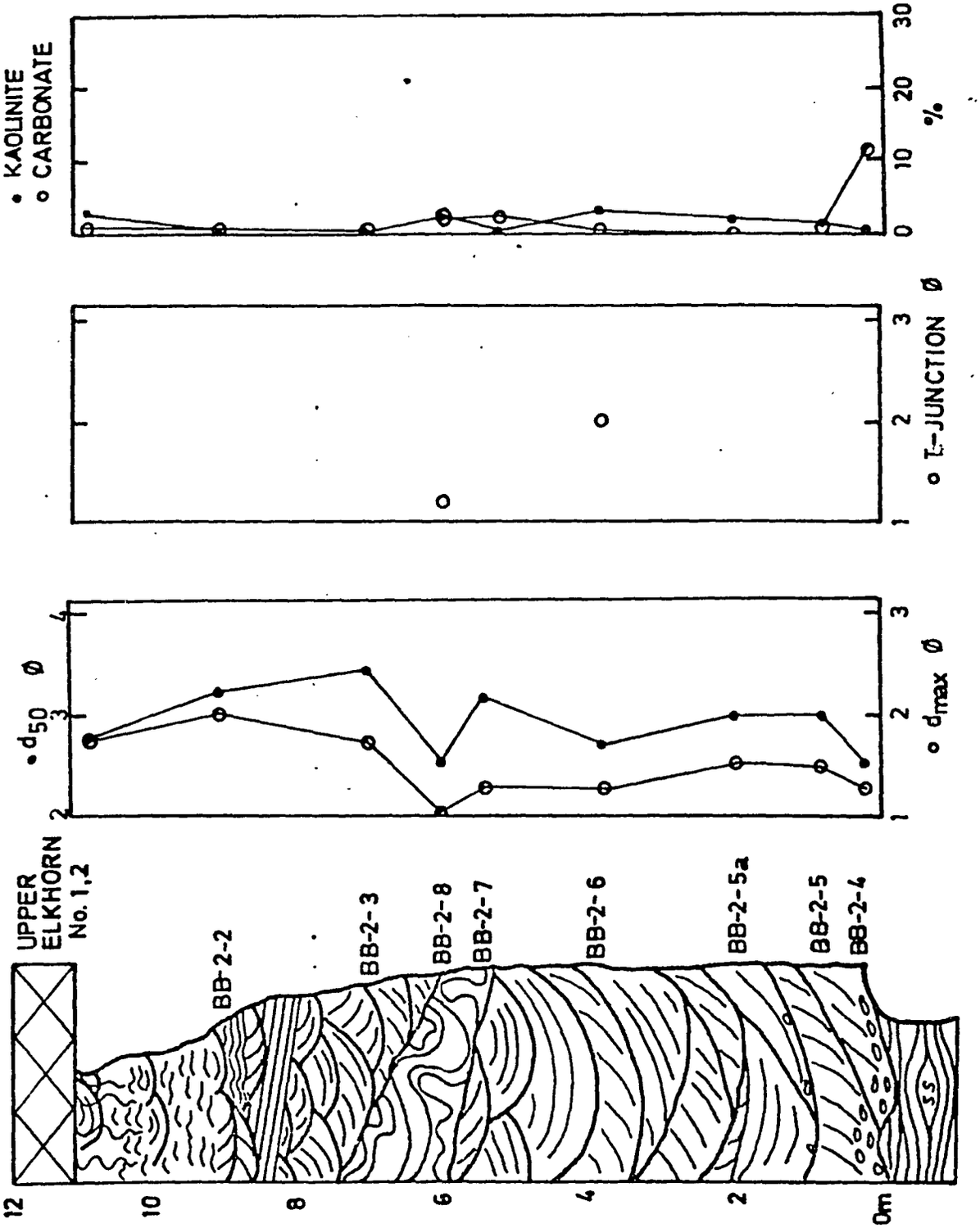

FIGURE 29. Vertical profile of fluvial deposits in the Harold Sandstone at HA-1.

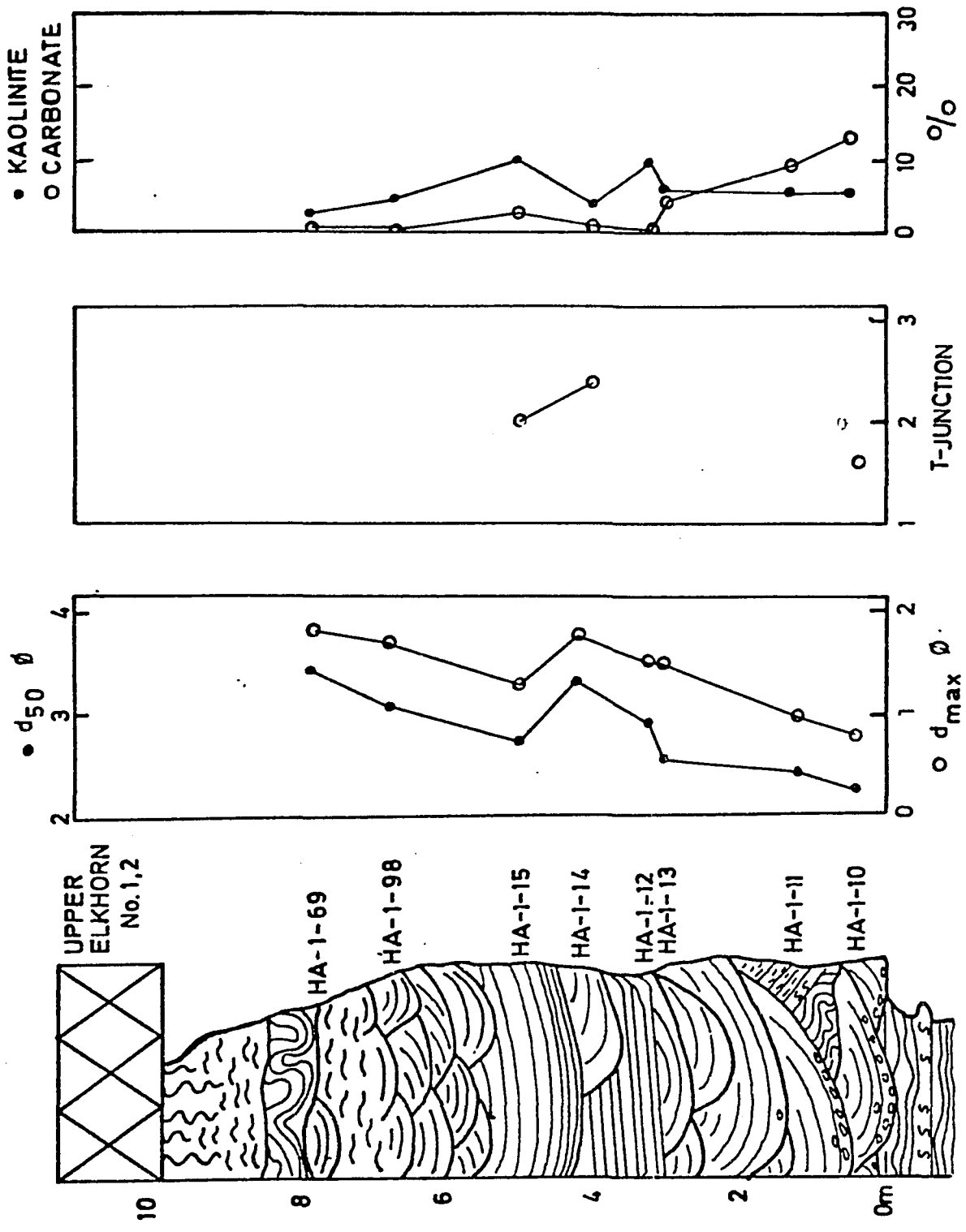

FIGURE 30. Vertical profile of fluvial deposits in the Harold Sandstone at HA-2.

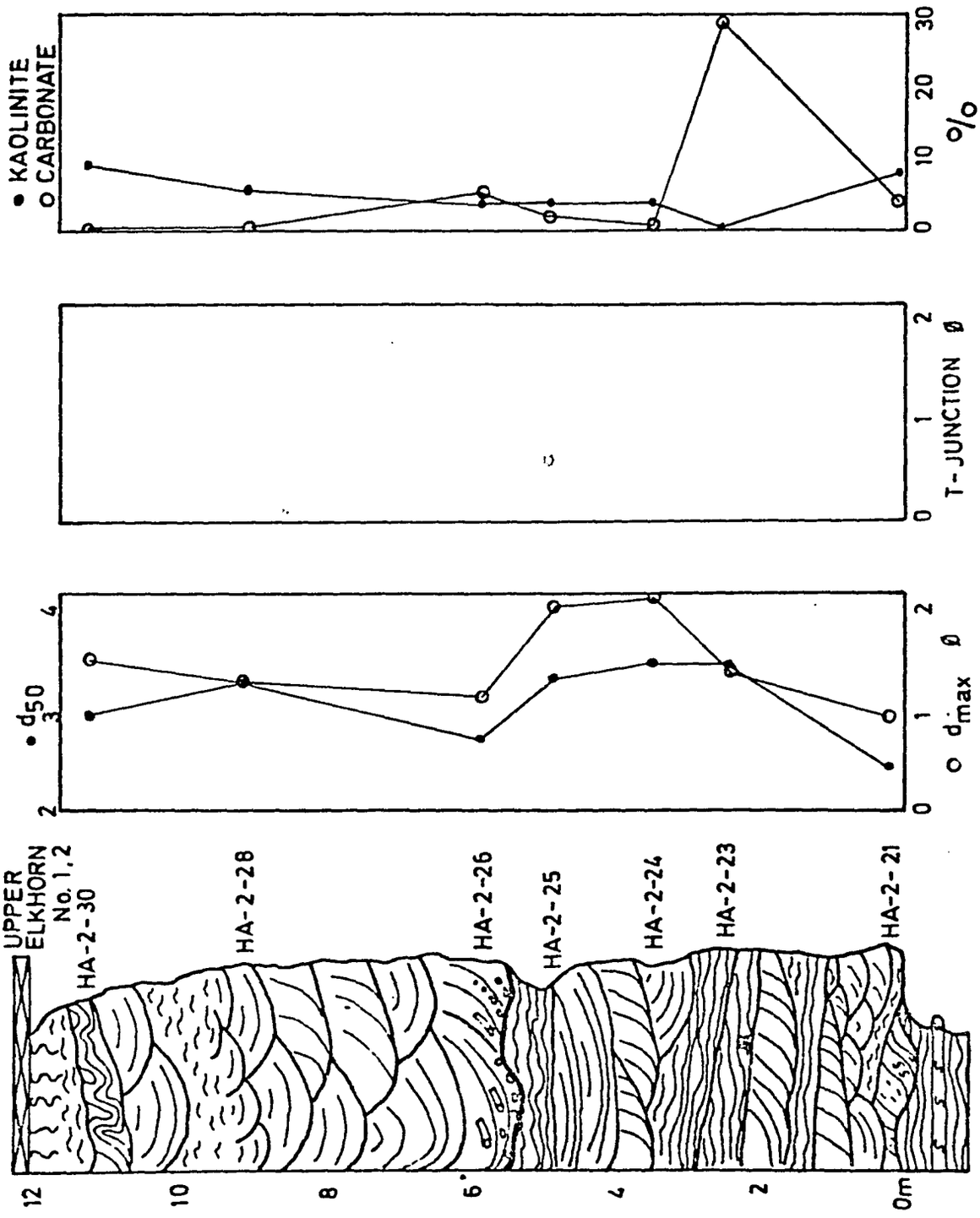

FIGURE 31. Vertical profile through fluvial deposits in the Allen Sandstone at HA-23.

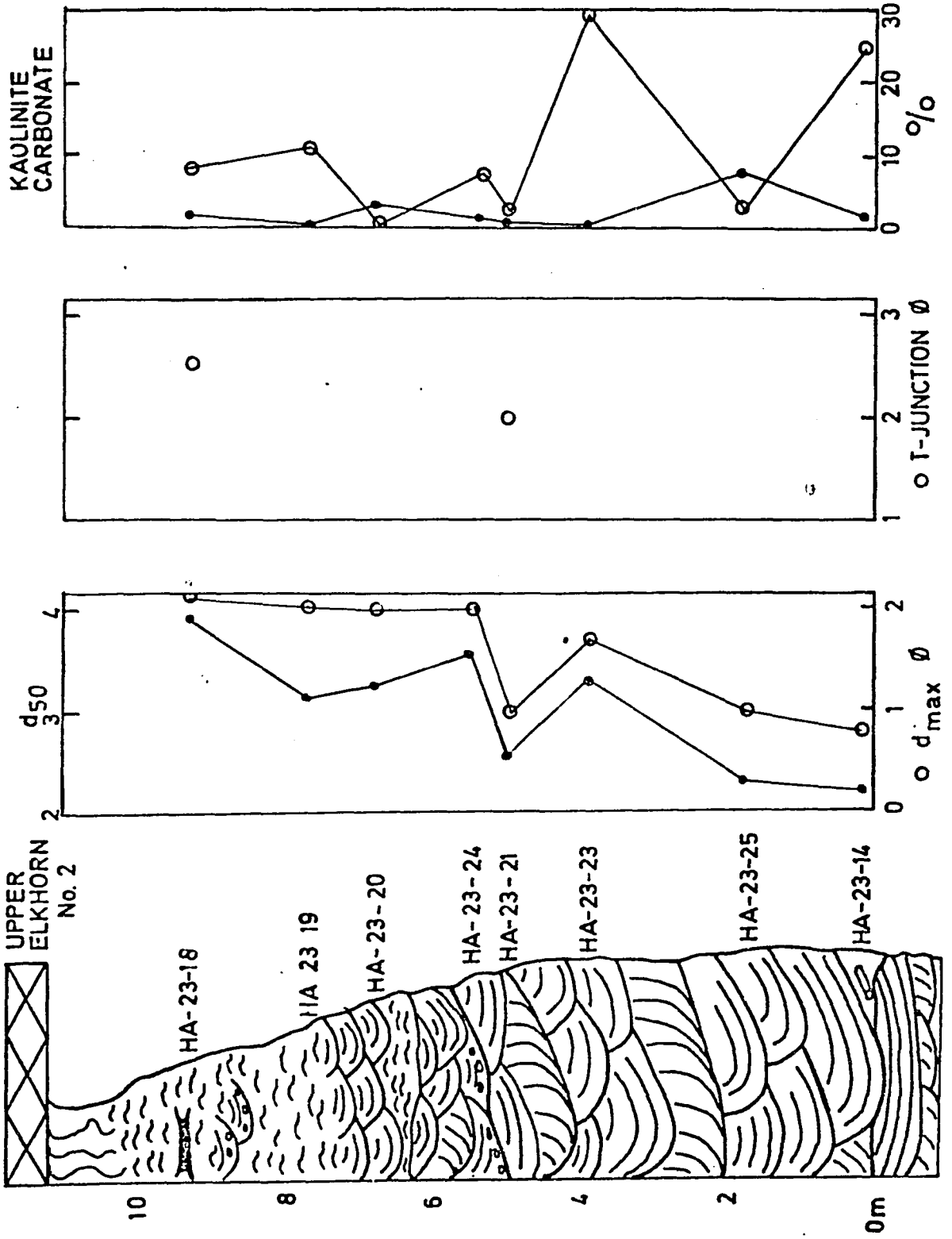

FIGURE 32. Vertical profile through fluvial deposits in Allen Sandstone at HA-27.

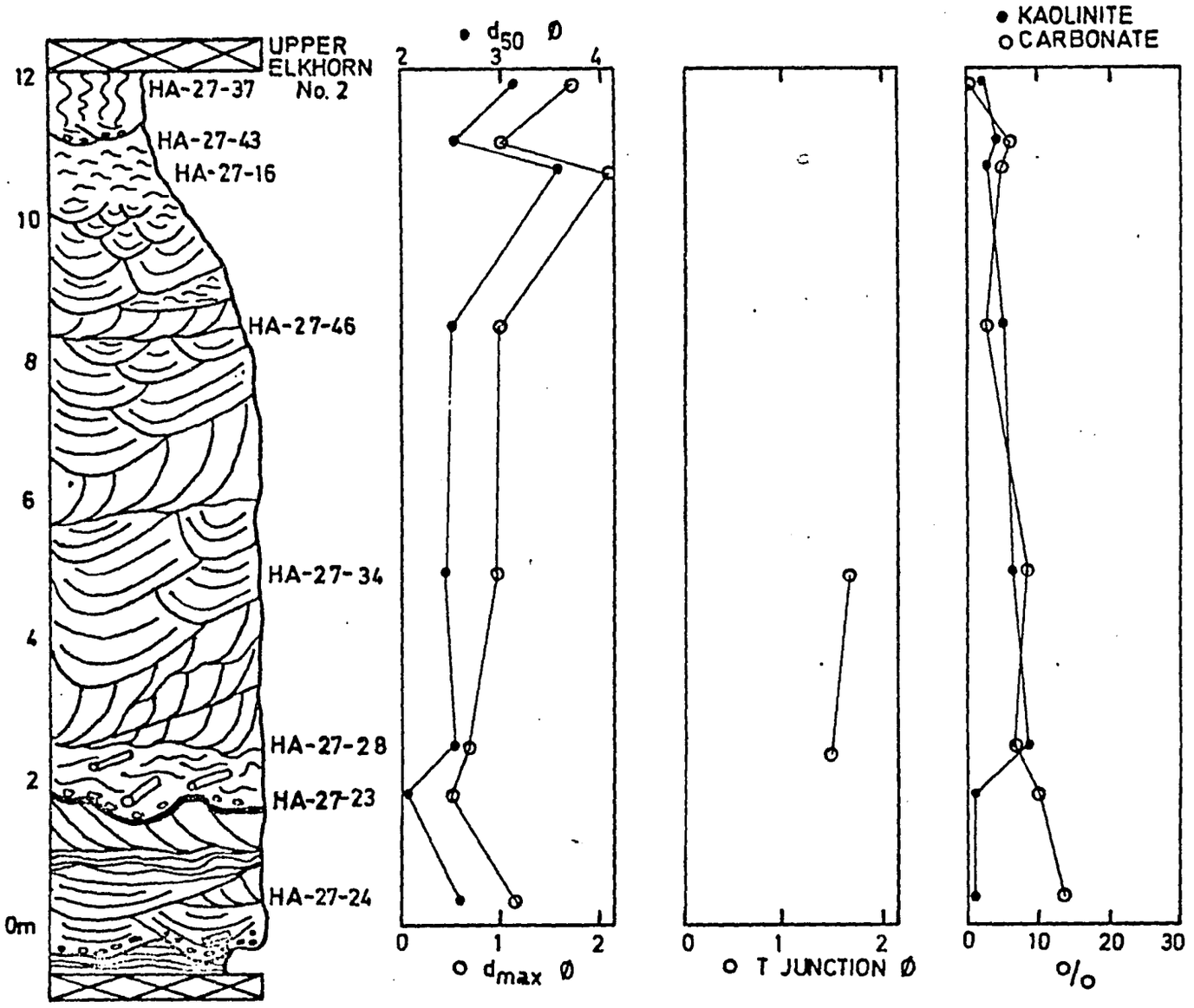

FIGURE 33. Vertical profile through fluvial deposits in the Allen Sandstone at HA-29.

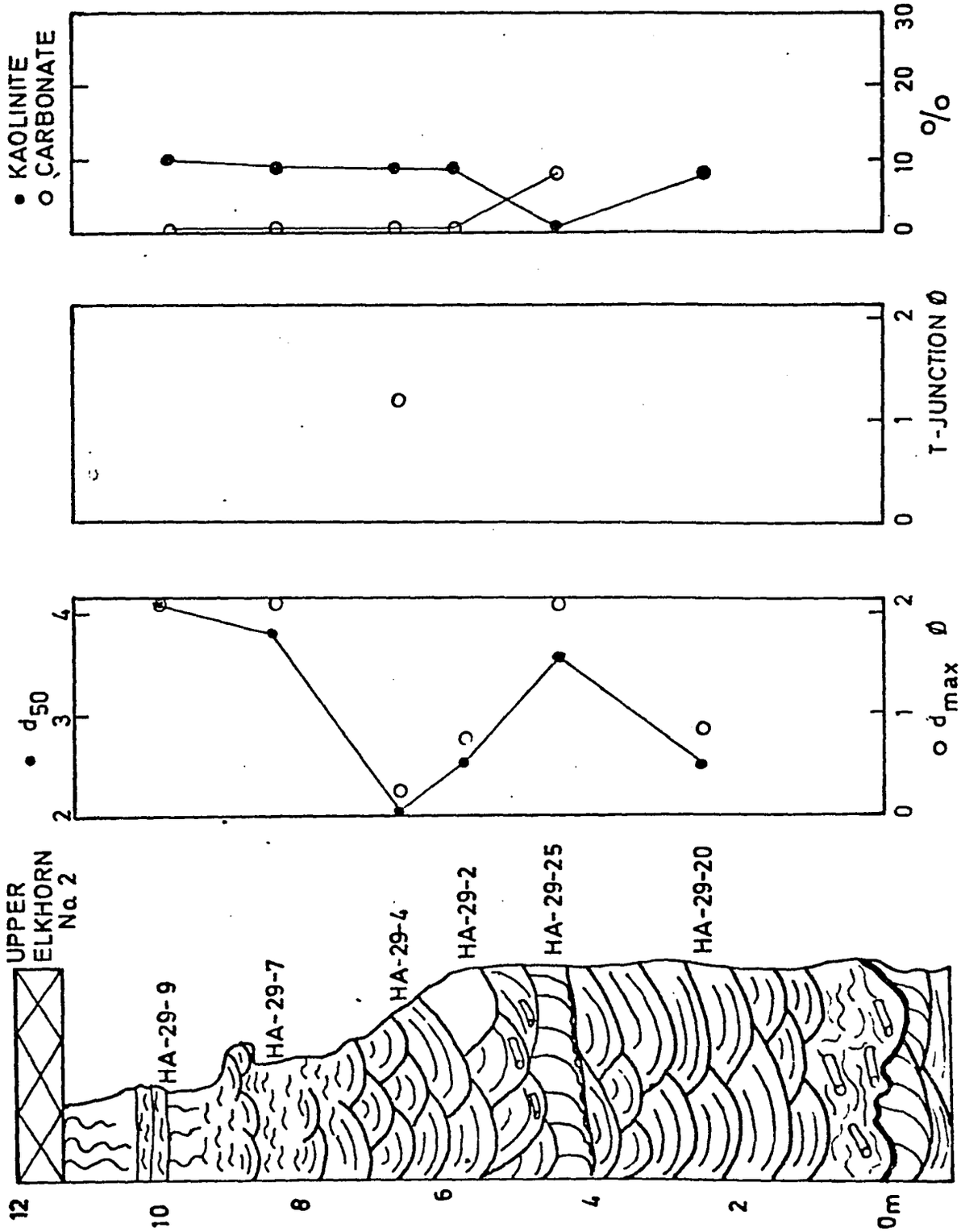

FIGURE 34. Vertical profile through fluvial deposits in the Allen Sandstone at LA-3.

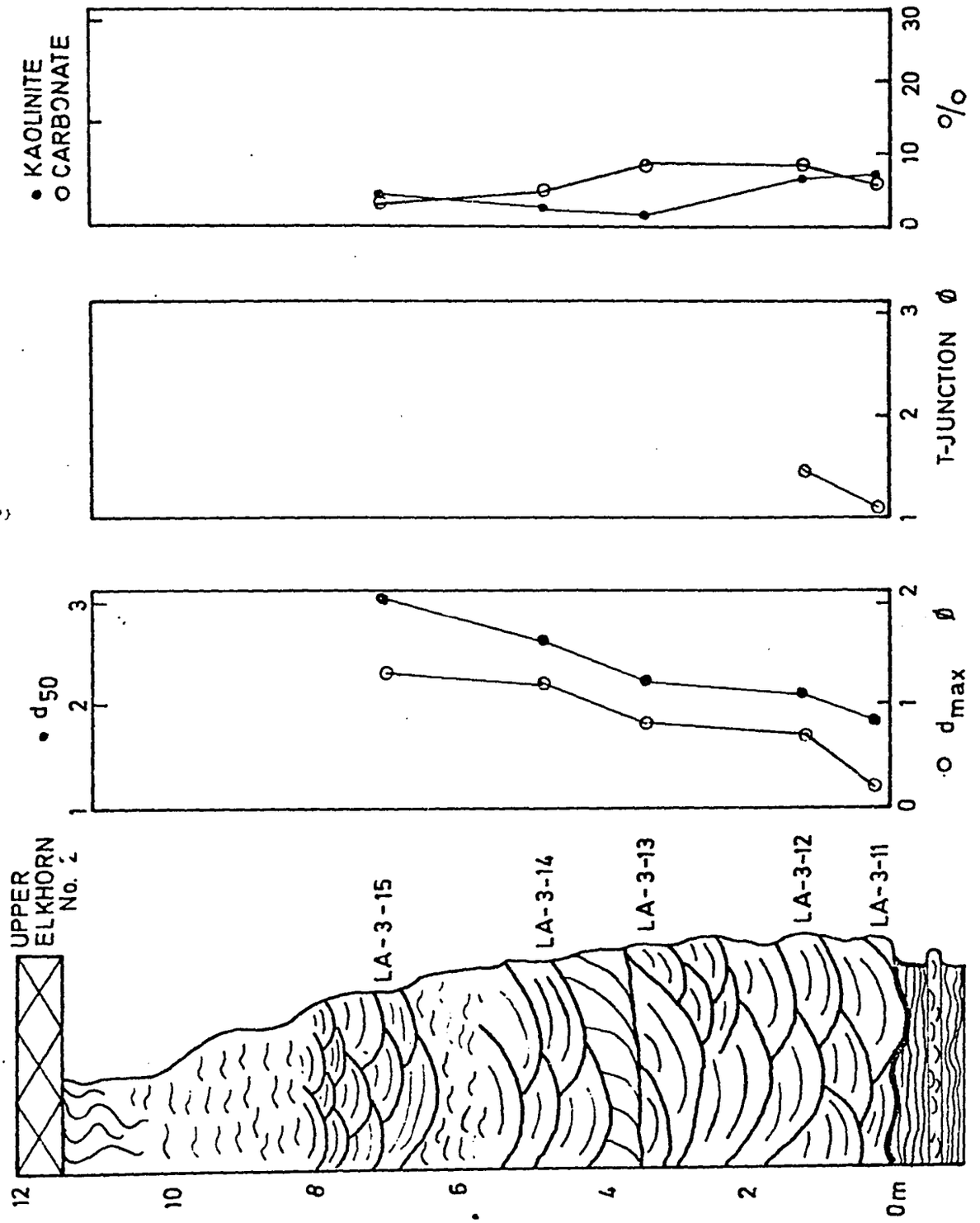

FIGURE 35. Vertical profile through fluvial deposits in the Allen Sandstone at PR-7.

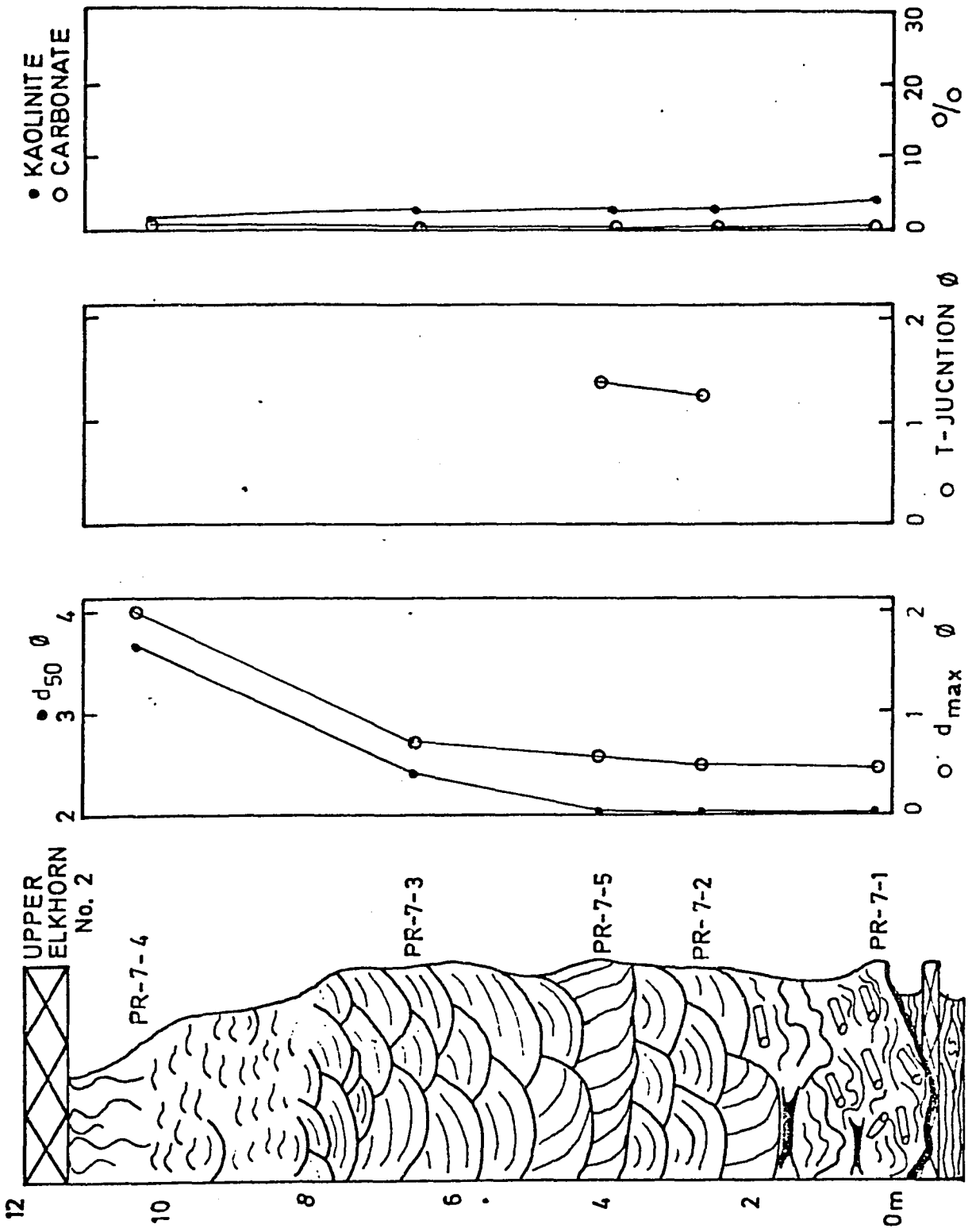

FIGURE 36. Vertical profile along point bar surface in Harold Sandstone at BB-2.

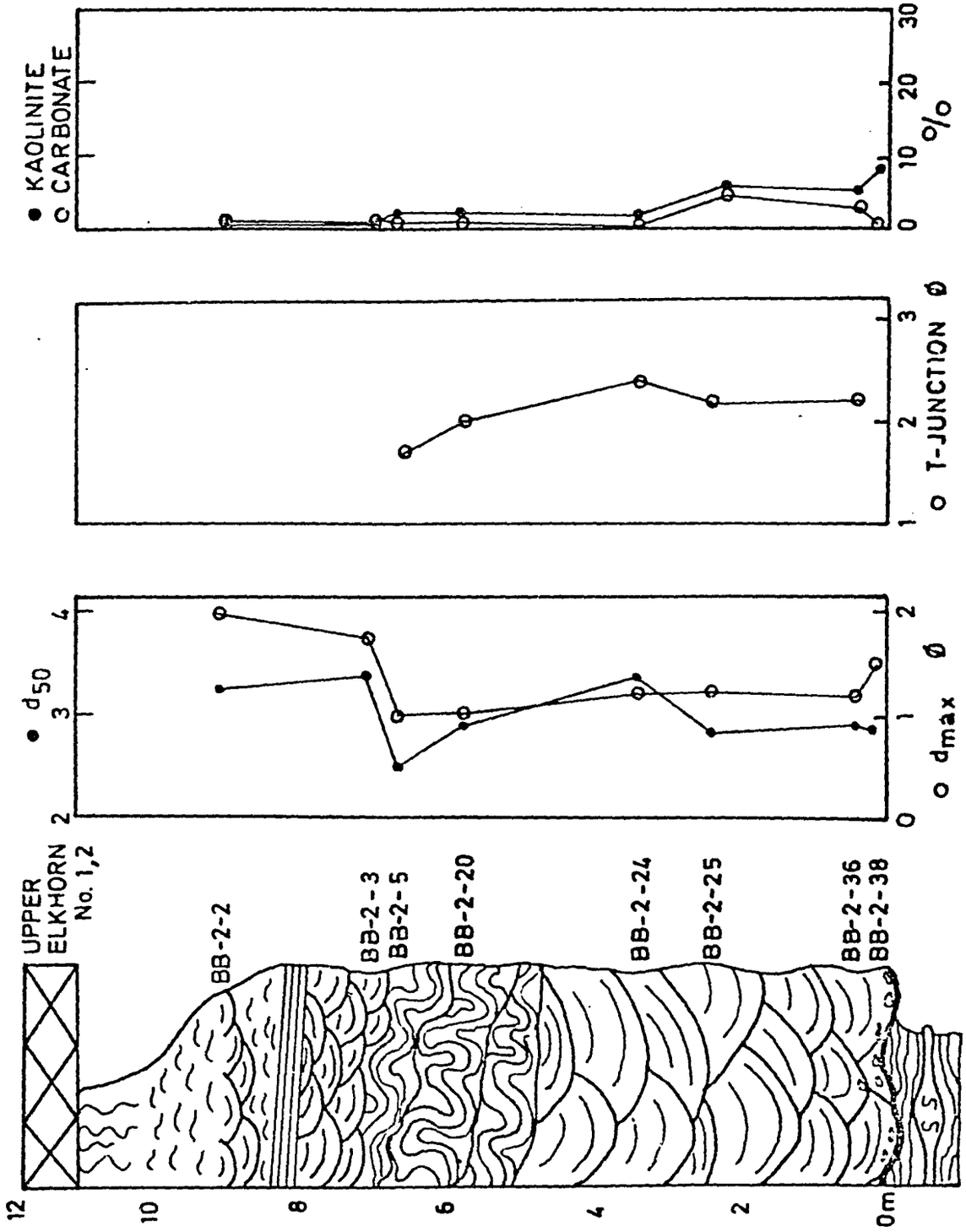

FIGURE 37. Vertical profile along point bar surface in Harold Sandstone at HA-1.

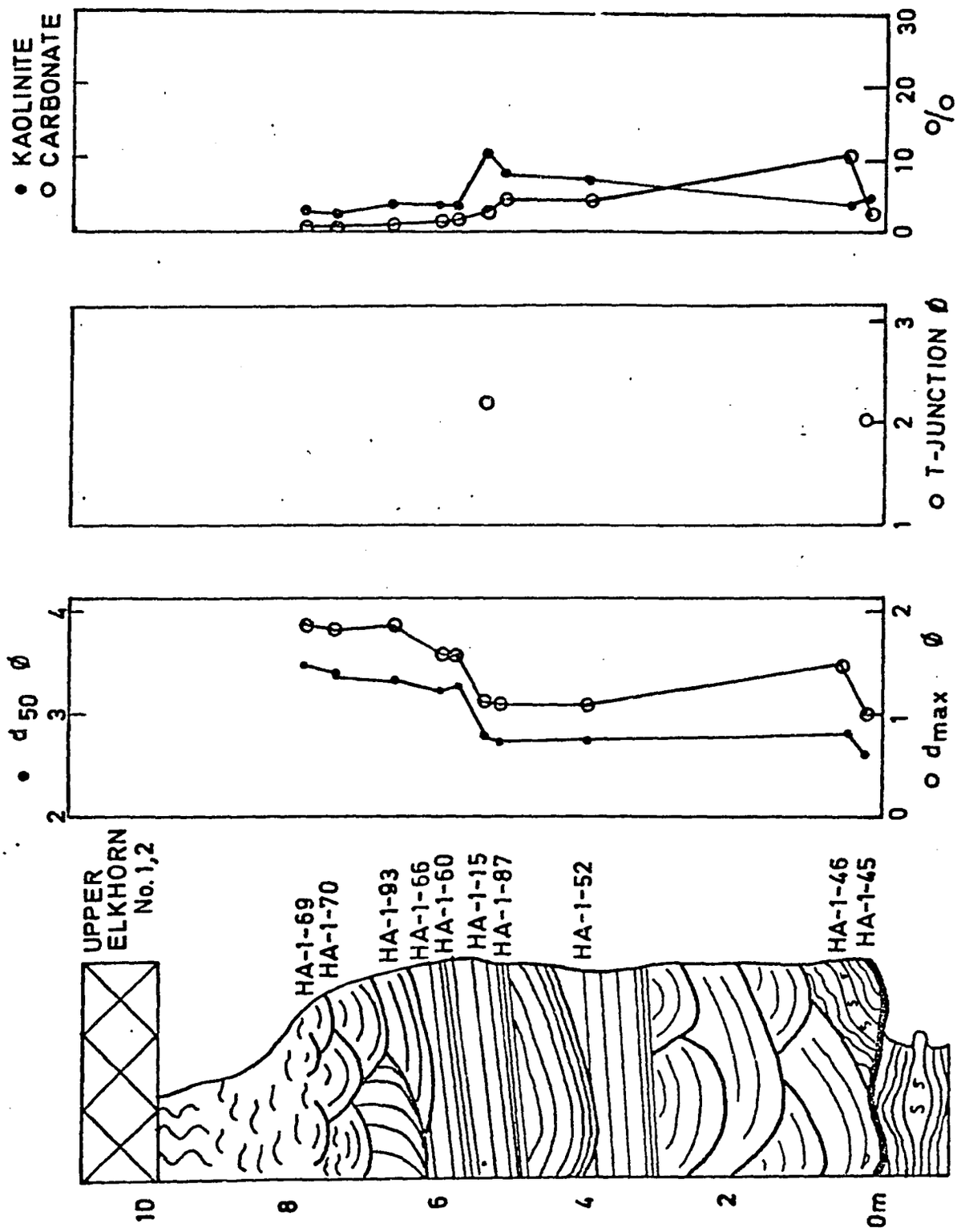

FIGURE 38. Photograph of slightly imbricated siderite pebbles at the base of some fluvial sandstone. From the base of the Harold Sandstone at HA-1.

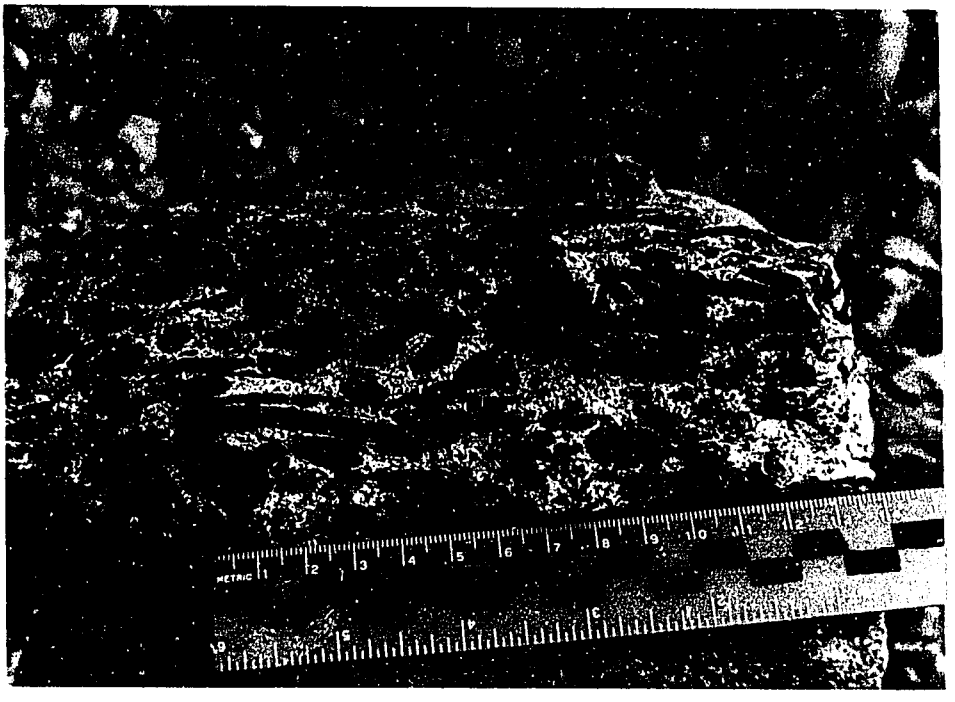

FIGURE 39. Photograph of slump blocks in the base of the Harold Sandstone at HA-1. Slump blocks are composed of contorted interchannel bay sediments that are interbedded with siderite lag pebbles and coarse sand lenses. Slump block is approximately 0.5 meters thick.

FIGURE 40. Photograph of collapsed zones around decayed logs and stems from base of the Allen Sandstone at PR-6. Note ruler on right side by drill hole for scale.

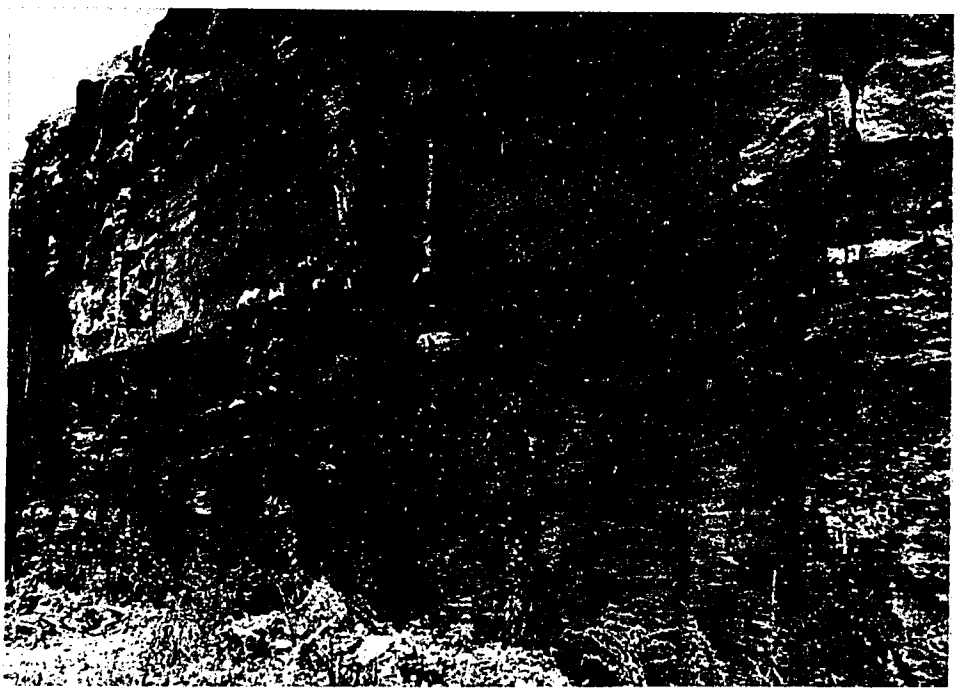

Above this basal conglomeratic zone is a thick zone (5 meters) of uniform, large festoon cross-beds, up to one meter thick (Figure 41). Erosional truncation is common and individual bedforms can be traced for a maximum of five meters in the direction of migration. Concentrations of fossil plant litter and micaeous minerals are common in the base of troughs (Figure 42). Median grain size ranges from 2.0 - 3.0ϕ but tends to be constant through this zone.

Small to medium scale trough cross-beds, 20 to 50 centimeters thick, (Figure 43) occupy a 2 - 4 meter thick zone above the large trough cross-bedding. Grain size is finer, 3.0 - 3.5ϕ and contributes to the overall fining upward tendency. Maximum grain size is also finer in this zone. Convolutely laminated units are commonly developed (Figure 44) and can be traced for tens of meters.

Gently inclined, pseudo-parallel bedding (Figure 45) one to three meters thick composed of individual laminations one to three centimeters thick, occasionally occur interbedded with medium and small troughs. These beds could be confused with parallel beds, but close inspection indicates that they are trough cross-beds. Individual troughs attain maximum lengths of twenty-five meters and are slightly concave at their edges. Grain size tends to be coarser in these units than in the small and medium scale trough. Studies from modern environments (Lane, 1963; McDowell, 1965; Pryor, 1971; Singh, et.al., 1974; and Jackson, 1976) attribute this style of bedding to the migration of large sandwaves.

FIGURE 41. Photograph of large festoon cross-beds typically developed in the base of most fluvial sandstone. Current is out of photograph.

FIGURE 41a. Large trough cross-bed. Note spoon shaped appearance. Migration was from lower left to upper right.

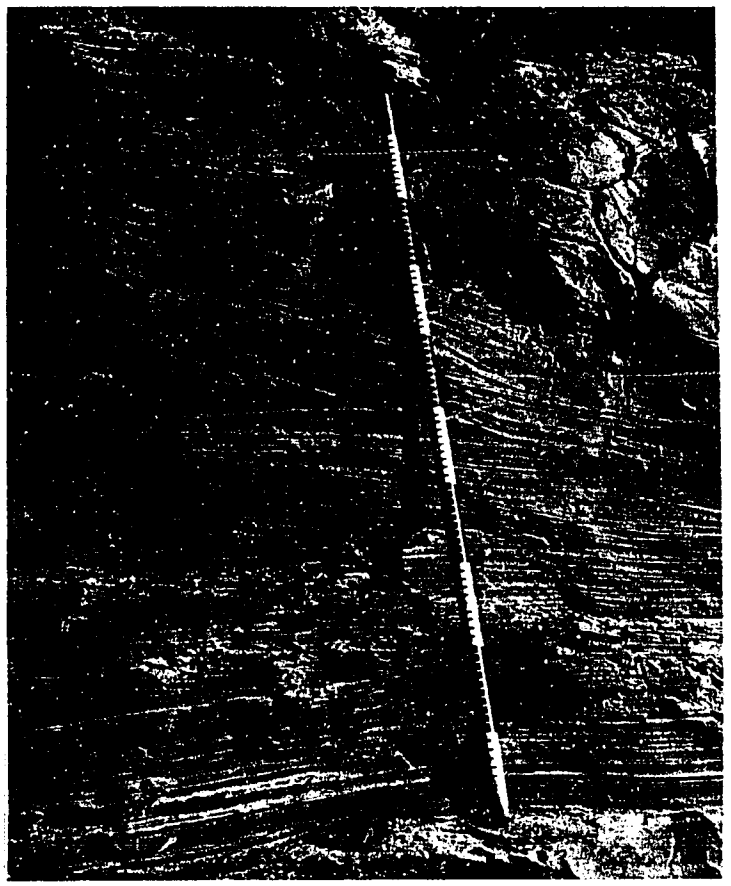

FIGURE 42. Photograph of macerated plant material that commonly occurs on the bedding planes in the base of trough cross-beds. Plant material generally shows no preferred orientation in such locations.

FIGURE 43. Photograph of medium to small scale trough cross-beds from the middle and upper part of most fluvial sandstones. Dark bands are layers of muscovite, plant material, coal grains and detrital siderite. Currents moved from right to left and into the photograph.

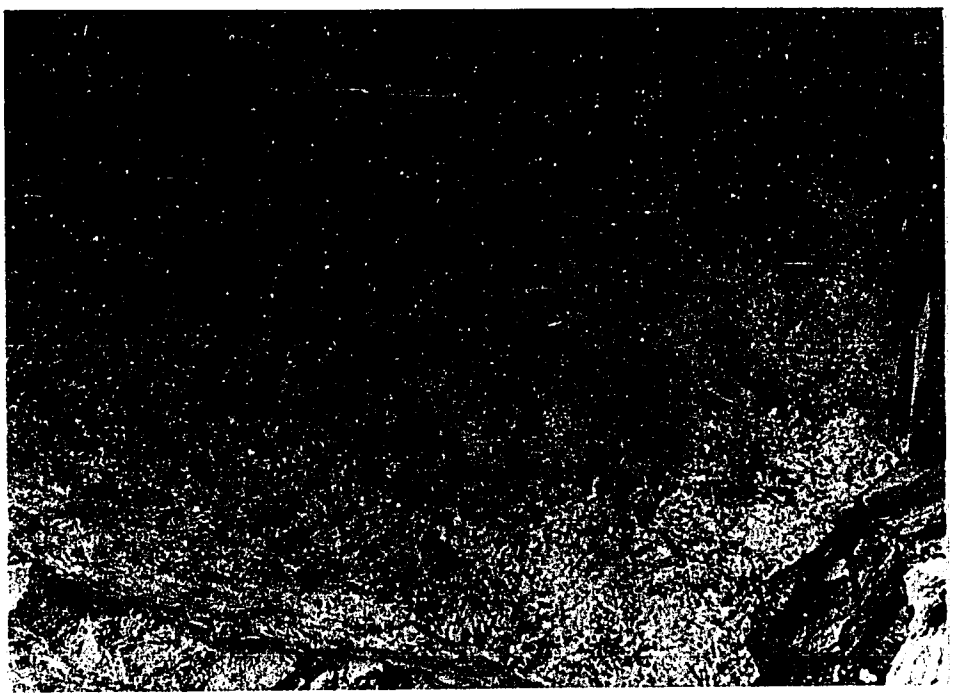

FIGURE 44. Photograph of convoluted zones that develop along point bar surfaces. Folds are visible in the clay drapes that mark many point bar surfaces. From BB-2 with Harold Sandstone.

FIGURE 44a. Close up of distorted lamination in the convoluted zone. Orientation of fold axes indicates that sediment slumped down the point bar surface and into the channel.

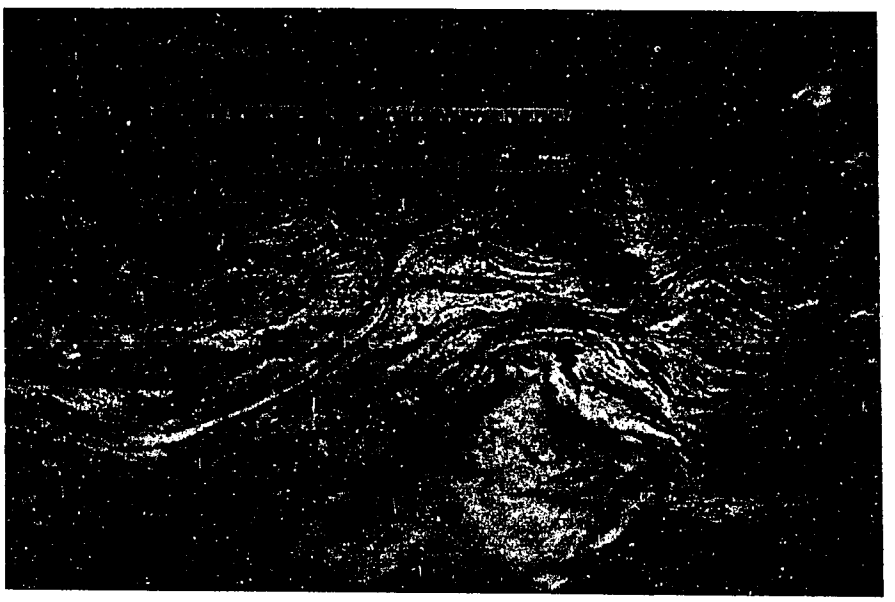

FIGURE 45. Photograph of pseudo-parallel bedding. Laminations are horizontal for 10-20 meters but become concave up and are eroded by the overlying pseudo-parallel beds as in 45a. Drill cores are about 1 meter apart for scale. Concentrations of plant material, muscovite and siderite grains mark bedding planes. From HA-1 in the Harold Sandstone.

FIGURE 45a. Concave upward nature of pseudo-parallel bedding. Notice erosional truncation at top of meter stick.

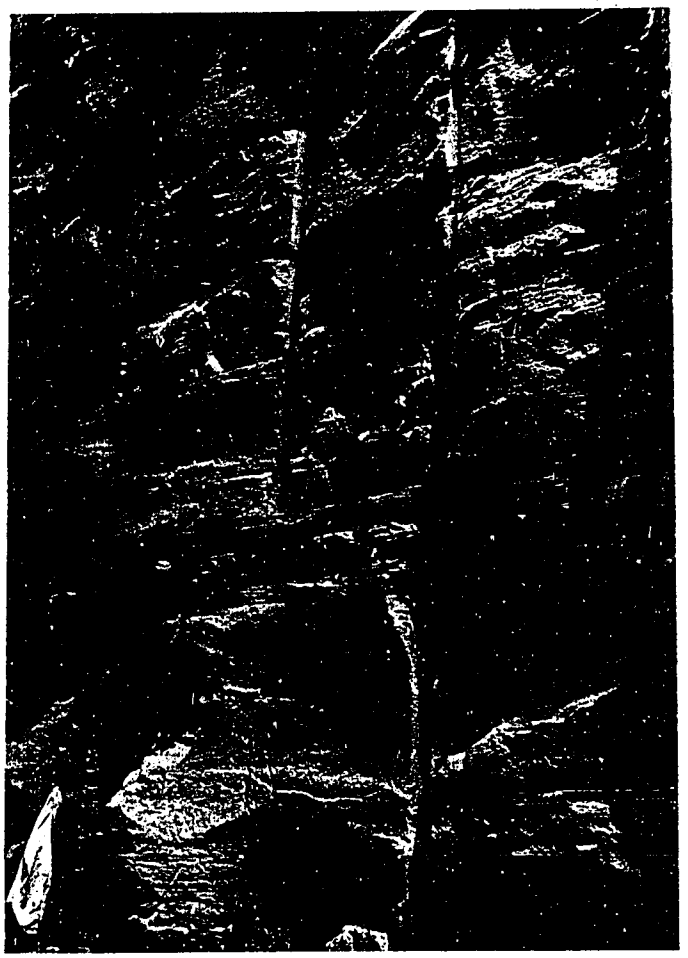

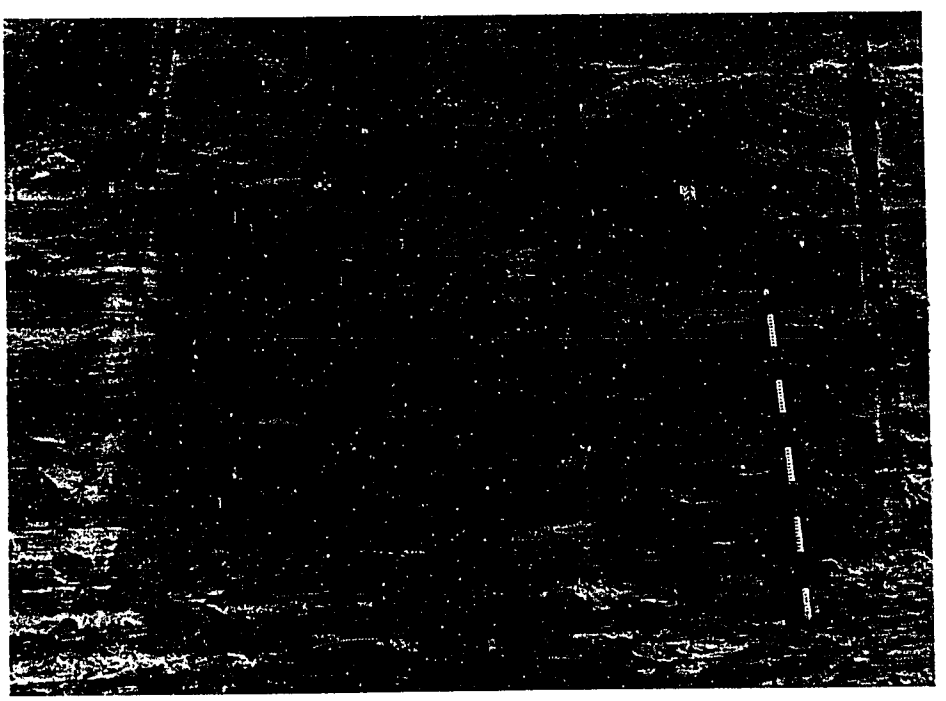

Above this zone is a one to three meter thick unit of small troughs (ten centimeters thick), small scour and fill structures, ripples and wavy lamination of very fine sand and coarse silt (3ϕ to 4ϕ) that are characteristic of upper point bar sedimentation. Occasionally, lenses of large scale trough cross-beds (Figure 28 and 30) seventy centimeters thick and rarely, planar cross-beds occur in this unit. Paleocurrent orientations from these large cross-beds (Table III) are significantly different from cross-bed orientations of the main channel. These deposits record the development of chute cutoffs (Edgar, 1973 and Zimpfler, 1973). Chute cutoffs are defined as small channels that cut across the inside of point bars (Friedman, 1945). They are active during periods of high flow, contain large scale bed forms and are usually oriented at slight angles to flow in the meander bend.

Above this zone is a 0.5 to 1.0 meter thick unit of extensively rooted, overbank silts and clays. Bedding is completely disrupted by Stigmaria. Occasionally a reddish-buff oxidized zone, one meter thick (Figure 32 and 47), indicative of subaerial exposure and soil development, occurs in these overbank deposits. The sequences of fining upward fluvial sandstones are invariably capped by a coal.

Crevasse Splay and Subaerial Levee: Areas of slightly higher elevation bordering and confining the fluvial channels are called subaerial levees. These ridges form in response to different river stages. Deposition results from overbank flow. Breaches in the levee system usually caused by peak discharges are called crevasse splays. Crevasse splay systems accomodate part of the river discharge and are generally active for short periods of time.

Baganz, et.al. (1975) aptly describes the geometry of a crevasse splay system that forms a split in the Upper Elkhorn No. 1, 2 coal. It is nearly five meters thick and can be traced for several miles along strike. This system is part of the Allen Sandstone which to the north occuppies the same interval between the Upper Elkhorn No. 1, 2 coal (Figure 4).

Figure 47, a composite vertical profile through this interval, illustrates the internal stratigraphy of the crevasse splay and the subaerial levee through which it has eroded. The lower part of the crevasse splay is composed of very fine grained (3.3Ø), small to medium scale trough cross-beds (twenty to fifty centimeters thick) that grade upward into rippled and parallel bedded sands (Figure 48). Climbing ripples are well developed (Figure 49) and interbedded with lenses of small trough cross-laminations. Large plant stems twenty to thirty centimeters in length commonly mark bedding planes (Figure 50). Erosional truncation is common and is marked by a clay chip lag (Figure 51). This sequence of sedimentary structures gradationally fines upward into wavy bedded coarse silts and clays containing abundant siderite nodules. Coleman (1975) and Arndorfer (1973) reported similar sequences of sedimentary structures from crevasse splays in the Mississippi River delta.

Laterally adjacent to the crevasse splay deposit is a sequence of oxidized, rooted, fine silts and clays of the subaerial levee.

FIGURE 46. Model for deposition of crevasse splay system at HA-9. Located in Panel I. The coal is the Upper Elkhorn No. 1. The Allen Sandstone corresponds to the fluvial system depicted in the upper left hand corner. (After Baganz, et.al., 1975)

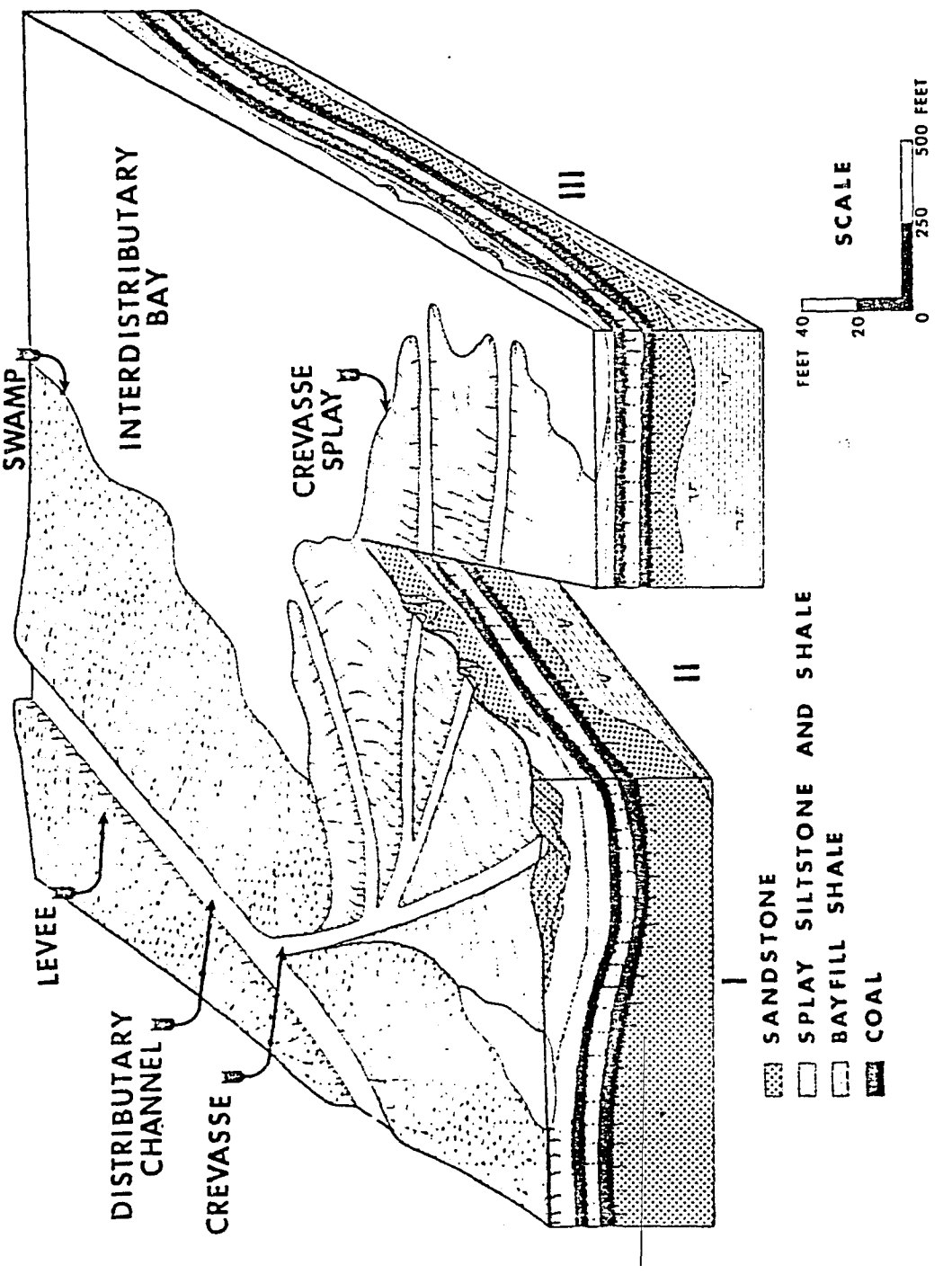

FIGURE 47. Vertical profile through the crevasse splay and subaerial levee in the Allen Sandstone at HA-9. An oxidized zone in the overbank deposits at HA-27 is also included for comparison. Sample HA-27-15 is from the underclay, sample HA-27-14 and 13 are from the B-horizon, sample HA-27-12 is from the C-horizon and sample HA-27-11 is from a clay drape on a rippled unit in the fluvial sandstone. Sample HA-9-8 is from the A-horizon, sample HA-9-7 is from the B-horizon and sample HA-9-6 is from the upper C-horizon.

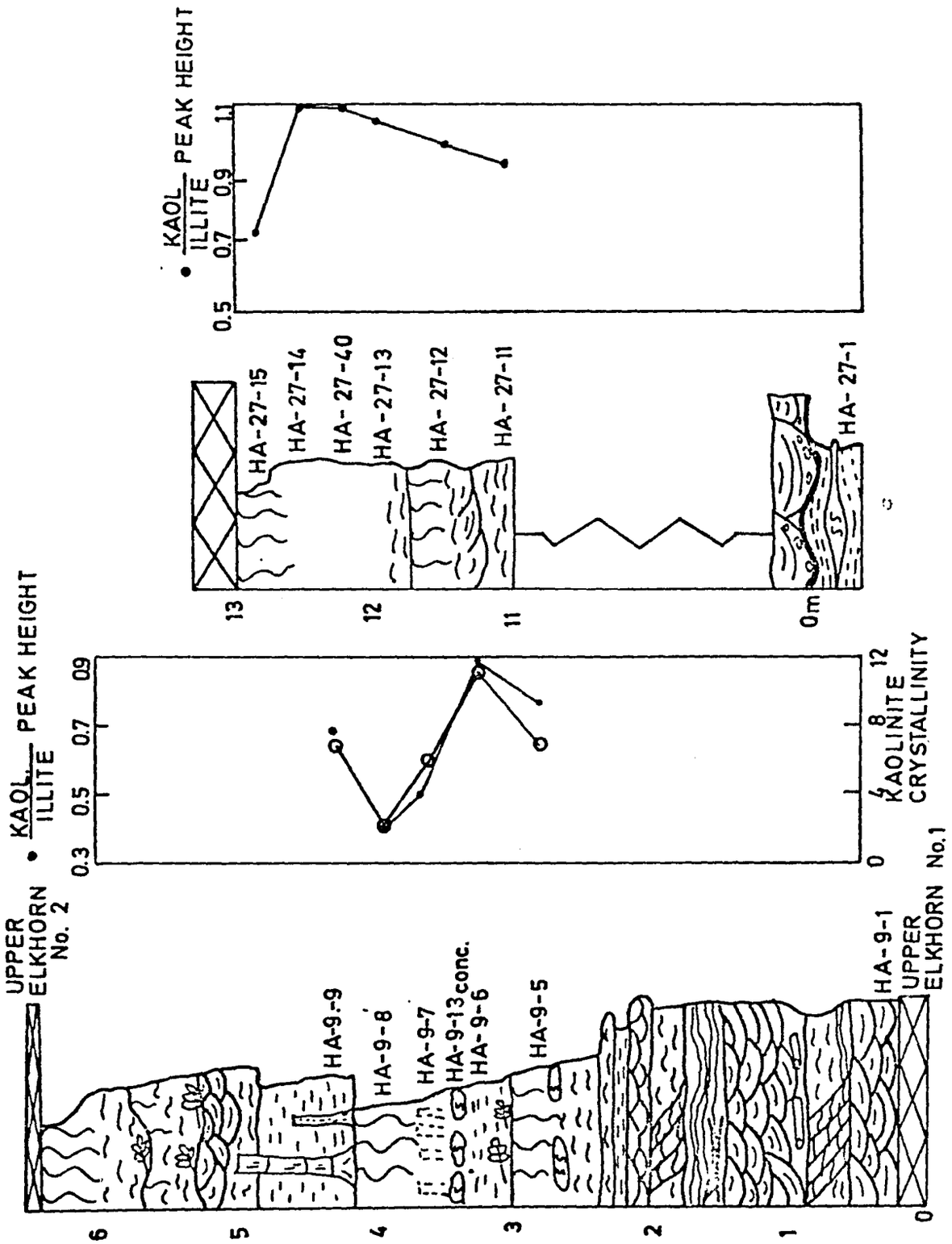

FIGURE 48. Photograph of parallel to wavy bedding in the crevasse splay at HA-9.

FIGURE 49. Photograph of climbing ripples in the crevasse splay deposit at HA-9. Ripples migrated from right to left. Ripple surfaces are marked by accumulation of siderite grains and macerated plant material.

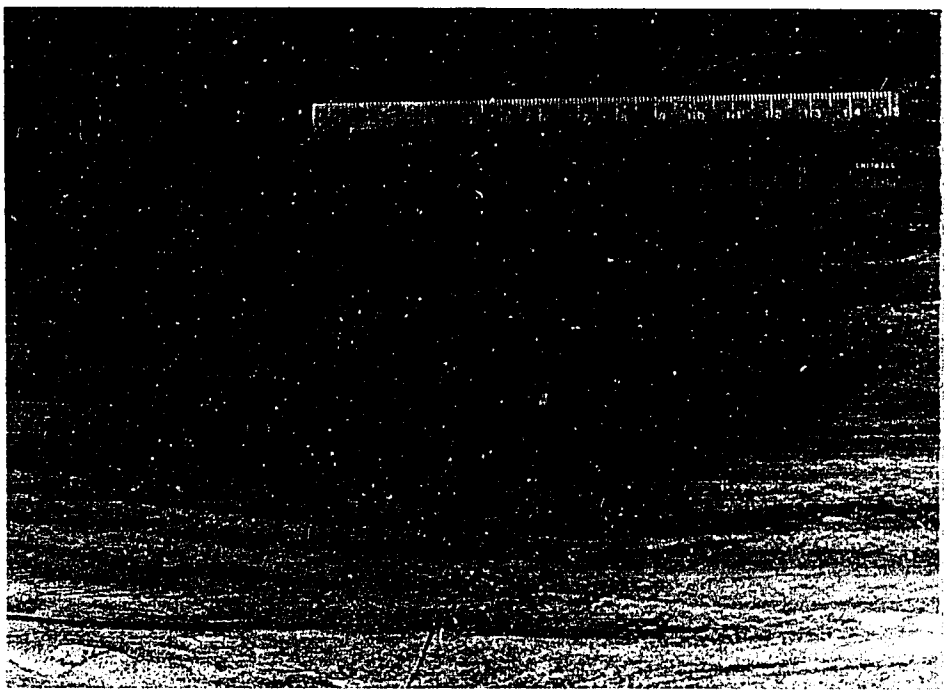

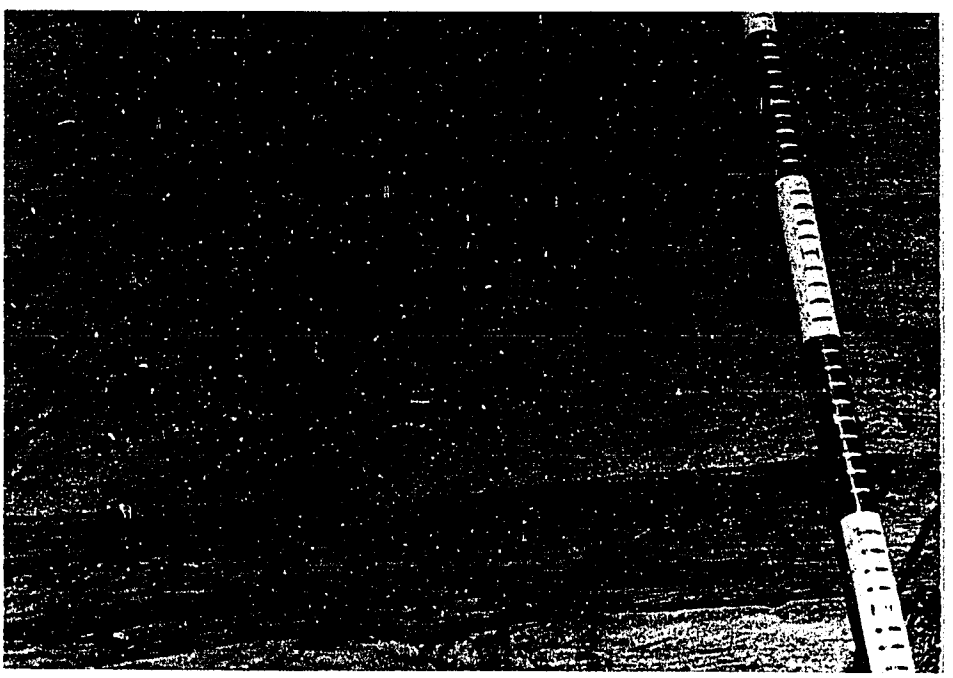

FIGURE 50. Photograph of large oriented plant stems on bedding planes in the crevasse splay deposit at HA-9.

FIGURE 51. Photograph of well developed clay chip conglomerate along erosional surfaces in the crevasse splay at HA-9. Clay chips are elongate and angular and were probably deposited close to the site of erosion. Currents flowed towards observer.

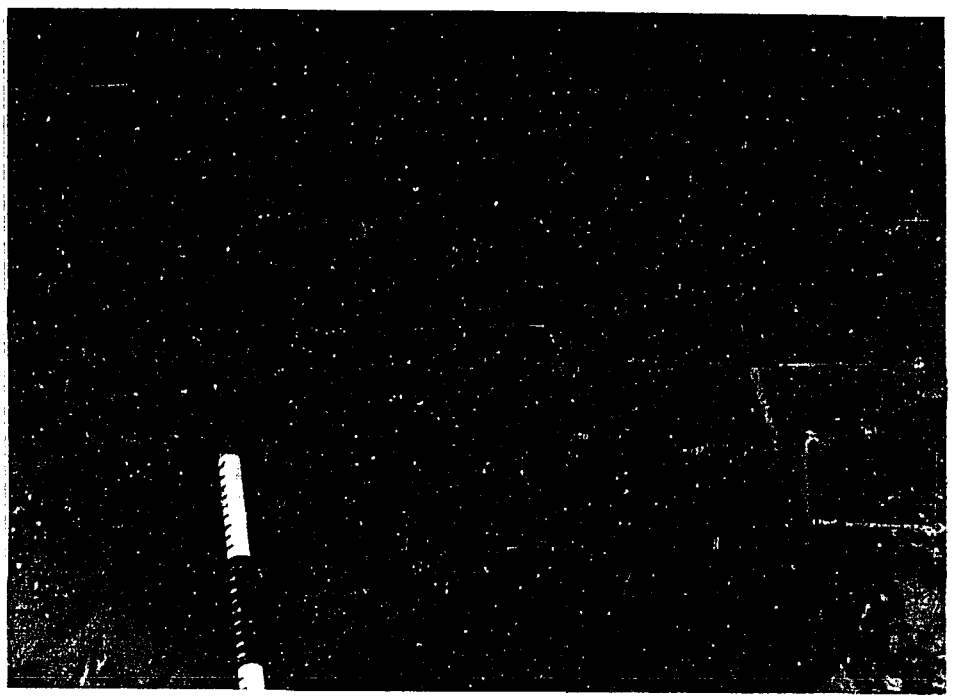

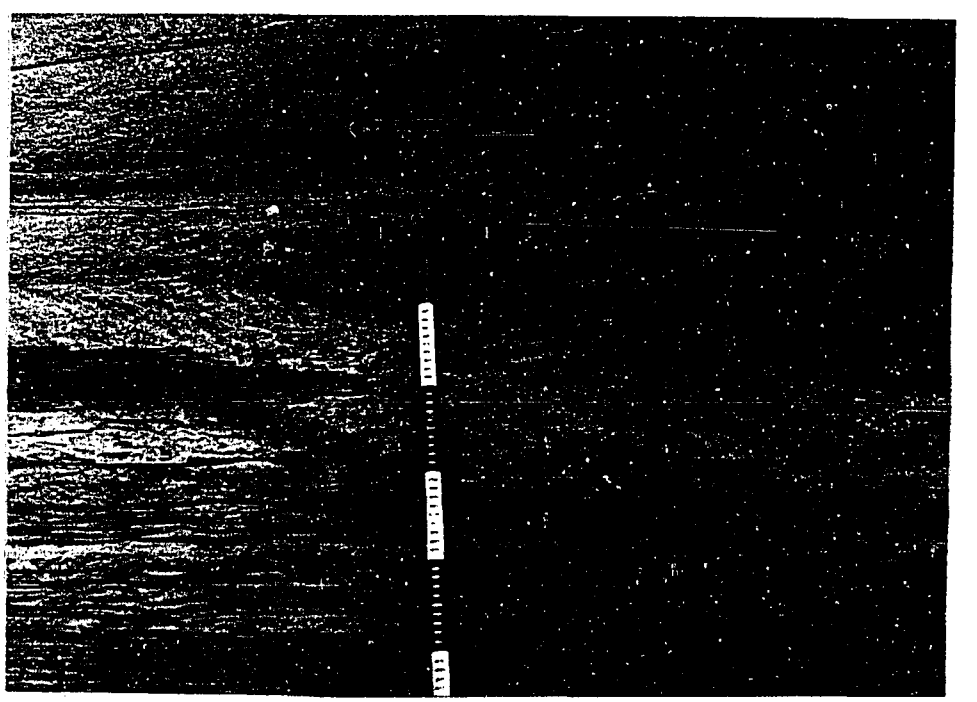

Figure 52 is a detailed profile through the oxidized zone of the subaerial levee. A, B and C-horizons typical of soil development (Hunt, 1972) are poorly developed but nevertheless present. In situ Lepidodendron and Calamites fossils are preserved above an oxidized, reddish-buff colored, clayey A-horizon, thirty centimeters thick (Figure 53). Below this is a forty centimeter thick, buff to gray, oxidized zone, exhibiting crude, blocky to prismatic structures typical of argillic B-horizons from warm to temperate climates. Clay films commonly coat grains and ped surfaces. These types of structures are generally attributed to migration into and neoformation of clays in the B-horizon (Birkeland p. 5, 1974). Profiles showing the vertical distribution of the relative abundance of kaolinite to illite (Figure 52) indicate that the B-horizon and upper part of the C-horizon are zones of relative kaolinite enrichment. Immediately below this zone, at the base of root penetration, is a well developed, horizontal zone of siderite nodules. Coleman (1975) notes similar occurrences of iron carbonates in levees of the Mississippi River delta. These nodules are composed of well developed spherulitic concretions. These spherulites have been observed in Carboniferous soils from England (Deans, 1934; Hallam, 1967; and Curtis, et.al., 1975) but have not been reported from Carboniferous soils in the United States.

Immediately below the siderite concretions is a zone of unoxidized, green to gray, horizontally bedded, fine silts and clays; the C-horizon. Abundant organic material, oxidized in the A and B-horizons, is preserved on bedding planes.

FIGURE 52. Detailed vertical profile through the soil zone in the crevasse splay at HA-9. See figure 47 for general location.

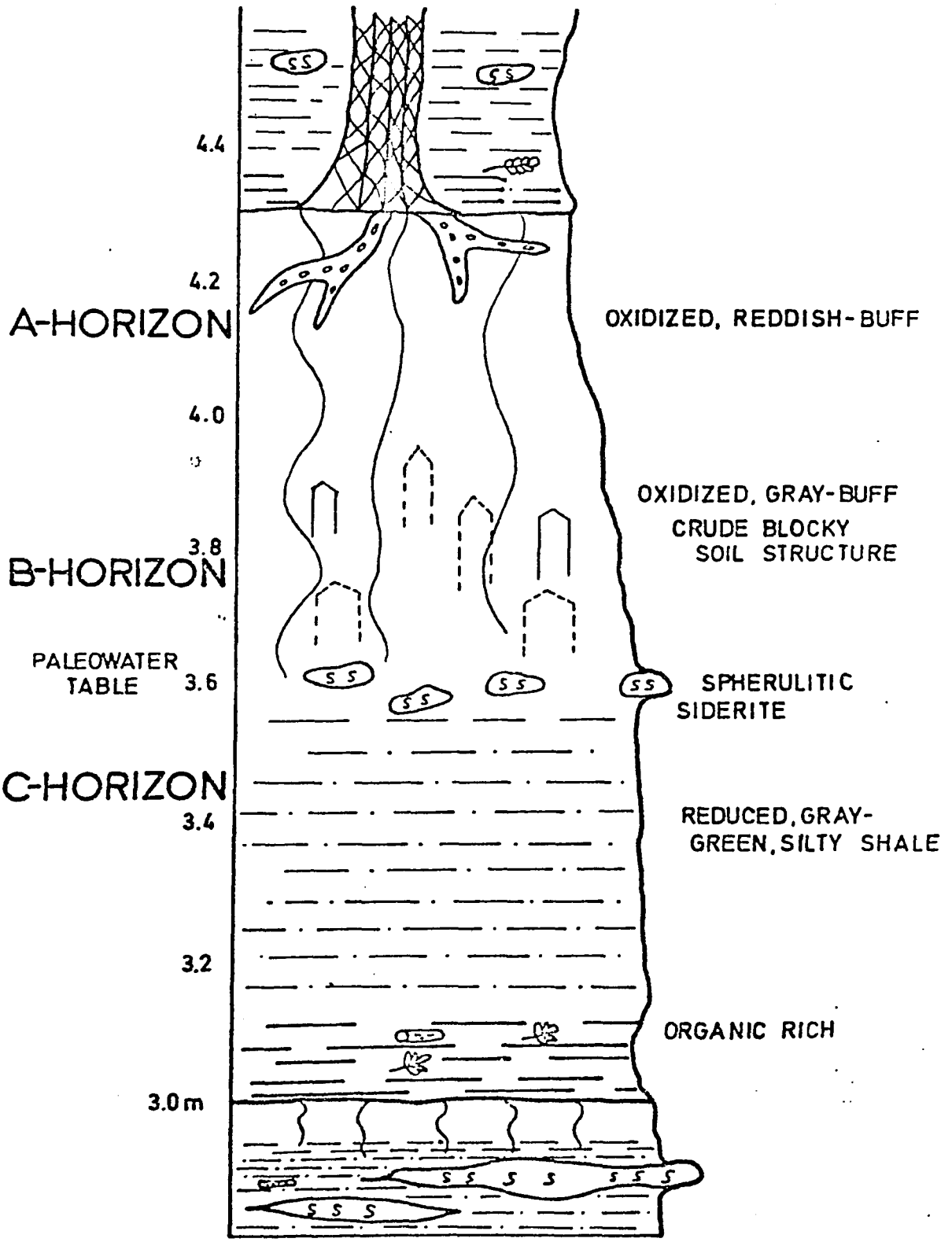

FIGURE 53. Photograph of *in situ* *Lepidodendron* located at top of A-horizon. A-horizon is recessed behind the meter stick. The B-horizon occurs at the base of the meter stick and the C-horizon occurs just above the base of the photograph.

FIGURE 54. Photograph of nesting traces of pelycopods *Lockeia* on the undersides of sheet sandstones from restricted marine zones.

Marine Zones: Marine zones were not studied in detail in this report but several samples were collected from documented marine environments (Jillson, 1919 and Baganz, et.al., 1975) for use in comparison with other depositional environments. Restricted marine zones commonly display current rippled, fine grained, sheet sandstones with abundant nesting traces of a single type of pelycopod, Lockeia (Figure 54). Tidal channels, seven meters thick, occasionally cut through these restricted marine sheet sands (Figure 55). They were examined in some detail for comparison with fluvial channels. Poor development of point bars indicates some channel migration. Sandstones from these point bars are composed of rippled, extensively bioturbated (Figure 56), medium grained (1.8ø) sand. Inclined point bar surfaces commonly exhibit wavy bands of burrowed siderite up to three centimeters thick.

Additional Criteria

In this section the previous environmental assignments are tested using several different techniques. Log-probability plots of grain size distributions and the derived textural parameters, petrography and clay mineralogy will be discussed.

Log-probability curves of grain size distributions displaying straight line segments have been used to describe depositional processes during sedimentation. Visher (1969), Sagoe and Visher (1977) and Glaister and Nelson (1974) successfully used this technique to separate deposits from various depositional environments. Representative log-probability plots from the depositional environments sampled in this study are shown in figure 57. Samples from any particular

FIGURE 55. Photograph of tidal channel. Point bar sands are developed on east side of channel about one inch above car. Restricted marine sheet sandstones are well developed to the right. On the left a bioturbated silty shale fills the channel. The Blairtown Sandstone is visible as the white band that extends across the middle of the photograph.

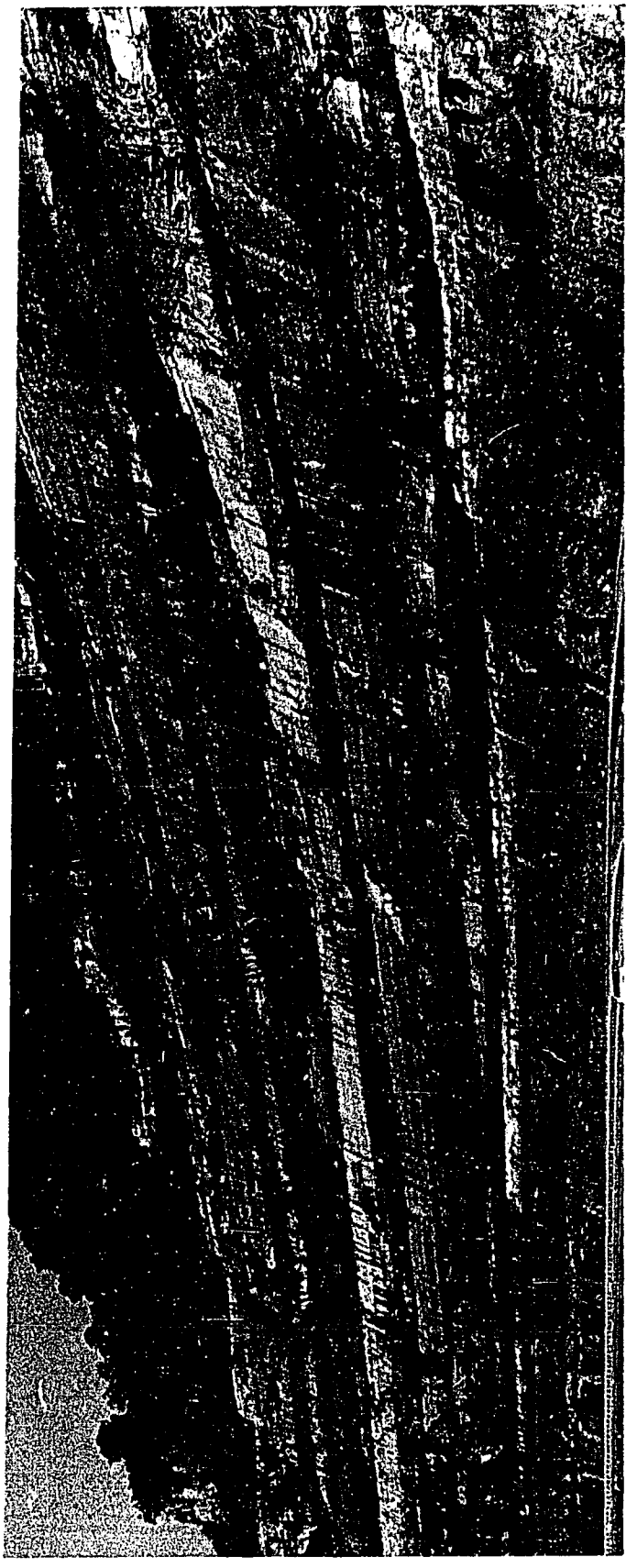

FIGURE 56. Photograph of bioturbation on point bar surfaces of tidal channels.

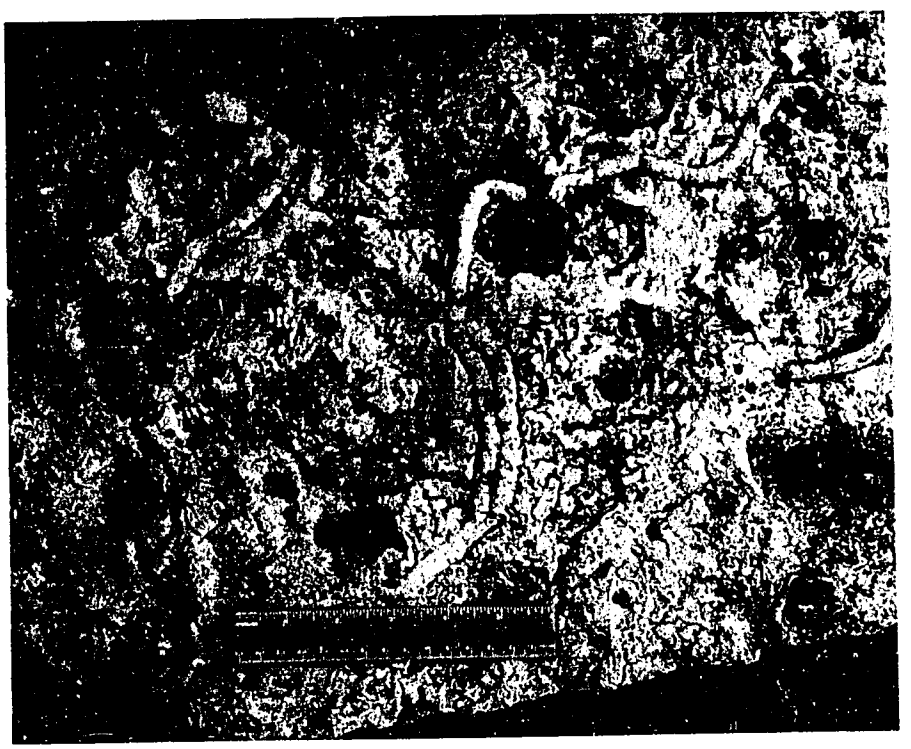

FIGURE 57. Representative log-probability plots of grain size distribution curves of samples from different environments.

A. 1) microtrough laminations from top of bay fill
   2) rippled to wavy beds from middle of bay fill
   3) wavy to horizontal beds from base of bay fill

B. 1) marine sheet sandstone
   2) point bar in tidal channel

C. 1, 2) large trough cross-beds from base of fluvial deposit
   3) small to medium trough cross-beds from middle of fluvial deposit
   4) rippled beds from upper part of fluvial deposit

D. 1) small troughs from base of channel mouth bar
   2, 3) ripples from middle of typical vertical section
   4) wavy beds from upper part of channel mouth bar

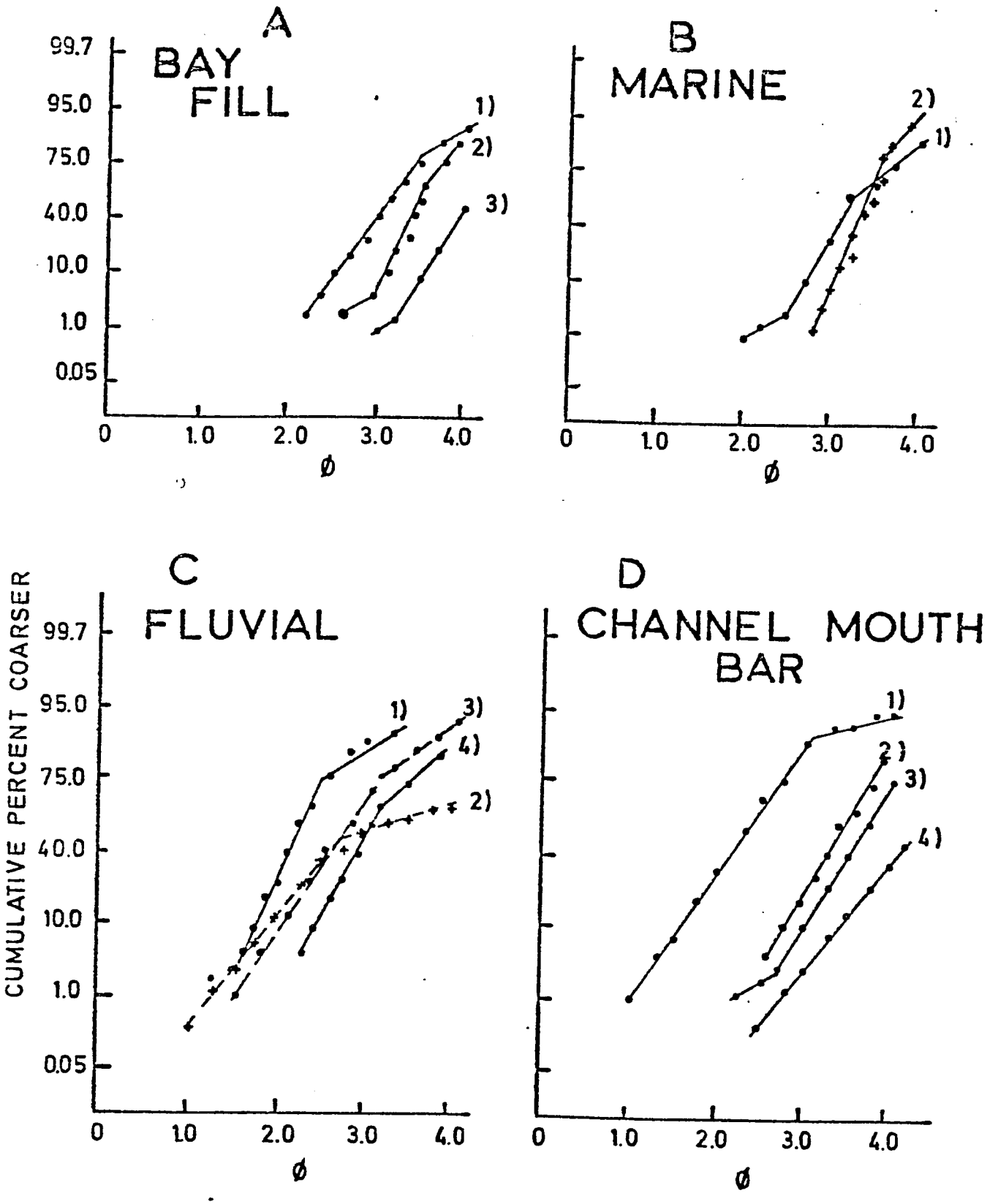

environment do not display uniquely shaped log-probability plots. There is a tendency for fluvial samples to display three straight line segments and channel mouth bars only two segments, but this is not consistent.

For more than thirty years workers have attempted to identify sedimentary environments on the basis of textural parameters, namely, mean or median, standard deviation, skewness and kurtosis. Recent papers by Folk and Ward (1957), Mason and Folk (1958), Friedman (1961) and Shepard and Yound (1961) suggest that the above statistical grain size parameters may be sensitive indicators of depositional environments. In particular, cross-plotting was advocated because it was thought to set up fields that were diagnostic of depositional environments (Passega, 1964; Moila and Weiser, 1968). Glaister and Nelson (1974) and Amaral and Pryor (1977) concluded, however, that textural parameter plots were not sensitive enough to discriminate among depositional environments.

Textural parameters from various fluvio-deltaic environments studied in this report are summarized in table IV. Cross-plots of standard deviation and skewness versus median grain size are shown in figures 58 and 59 respectively. Separation of fluvial from nonfluvial samples is achieved in the plot of standard deviation versus median size, with nonfluvial samples tending to have a lower standard deviation for a given median size, that is, better sorting. The plot of skewness versus median size does not show the separation of fluvial from nonfluvial samples. There is a slight tendency for fluvial samples to have higher skewness values, indicating more fine material, that is, more matrix.

TABLE IV

GRAIN SIZE TEXTURAL PARAMETERS DERIVED FROM LOG PROBABILITY CURVES ARRANGED TO COINCIDE WITH VERTICAL PROFILES

Sample No.	Vertical Profile Position[1]	Maximum Diameter (ø)	Median (ø)	Standard Deviation	Skewness	T-Junction[2] (ø)
Fluvial Point Bar Surfaces						
Harold Sandstone						
BB-2-38	0.1	1.50	2.93	0.62	0.171	
BB-2-36	0.5	1.25	2.97	0.67	0.130	1.8_R
BB-2-25	2.4	1.25	2.83	0.67	0.144	1.7_R
BB-2-24	3.4	1.25	3.27	0.64	0.142	2.0_R, 2.4_T
BB-2-20	5.8	1.00	2.94	0.76	0.142	1.6_R
BB-2-15	6.7	1.10	2.45	0.65	0.151	1.3_R
BB-2-8	6.0	1.10	2.56	0.72	0.163	1.1_R
BB-2-3	7.0	1.75	3.37	0.67	0.149	
BB-2-2	9.0	2.00	3.21			
HA-1-45	0.3	1.00	2.66	0.56	0.135	1.6_R, 2.0_T
HA-1-46	0.4	1.50	2.85	0.64	0.164	
HA-1-52	4.2	1.05	2.68	0.61	0.145	
HA-1-87	5.0	1.05	2.70	0.61	0.153	1.8_R, 2.1_T
HA-1-15	5.2	1.10	2.77	0.60	0.137	2.0_T
HA-1-60	5.7	1.60	3.27	0.64	0.128	
HA-1-66	5.9	1.60	3.19	0.77	0.109	
HA-1-93	6.7	1.80	3.19	0.62	0.139	
HA-1-70	7.3	1.70	3.31	0.72	0.125	
HA-1-69	7.5	1.75	3.41	0.71	0.097	
Fluvial Vertical Profiles						
Harold Sandstone						
BB-2-4	0.1	1.25	2.57	0.62	0.147	
BB-2-5	0.7	1.50	3.03	0.81	0.177	
BB-2-5a	2.2	1.50	2.98	0.67	0.175	
BB-2-6	3.8	1.25	2.70	0.62	0.176	1.6_R, 2.0_T
BB-2-7	5.5	1.25	3.19			
BB-2-8	6.0	1.00	2.56	0.72	0.163	1.2_T
BB-2-10	10.8	1.75	2.78			

Sample No.	Vertical Profile Position[1]	Maximum Diameter (ø)	Median (ø)	Standard Deviation	Skewness	T-Junction[2] (ø)
HA-1-10	0.1	0.75	2.21	0.53	0.116	1.0_R, 1.6_T
HA-1-11	1.3	1.00	2.41	0.57	0.136	
HA-1-12	3.0	1.50	2.95	0.65	0.098	
HA-1-13	3.0	1.50	2.53	0.68	0.142	
HA-1-14	4.2	1.60	3.31			1.9_R
HA-1-15	5.0	1.30	2.70	0.61	0.137	2.0_T
HA-1-98	6.7	1.84	3.08	0.83	0.170	
HA-1-69	7.6	1.80	3.41		0.100	
Allen Sandstone						
HA-23-14	0.9	0.80	2.20	0.62	0.127	
HA-23-25	2.7	1.10	2.33	0.53	0.140	
HA-23-23	4.8	1.75	3.30	0.46	0.104	2.8_T
HA-23-21	5.9	1.00	2.54	0.56	0.192	1.6_R, 2.0_T
HA-23-24	6.4	2.00	3.61	0.54	0.105	
HA-23-20	7.0	2.00	3.23	0.64	0.120	
HA-23-19	8.6	2.00	3.14	0.62	0.176	
HA-23-18	9.9	2.25	3.82			2.3_R, 2.7_T
HA-29-20	2.3	0.85	2.57	0.56	0.090	
HA-29-25	4.3	2.30	3.55			
HA-29-2	5.5	0.70	2.49	0.73	0.166	
HA-29-4	6.3	0.25	1.90	0.66	0.181	0.8_R, 1.2_T
HA-29-7	8.5	2.25	3.79			
HA-29-9	9.5	2.75	4.10			
LA-3-11	0.1	0.30	1.86	0.58	0.186	1.1_T
LA-3-12	1.2	0.75	2.27	0.87	0.219	1.1_R
LA-3-13	3.4	0.85	2.31	0.67	0.188	
LA-3-14	4.4	1.10	2.58	0.81	0.216	
LA-3-15	6.9	1.25	3.04			
PR-7-1	0.1	0.40	1.88	0.61	0.136	
PR-7-2	2.6	0.40	1.94	0.54	0.148	0.9_R
PR-7-5	4.0	0.50	2.01	0.70	0.156	1.0_R
PR-7-3	6.5	0.75	2.45	0.72	0.142	
PR-7-4	10.4	2.30	3.63			
Individual Trough Cross-bed[3]						
HA-2-36	0.02	1.00	2.38	0.73	0.184	1.2_R
HA-2-37	0.1	1.10	2.31	0.75	0.187	
HA-2-38	0.3	1.10	2.26	0.74	0.202	
HA-2-39	0.7	1.00	2.25	0.76	0.190	1.5_T

Sample No.	Vertical Profile Position[1]	Maximum Diameter (Ø)	Median (Ø)	Standard Deviation	Skewness	T-Junction[2] (Ø)
Fluvial and Channel Mouth Bars						
Allen Sandstone						
HA-2-21	0.1	0.90	2.44	0.57	0.105	
HA-2-23	2.5	1.65	3.40	0.56	0.095	
HA-2-24	3.5	2.10	3.43	0.60	0.131	
HA-2-25	4.9	2.00	3.24	0.58	0.127	
HA-2-26	5.3	1.10	2.76	0.73	0.114	
HA-2-28	9.2	1.20	3.24	0.83	0.105	
HA-2-30	11.0	1.50	2.95	0.78		
HA-27-24	0.3	1.15	2.60	0.48	0.121	
HA-27-23	2.1	0.50	1.84	0.48	0.148	
HA-27-28	2.7	0.65	2.53	0.65	0.126	1.0_R, 1.5_T
HA-27-34	5.3	1.00	2.45	0.55	0.123	1.3_R
HA-27-46	8.8	1.00	2.50	0.64	0.194	
HA-27-16	11.2	2.25	3.59	0.55	0.081	
HA-27-46	11.3	1.00	2.50	0.76	0.138	
HA-27-37	12.2	1.75	3.10			
Blairtown Sandstone						
BB-3-27	0.8	2.30	3.73			2.8_R
BB-3-8	1.4	1.60	3.18	0.64	0.163	
BB-3-30	3.0	0.75	2.22	0.62	0.119	
BB-3-9	5.6	0.80	2.45	0.99	0.158	
BB-3-10	10.4	2.30	4.02			2.5_R
Crevasse Splay						
Allen Sandstone						
HA-9-1	0.3	1.60	3.34	0.67	0.181	2.3_R
Channel Mouth Bars Vertical Profile						
Allen Sandstone						
IA-9-1	0.1	0.85	2.24	0.50	0.153	
IA-9-2	1.8	1.50	3.11			1.8_R
IA-9-3	4.0	2.50	3.76			
IA-9-3a	4.5	2.75	4.08			
IA-9-4	7.0	2.40	4.07			
IA-9-5	2.0	2.25	3.93			3.9_R, 2.7_T

Sample No.	Vertical Profile Position[1]	Maximum Diameter (ø)	Median (ø)	Standard Deviation	Skewness	T-Junction[2] (ø)
Channel Mouth Bar Lateral Profile						
Blairtown Sandstone						
BB-3-8	80	1.60	3.18	0.64	0.163	
BB-3-27	73	2.30	3.73			2.8_R
BB-3-28	60	2.30	3.82			
BB-3-29	35	2.40	3.76			2.7_R
BB-3-34	180	2.60	4.02			
Bay Fill Vertical Profile						
BB-3-4	0.1	3.25	5.10			
BB-3-37	1.5	3.10	4.50			
BB-3-7	4.2	2.20	3.52			
BB-3-20	7.5	1.75	3.35		0.110	
BB-3-17	8.0	1.70	3.16		0.122	
BB-3-18	9.8	3.10	4.00			
Bay Fill Lateral Profile						
BB-3-1	560	3.00	4.10			
BB-3-2	450	2.85	4.00			
BB-3-39	400	2.10	4.15		0.128	2.7_R, 3.0_T
BB-3-6	340	2.15	4.00			2.7_R
BB-3-7	250	2.05	3.50			
BB-3-31	150	1.80	3.30			
BB-3-8	80	1.60	3.20	0.64	0.163	
Marine Sheet Sandstone						
BB-3-A		2.00	3.37	0.46	0.203	2.5_R, 2.9_T
BB-3-B		2.00	3.40	0.33	0.078	
Marine Tidal Channel						
BB-3-M		1.80	3.31		0.085	
Composite Fluvial Samples						
1	0 - 2		2.23	0.65	0.117	
2	2 - 4		2.73	0.65	0.163	
3	4 - 6		2.90	0.79	0.142	
4	6 - 8		3.20	0.68	0.172	
5	8 - 10		3.70			

[1] All samples are located on vertical and lateral profiles. Position is in meters above base of vertical profile except lateral profiles where distances are in meters west of arbitrary data.

[2] For explanation of T-Junction see Appendix II and Figure 66.

[3] Distance is in meters above base of trough from base of fluvial channel at HA-2.

FIGURE 58. Plot of standard deviation versus median grain size for samples from all environments. Fluvial samples tend to be better sorted.

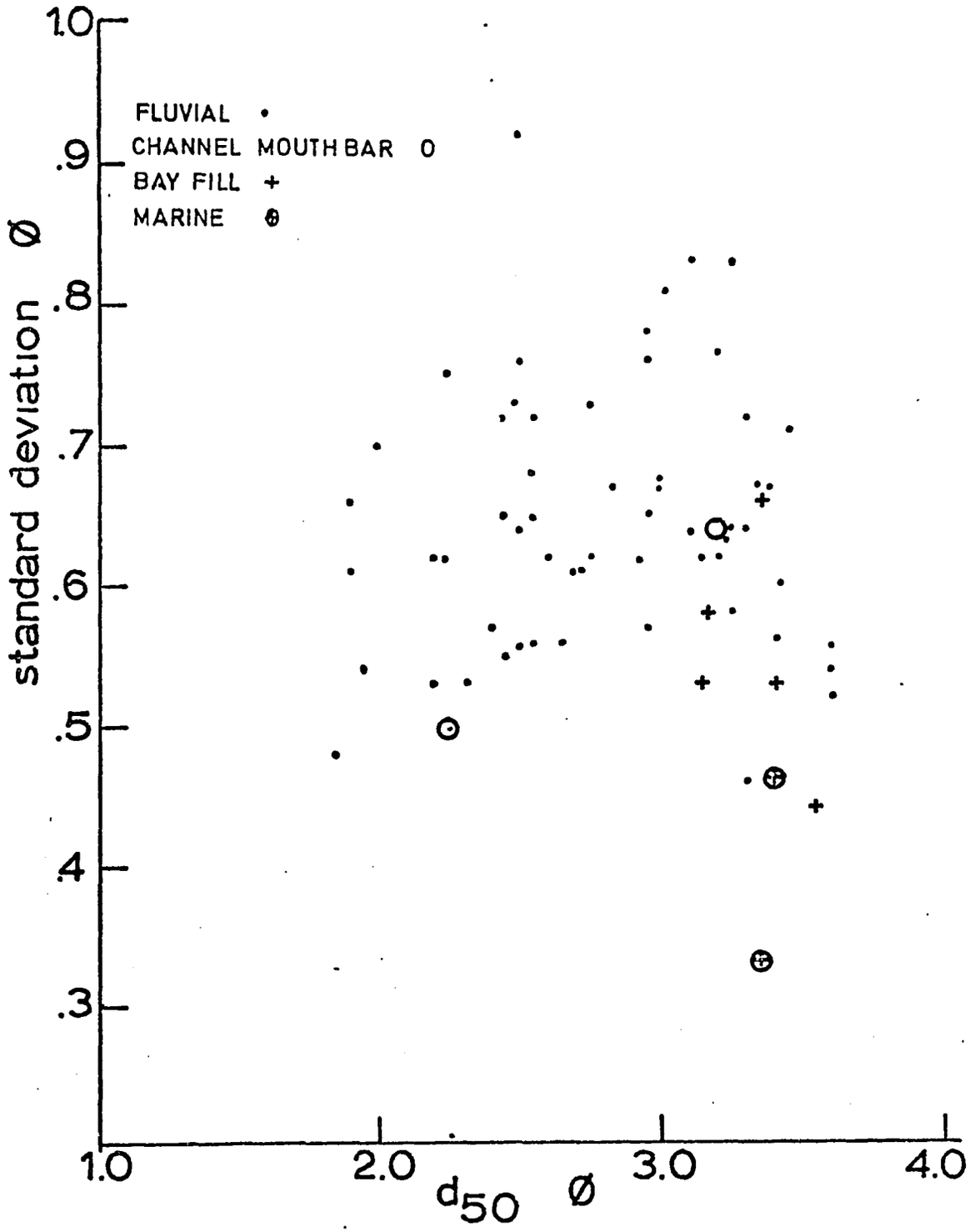

FIGURE 59. Plot of skewness versus median grain size for sample from all environments. Separation of environments is poor but fluvial samples tend to be more positively skewed than nonfluvial samples.

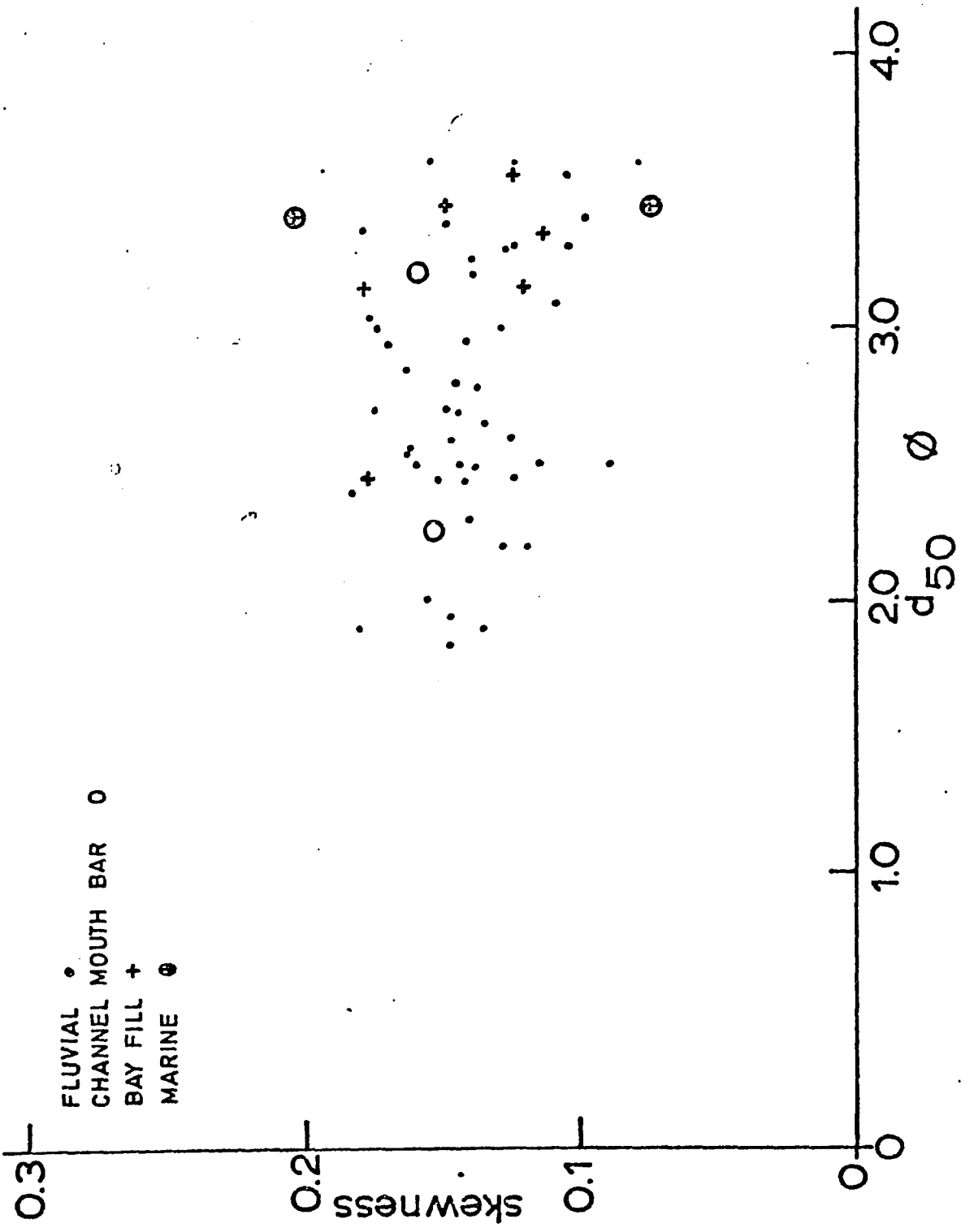

Petrology has been used successfully to discriminate among depositional environments by Davies, et.al., (1975). Petrographic analysis of samples, summarized in table V, by depositional environment, indicates that fluvial samples can be classified (Folk, 1968) as feldspathic litharenites and nonfluvial samples as sublitharenites. Nonfluvial samples tend to have a higher ratio of quartz to feldspar plus rock fragments. Using Pettijohn's (1957) terminology that includes matrix, fluvial samples are protoquartzites near the channel bottom but grade upward into subgraywackes or lithic graywackes where the matrix exceeds ten to fifteen percent of the total sample. Nonfluvial samples tend to plot as protoquartzites, reflecting a lower matrix content than fluvial samples with the same median grain size. In general, these sandstones fit the description of a first cycle, immature sandstone. The petrology and diagenesis is described in detail in Appendix IV.

In an attempt to discriminate among depositional environments, petrographic data was subjected to cluster analysis. This technique has been used successfully by BeMent (1976) and Short (1977) for sandstones of Carboniferous age in eastern Kentucky. Cluster analysis shows the interrelationships of samples in a similarity coefficient matrix of variables. These relationships may be represented by dendritic networks or dendograms, tree-like hierarchial charts where samples with the highest similarity are linked first.

Variables used in this cluster analysis were total quartz, total rock fragments, total feldspar and total mica. Since composition is a function of grain size (Ferm, 1962; Davies, et.al., 1975),

TABLE V

PETROLOGY OF HAROLD AND ALLEN SANDSTONES
ARRANGED BY DEPOSITIONAL ENVIRONMENT*
(Values in Percent)

Sample No.	Quartz[1]	Feldspar	Mica[2]	Rock Fragments[3]	Clay Matrix[4]	Detrital Dolomite	Authigenic Siderite[5]	Authigenic Iron Dolomite	Authigenic Kaolinite
Fluvial									
Harold Sandstone									
BB-2-4	50.0	10.0	6.0	9.7	6.0			12.3	6.0
BB-2-5	52.0	9.0	4.0	24.0	8.0		1.0		1.0
BB-2-5a	54.0	8.0	9.5	21.0	6.0				2.0
BB-2-6	54.0	9.0	5.0	21.0	8.0				3.0
BB-2-7	54.5	8.0	7.0	21.5	4.0		3.5		
BB-2-8	53.0	12.0	8.5	17.0	11.0		3.5		
BB-2-10	59.0	4.5	3.0	12.5	17.0		1.0		3.5
BB-2-38	63.5	7.5	4.5	15.5	9.0				7.0
BB-2-36	56.5	5.5	5.5	16.0	10.5		3.0		3.0
BB-2-25	60.5	7.0	7.0	10.5	6.0		4.5		4.5
BB-2-24	58.0	5.0	6.5	17.5	10.0		0.5		2.5
BB-2-20	54.0	7.5	6.0	22.0	9.5		1.0		3.0
BB-2-15	68.5	6.5	3.0	15.5	5.0				2.5
BB-2-3	53.0	5.0	10.5	14.5	17.0				
BB-2-2	59.0	7.0	6.0	15.5	10.5				
HA-1-41	62.0	6.0	6.0	12.0	5.5		3.5		4.0
HA-1-45	58.5	4.0	3.5	16.0	4.5	0.5	1.0	9.0	4.0
HA-1-52	63.5	8.0	4.0	14.0	5.0		1.0	3.0	6.5
HA-1-87	63.5	7.0	4.0	12.0	6.5		1.0	1.0	8.0
HA-1-15	56.0	4.5	7.0	11.5	7.0		3.0		10.5
HA-1-60	62.5	8.5	6.5	13.0	9.5		2.5		3.5
HA-1-66	65.5	7.0	6.0	11.5	9.5		1.0		9.5
HA-1-93	65.0	5.0	7.5	8.0	10.0		1.5		4.0
HA-1-70	56.0	8.5	6.5	14.5	10.5		1.0		2.0

Sample No.	Quartz[1]	Feldspar	Mica[2]	Rock Fragments[3]	Clay Matrix[4]	Detrital Dolomite	Authigenic Siderite[5]	Authigenic Iron Dolomite	Authigenic Kaolinite
Fluvial									
Allen Sandstone									
HA-23-14	51.0	8.5	5.0	11.0	3.5		1.5	23.0	1.5
HA-23-25	60.5	10.0	4.5	8.0	3.5		2.5		7.5
HA-23-2	34.5	8.5	10.5	14.0	1.0			31.5[6]	
HA-23-24	56.5	8.0	7.0	15.0	9.5		1.0	0.5	2.5
HA-23-20	67.0	8.5	7.0	8.5	5.5		1.5		2.5
HA-23-18	46.0	10.0	15.5	3.0	16.0			.8.0	2.0
HA-27-23	62.0	12.5	3.0	21.0	1.0				1.0
HA-27-28	55.0	10.0	5.0	12.0	4.5	1.0	0.5	3.5	8.5
HA-27-34	57.5	7.0	6.0	12.0	2.0		0.5	9.0	6.0
HA-27-46	57.0	11.5	7.0	10.0	8.5		2.5		4.5
HA-27-43	60.5	9.0	6.0	13.0	3.5	1.0	1.5	4.5	5.0
HA-27-16	53.5	9.5	14.0	7.0	11.0		1.5		3.5
PR-7-1	55.5	13.0	2.0	19.5	2.0		3.5		4.5
PR-7-3	57.0	12.0	6.5	18.0	5.0				2.0
Blairtown Sandstone									
BB-3-30	60.5	12.0	3.0	15.5	3.5	0.5		1.5	4.0
BB-3-9	63.5	5.0	7.0	14.5	4.0	1.0		2.0	5.0
BB-3-10	48.5	4.0	8.5	15.5	12.5	2.0	8.0	0.5	2.0
Channel Mouth Bar									
Allen Sandstone									
LA-9-1	63.0	12.0	4.5	16.0	1.5	0.5	3.5	8.5	1.5
LA-9-2	51.0	11.0	8.5	13.5	6.0	2.5	5.0	4.5	
LA-9-3	52.5	7.0	7.0	8.5	11.5	2.5	3.0	8.5	0.5
LA-9-3a	49.5	6.0	15.5	12.0	12.0	6.0	2.0	3.0	
LA-9-4	46.0	10.0	15.0	2.0	20.0	3.0	3.0	2.0	1.0
LA-9-5	52.5	9.5	12.0	9.5	12.0		5.0		0.5

Sample No.	Quartz[1]	Feldspar	Mica[2]	Rock Fragments[3]	Clay Matrix[4]	Detrital Dolomite	Authigenic Siderite[5]	Authigenic Iron Dolomite	Authigenic Kaolinite
Blairtown Sandstone									
BB-3-8	52.5	4.5	5.5	10.5	5.0	1.5	7.0	7.0	6.0
BB-3-27	66.0	9.0	6.5	5.5	8.5	3.0	2.0	12.5	1.0
BB-3-34	48.0	7.5	6.5	5.5	9.0	7.5	7.0	9.0	
Bay Fill									
Blairtown Sandstone									
BB-3-1	42.5	3.0	18.5	5.0	8.0	2.5	19.0	1.0	
BB-3-2	53.0	7.0	11.5	5.5	9.5	5.0	3.5	3.5	2.5
BB-3-6	45.5	6.0	5.5	14.5	9.0	3.0	5.5	9.0	2.5
BB-3-7	50.0	9.0	5.0	10.0	8.0	3.5	5.0	6.5	3.0
BB-3-20	48.5	9.5	3.5	10.5	9.0	4.5	4.0	10.5	1.5
Marine									
Blairtown Sandstone									
BB-3-B	62.0	6.0	10.0	6.0	6.0	1.0	3.0	2.5	2.5
BB-3-A	60.5	1.5	8.0	7.0	5.5	3.5	6.0	8.5	
BB-3-M	64.0	8.5	7.0	9.0	13.0	1.0	10.0	0.5	
Crevasse Splay									
Allen Sandstone									
HA-9-1	62.0	6.5	5.0	12.5	11.5				3.0
Abandoned Channel Fill									
HA-22-2	54.0	7.5	5.5	14.5	3.5	3.5	1.0	10.5	

* See vertical and lateral profiles for exact location.

1 Includes all quartx minus chert.

2 Includes muscovite, chlorite and biotite.

3 Includes igneous, metamorphic and sedimentary rock fragments plus chert, detrital coal and siderite.

4 Less than 62 microns.

5 Authigenic, euhedral rhombs less than 50 microns, often replacing chlorite and organic material.

6 X-ray peak indicates iron-rich calcite.

samples were first arbitrarily divided into two groups, one group with a median greater than 0.45ϕ and one group with a median less than 0.45ϕ.

Samples from the first group are all fluvial samples from the Allen, Harold and Blairtown Sandstone. Figure 60, a dendogram of this group, shows an unexpected, yet rather good separation of Harold Sandstone samples from the Allen and Blairtown samples. The Allen and Blairtown samples tended to have more feldspar.

All depositional environments studied in this report are represented in the second group, but no discernable clustering by environment was apparent. However, when total carbonate and authigenic kaolinite were added as two more variables, clustering into fluvial and nonfluvial environments was excellent (Figure 61). Fluvial samples tended to have more authigenic kaolinite while channel mouth bars, interchannel bays and marines sampled tended to have more total carbonate. This is apparent in several vertical profile plots of percent total carbonate and kaolinite (Figures 11, 17 and 30).

Samples from all depositional environments were analyzed for clay mineral content (Figure 62). The dominant clay minerals from all environments are illite and kaolinite with subordinate amounts of expandable layered clays and 14 Angstrom chlorite. Glycolation indicates that the expandable clays occur as a shoulder on the 10 Angstrom peak and are interlayered smectite. Marine clays tend to have more expandable layered clays than fluvial clays. Rusnak (1957), Hopkins (1958) and Potter, et.al., (1968) report similar bulk composition from Pennsylvanian age sediments in the Illinois Basin.

FIGURE 60. Dendogram of samples with median grain size greater than 0.45Ø. Variables used in the cluster analysis are total quartz, total feldspar, total rock fragments and total mica. This technique separated Harold Sandstone from Allen Sandstone with 78% accuracy. Only fluvial samples are included. "+" indicates that sample was incorrectly grouped. Data from table V.

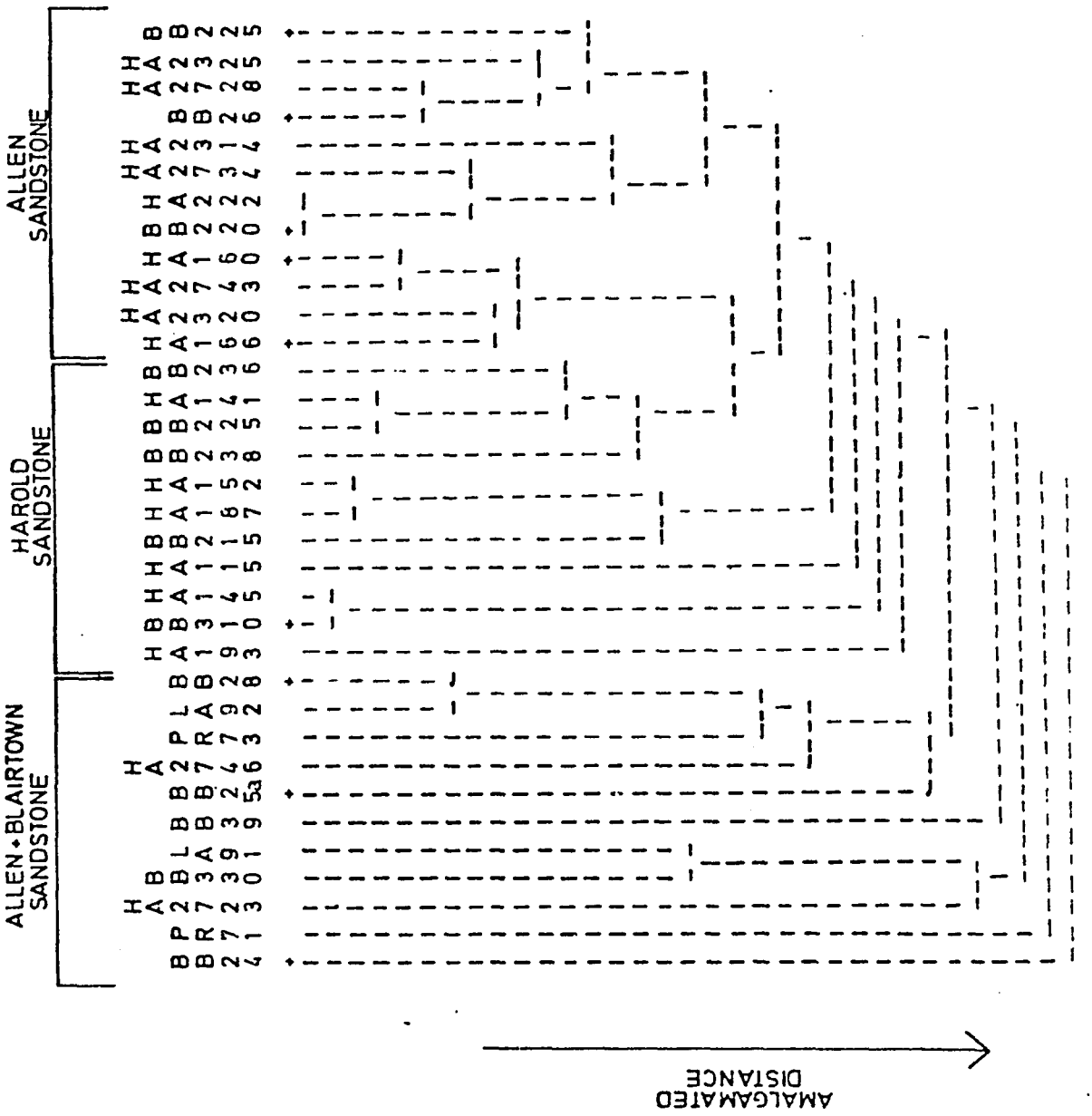

FIGURE 61. Dendogram of samples with median grain size less than 0.45Ø. Variables used in the cluster analysis are total quartz, total feldspar, total rock fragments, total mica, total carbonate and authigenic kaolinite. All depositional environments are represented. The cluster analysis was 80% successful in separating fluvial from non-fluvial samples. "+" indicates that sample was incorrectly grouped. Data from table V.

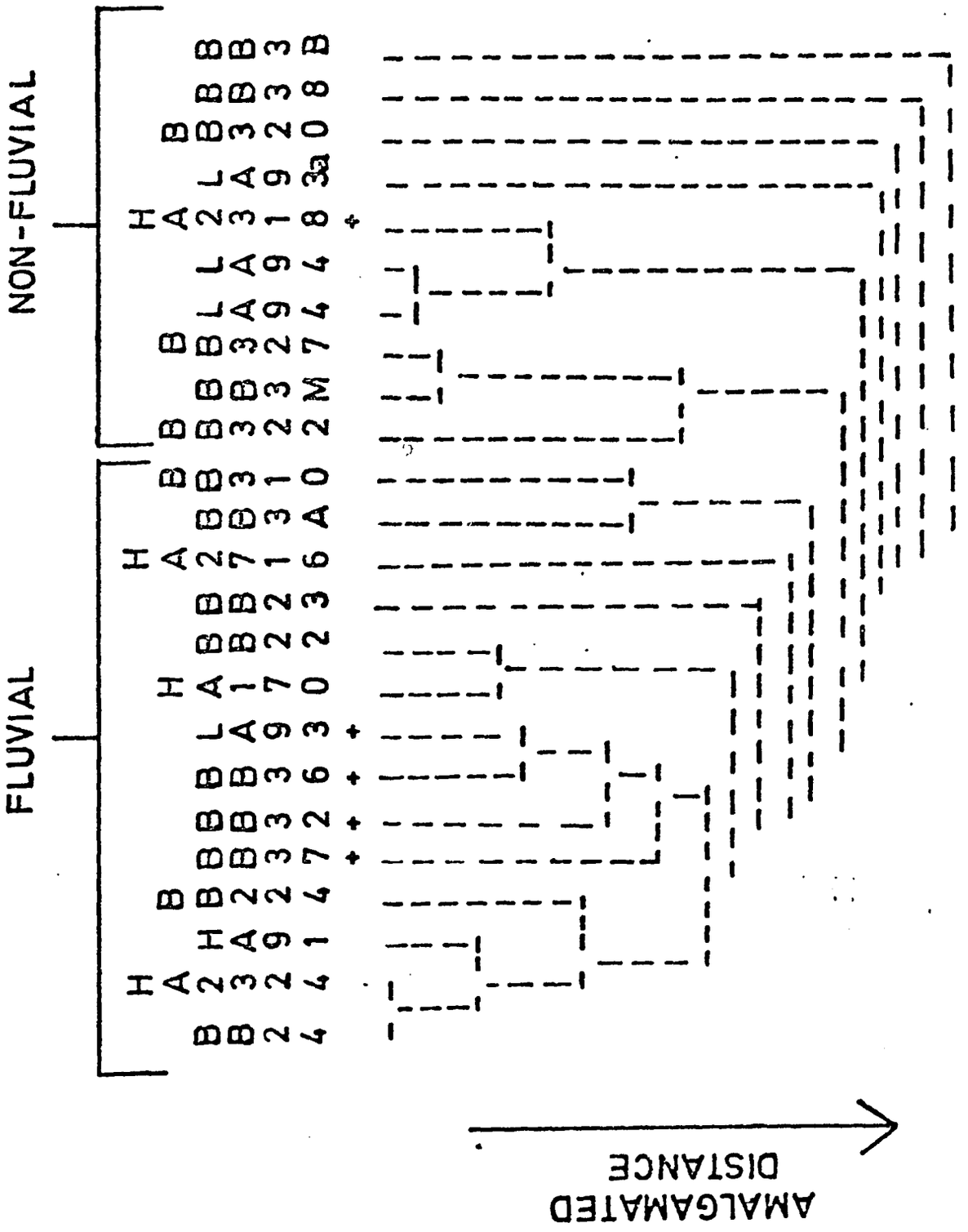

FIGURE 62. Plot of X-ray patterns. Kaolinite and illite are the dominant clay minerals with subordinate amounts of chlorite and mixed layered clays. HA-1-97 is from a clay drape and a fluvial point bar surface in the Harold Sandstone. BB-2-29 is from the clay plug in the abandoned meander in the Harold Sandstone. BB-2-31 is from the underlying bay fill sediments. BB-3-X is from the silty-shale fill in the tidal channel. HA-3-A is from the marine sheet sandstone at BB-3. Kendrick is from the Kendrick marine zone of Jillson (1931). Kendrick glycolated shows that some expandable clays are present in the marine clays. HA-2-19 was heated to 550° C to remove kaolinite.

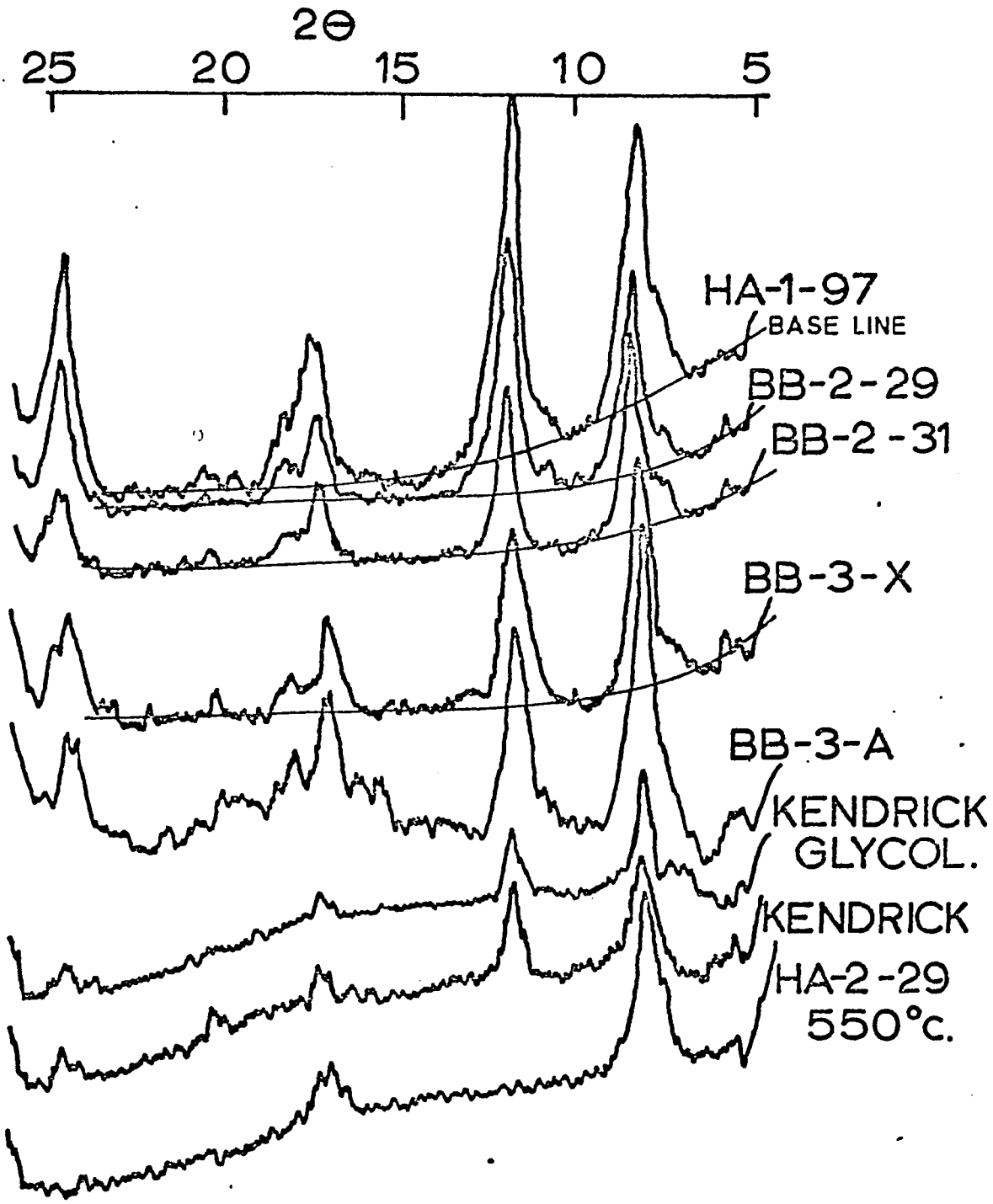

Cross-plotting of illite (001) peak and kaolinite (001) peak (see Appendix for methodology) separated fluvial from nonfluvial samples (Figure 63). Fluvial samples, mostly from clay drapes on point bar surfaces, had a kaolinite to illite ratio greater than one, whereas nonfluvial samples had ratios less than one. Samples taken from the clay plug in the abandoned meander in the Harold Sandstone plotted in the fluvial field. Whereas samples from the underlying, truncated bay fill plotted in the nonfluvial field. However, samples from the abandoned meander fill in the Allen Sandstone plotted just inside the nonfluvial field.

Summary

A number of techniques have been used in this study to determine depositional environments of sandstones, siltstones and shales from the lower and upper delta plain. Initial assignments were based on vertical and lateral straigraphic relationship, nature of bounding surfaces, internal sedimentary structures and grain size (Table VI). Additional criteria based on log-probability plots, textural parameters, clay mineralogy and petrography only served to confirm the fluvial or nonfluvial character of the initial environmental assignments. None of the additional methods were sensitive enough to discriminate precisely among depositional environments, but when used in conjunction with basic stratigraphic data, are valuable tools to aid in environmental identification.

In the analysis of paleohydrology of fluvial sandstones it is important to be able to distinguish among fluvial channels, channel mouth bars and marine tidal channels. At several localities (Figures 14, 30 and 32) the fluvial channel system has truncated channel mouth bar sandstones and differentiation of the two deposits is difficult.

FIGURE 63. Cross-plot of kaolinite (001) peak and illite (001) peak. Fluvial samples have ratios greater than 1 whereas nonfluvial samples have ratios less than 1.

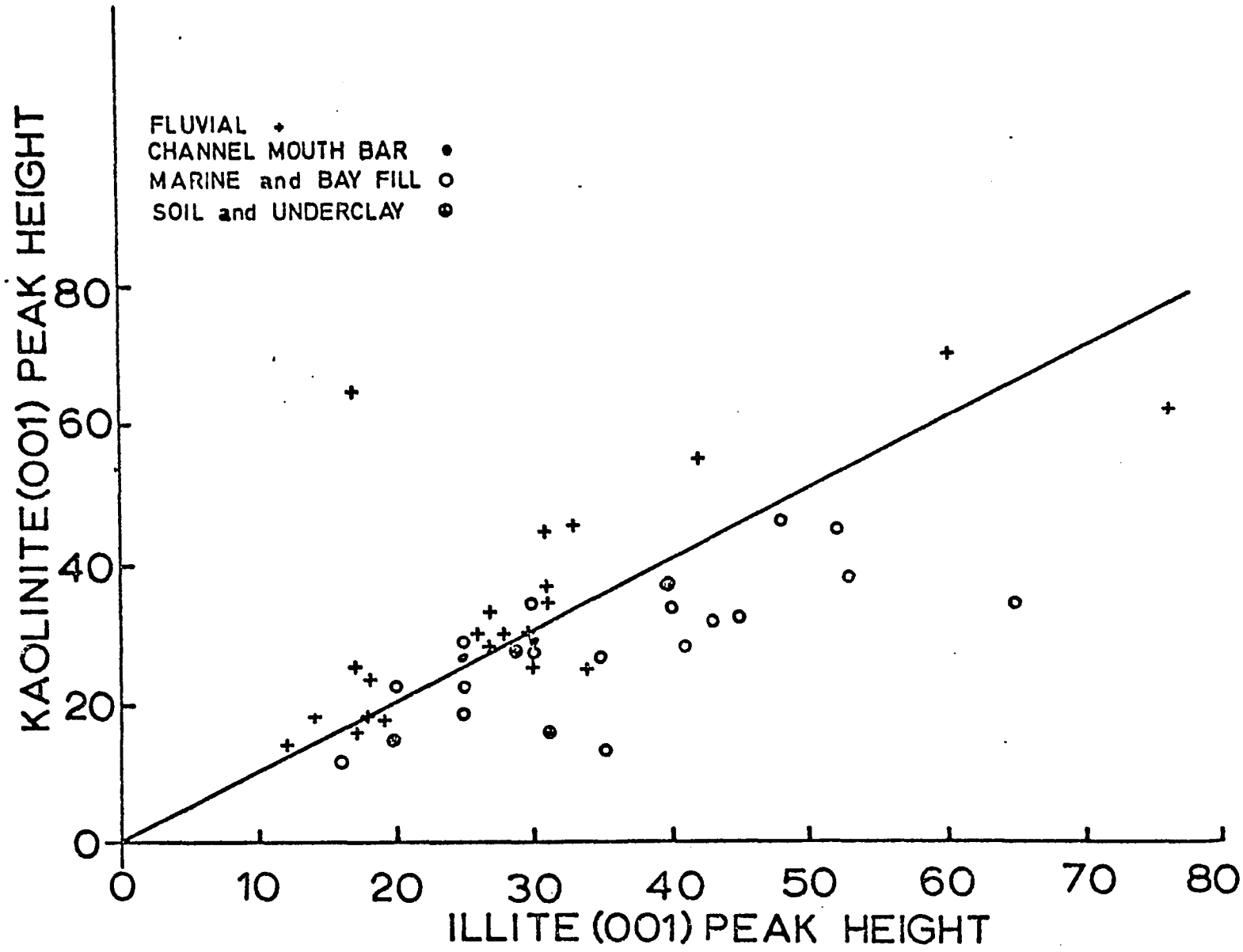

TABLE VI

OCCURENCE OF SEDIMENTARY STRUCTURES IN DEPOSITIONAL ENVIRONMENTS

Criteria	I	II	III	IV	V	VI
Trough cross-lamination						
Large, greater than 0.5 m.	A	A	D	R-A	A	A
Medium to small, 0.1 to 0.5 m.	A	R-C	C	C	A	A
Micro, less than 0.01 m.	R-C	C	R-A	C	D	C
Ripple lamination						
Current	R-C	C	R-C	A	R-C	C-D
Wave	C	C	A	A	C	A
Ripple drift	A	R-C	A-R	C	A	A
Horizontal to wavy laminations	D	R-C	A-R	R-C	A-R	A-R
Convoluted laminations	A	C	C	A-R	A	A
Microfaulting	A	R-C	C-C	A-R	A	A
Primary bedding surfaces						
Subhorizontal and and laterally continuous	D	A	A	A	R-C	A
Gently inclined (2° - 5°)	A-R	C-D	C	A	A	C-D
Moderately inclined (less than 10°)	A	A-R	D	A	A	A
Current parallel to strike of primary bedding surface		A-R	D			D
Current down dip of primary bedding surface		D	A-R			A-R
Erosional truncations	A-R	R-C	D	C	R	R-C
Lag Conglomerate	A	A-R	C	R-C	A	R-C
Plant Material						
Finely divided	D	C-D	C	C	A	C
Large stems and logs	A	A-R	C	C	A	A

Criteria	I	II	III	IV	V	VI
Fining upward cycle	A	C	D	D	A	R-C
Coarsening upward cycle	D	R-C	A	A	R-C	A-R
Oxidized zones	A	A	R-C	C	A	A
Burrows	R-C	A	A	A	R-C	D
Modules	C-D	A	A	R-C	A	A-R

I Interchannel bay
II Channel mouth bar
III Fluvial channel
IV Crevasse splay - subaerial levee
V Restricted marine
VI Tidal channel

D Dominant
C Common
R Rare
A Absent

A conspicuous erosional surface containing abundant macerated plant material, logs, stems, clay and siderite pebbles usually separate the two. There is usually an abrupt change in bedding style and grain size at this erosion surface.

Channel mouth bar and tidal channel deposits are ripple bedded to a great extent whereas basal fluvial sandstones are trough cross-bedded. Bedding tends to be more continuous with less erosional truncation in channel mouth bars and tidal channels. Tidal channel sands are extensively bioturbated.

All three deposits exhibit inclined primary bedding surfaces. Paleocurrent orientations are nearly parallel to inclined primary bedding on channel mouth bars, but are usually perpendicular to point bar surfaces in fluvial channels. Thin layers of bioturbated siderite usually line tidal point bar surfaces whereas clay drapes often occur on fluvial point bar surfaces.

PALEOHYDROLOGY AND PALEOMORPHOLOGY

General Statement

Quantitative analysis of the paleohydrology and paleomorphology of fluvial systems in the Breathitt formation is the most important aspect of this research. This analysis is made possible, in part, by recent advances in understanding the nature of open channel flow and sediment transport and, in part, by the nature of superb exposures of ancient fluvial channels in eastern Kentucky. Recognition of abandoned meander channels, previously not described in paleohydraulic studies, permit accurate determination of fluvial channel dimensions. This will allow critical evaluation of most aspects of the established methodology for paleomorphologic calculation. Hydraulic and sedimentologic data from recent fluvial environments will be used to test a new methodology for calculating velocity of flow in ancient, fluvial systems. Additionally, a new method will be developed to calculate discharge.

Within the past fifteen years, literature on the hydrology and morphology of ancient fluvial systems has expanded rapidly. Table VII summarizes all important publications. Pertinent equations relating to these publications are listed in table VIII.

Several different methods have been devised to estimate hydraulic and morphologic parameters of ancient fluvial channels, but they can be generalized into a useful flow chart (Figure 64). This methodology is based on studies of ancient fluvial sandstones (Allen, 1963, 1965, 1970; Moody-Stuart, 1966) and quantitative studies of modern fluvial environments (Schumm, 1963, 1968, 1971, 1972). However, it is susceptible to several forms of criticism.

TABLE VII

SUMMARY OF METHODS USED IN PALEOHYDRAULIC CALCULATIONS

Author	Parameter Measured from Field Data	Parameter Calculated from Field Data	Parameter Calculated from Previously Estimated Parameter	Remarks
Schumm (1960, 1968, 1971, 1972)	Channel width and depth, width-depth ratio, meander wavelength, sinuosity, slope, mean annual discharge and mean annual flood.	Same as column two. "M" (weighted mean percent silt and clay).		Developed basic paleohydraulic equations from modern environments, included error of estimate from regression equations relating outcrop parameters.
Allen (1965) Carboniferous England	Thickness and horizontal extent of point bar surfaces, preserved thickness of bedform.	Channel width and depth.		One of first attempts to relate certain outcrop dimensions to actual channel size. Related preserved bedform thickness to water depth.
Moody-Stuart (1966) Devonian Spitsbergen	Thickness and horizontal extent of point bar surfaces.	Channel width and depth.	Sinuosity	Arbitrarily decided channel width equals 1.5 times horizontal extent of point bar surfaces.
Maulde (1968)	Pebble or boulder diameter.	Maximum velocity of flood water.		
Allen (1970) Devonian of England and Appalachian Mountains	Thickness and horizontal extent of point bar surfaces, grain size and bedform distribution.	Channel width and depth, average velocity of flow.		Theoretical considerations of deposition in meandering streams, first attempt to use laboratory data (Guy, Simons and Richardson, 1965) in paleohydraulic calculations.

Author	Parameter Measured from Field Data	Parameter Calculated from Field Data	Parameter Calculated from Previously Estimated Parameter	Remarks
Cotter (1971)	Thickness and horizontal extent of point bar surfaces.	"M", channel width and depth, velocity.	Width-depth ratio, sinuosity, mean annual flood, mean annual discharge, meander wavelength, slope, flow velocity, drainage area and stream length.	Estimate of "M" based on limited data obscured by diagenesis. Velocity estimated from Manning equation and flume data of Nordin, et.al. (1965).
Mummedal (1973)	Median grain size, bedforms.	Velocity	Channel depth	Velocity calculated from flume data, similar to Allen (1970).
Leeder (1973) Method A	Thickness of fining upward cycle.	Channel depth	Channel width, wavelength, average discharge.	Method can be used if point bar surfaces are not preserved.
Method B	Thickness and horizontal extent of point bar surfaces.	Channel width and depth, M.	Width-depth ratio average discharge, wavelength, sinuosity.	Suggest substitution of width-depth ratio for "M", avoided error in estimating M, but may not be valid for low sinuosity streams.
Bellent (1976) Carboniferous U.S.A.	Thickness of preserved bedform, median grain size, bedform type.	Channel depth, flow velocity.	Channel width discharge, wavelength, sinuosity, slope, stream length and drainage basin area.	Estimated depth from preserved bedform thickness, assumed rectangular cross-section, assumed M from tables (Schumm, 1968), calculated error of estimating other parameters from given error in estimating channel depths.

Author	Parameter Measured from Field Data	Parameter Calculated from Field Data	Parameter Calculated from Previously Estimated Parameter	Remarks
Elliot (1976) Carboniferous England	Thickness and horizontal extent of point bar surfaces.	Channel depth and width.	Sinuosity, wavelength and discharge.	Uses method A and B of Leeder (1973).
Miall (1976) Cretaceous Banks Island, Canada	Thickness of preserved bedform, paleocurrent variation, median and maximum grain size.	Channel width and depth, average and maximum velocity, M.	Width-depth ratio, mean annual discharge, mean annual flood, sinuosity, drainage area.	Used data of Sundborg (1950) and Guy, Simons and Richardson (1965) to estimate velocity, assumed value of M from tables (Schumm, 1968).
Nami (1976) Jurassic England	Thickness and horizontal extent of point bar surfaces, meander radius.	Channel width and depth.	Meander wavelength and discharge.	First use of radius of curvature.
Padgett (1976) Carboniferous Morocco	Thickness of point bar surfaces, radius of curvature of meanders.	Channel width, channel depth, M, wavelength.	Discharge, slope, velocity.	Assumed rectangular cross-section of river in calculating velocity, estimate of M is based on little hard evidence.

TABLE VIII

PALEOHYDRAULIC EQUATIONS GROUPED BY PARAMETERS

DEPTH		
From geometry of abandoned meanders	(1a)	
d = thickness of fining upward cycle	(2)	Allen, 1965
$\log d = 0.89 + 0.83 \log H_m$	(2a)	Allen, 1969
d = thickness of point bar surfaces	(3)	Allen, 1965
WIDTH		
From geometry of abandoned meanders	(1b)	
w = 1.5 x (horizontal extent of point bar	(4)	Moody-Stuart, 1966
$w = 6.8\ d^{1.54}$	(4a)	Leeder, 1973
$w = 2.2\ Q^{0.56}$	(4b)	Foweracker, 1963
CROSS-SECTIONAL AREA		
From geometry of abandoned meanders	(1)	
SEDIMENT LOAD		
$M = (Sc \times w) + (S_b \times d) / w + 2d$	(5)	Schumm, 1963
WIDTH-DEPTH RATIO		
$w/d = 225\ M^{-1.08}$	(6)	Schumm, 1963
From geometry of abandoned meanders	(30)	geometry
VELOCITY		
$V = 1.49/n\ (R^{0.67}\ S^{0.5})$	(14)	Manning
graphic, based on grain size, bedforms	(28)	Sundborg, Guy, 1966
graphic, based on size distribution	(29)	Gardner, 1977
$V_{max} = 9 \times (\text{diameter})^{\frac{1}{2}}$	(29a)	Maulde, 1968
DISCHARGE		
$Q = VA$	(7)	
$Qm = wM^{0.37}/37$	(8)	Schumm, 1968
$Qm = w^{2.43}/18\ F^{1.13}$	(8a)	Schumm, 1968
$Qma = 16\ w^{1.56}/F^{0.66}$	(8b)	Schumm, 1968
$\log Qma = 0.268 - 1.47 \log M - 1.38 \log W$	(8c)	Schumm, 1968
MEANDER WAVELENGTH		
$Lm = 10.9\ w^{1.01}$	(10)	Leopold, Wolman, 1960
$Lm = 1890\ Qm^{0.34}/M^{0.74}$	(15)	Schumm, 1968
$Lm = 234\ Qma^{0.48}/M^{0.74}$	(16)	Schumm, 1968
$Lm = 30\ Q^{0.5}$	(18)	Dury, 1965
$Lm = 106\ Q^{0.46}$	(17)	Carlston, 1965

MEANDER AMPLITUDE

$A = 14.2\ Q^{0.5}$	(19)	Foweracker, 1963
$A = 2.7\ w^{1.1}$	(11)	Leopold, Wolman, 196
From geometry of abandoned meander	(11a)	

MEANDERBELT WIDTH

$Mb = 37.3\ w^{0.87}$	(12)	Foweracker, 1963
Mb = sand body width	(27)	geometry
$Mb = 60.5\ Q^{0.51}$	(20)	Foweracker, 1963

SLOPE

$S = 0.00146 / Q^{1} / 4$	(21)	Lane, 1957
$S = 60\ M^{-0.38}\ Qm^{-0.32}$	(26)	Schumm, 1968

SINUOSITY

$P = 0.94\ M^{0.25}$	(9)	Schumm, 1963
$P = 3.5\ (w/d)^{-0.27}$	(13)	Schumm, 1972

DRAINAGE BASIN AREA

graphic	(22)	Dury, 1965
$Db = (Lm/60)^2$	(23)	Hack, 1965

STREAM LENGTH

graphic	(25)	Leopold, Wolman and Miller, 1964

A - meander amplitude
d - channel depth
d_{50} - grain size median diameter
D_b - drainage basin area
F - width-depth ratio
f - Darcy-Weisbach friction coefficient
H_m - mean height of bedform
L_m - meander wavelength
M - weighted percent silt-clay in perimeter
M_b - meander belt width
n - Manning's coefficient
P - sinuosity
Q - average discharge
Q_m - mean annual discharge
Q_{ma} - mean annual flood
R - hydraulic radius
S - slope
S_b - percent silt-clay in channel banks
V - velocity
Sl - stream length
V_{max} maximum velocity

FIGURE 64. Generalized flow charg depicting the methodology of paleohydraulic calculations.

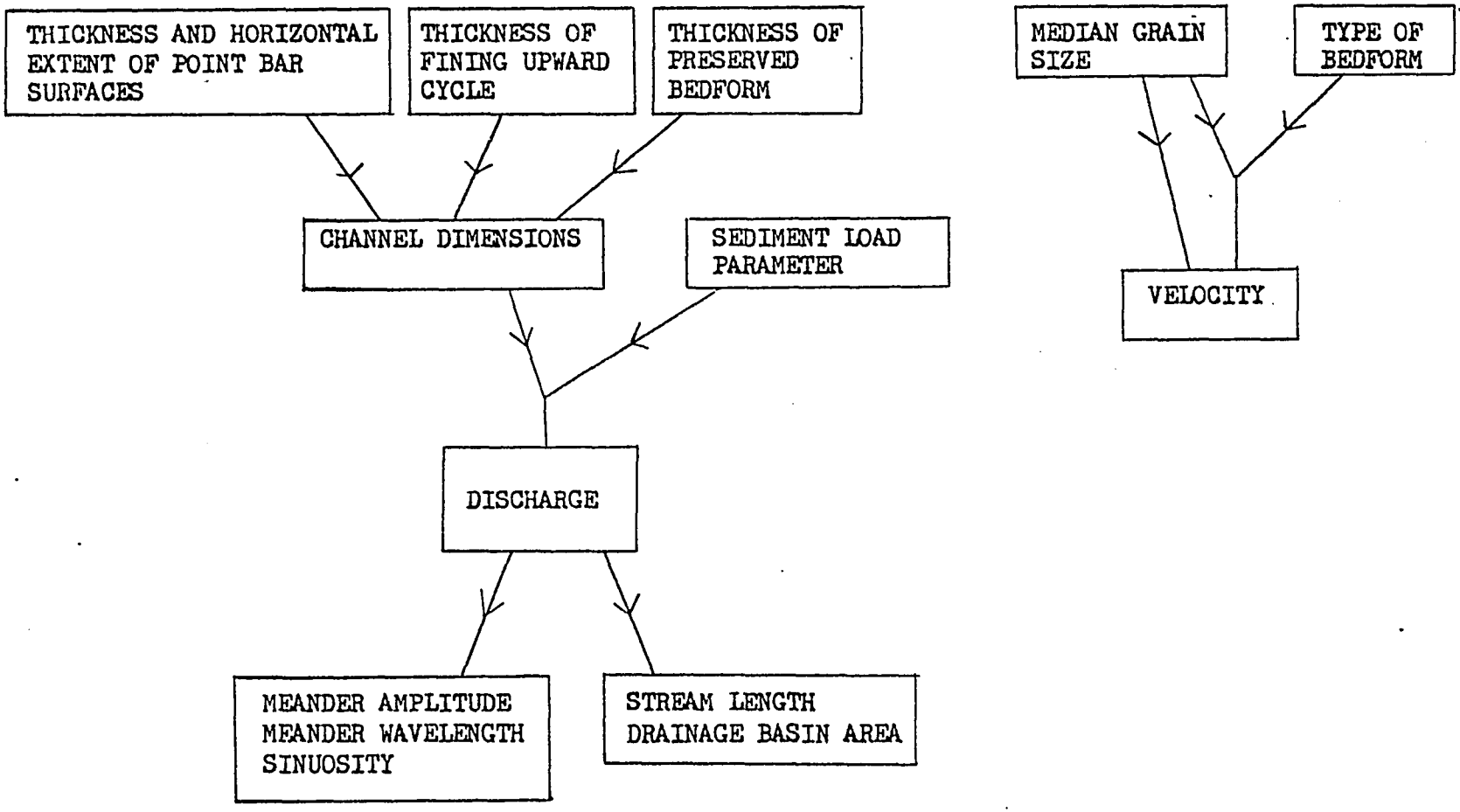

The conventional methodology for estimating channel dimensions is frequently criticized. It is important to realize that this methodology is an unfortunate result of the limitations of fluvial sandstone outcrops. The obvious first step in paleomorphologic calculation is to determine channel dimensions, namely, channel width, depth and cross-sectional area, but complete fluvial channels are rarely observed in outcrop. Therefore, it has been necessary to estimate channel dimensions from some attribute that is preserved in outcrop, preferably some attribute that is frequently preserved. Allen (1963, 1965) first noted that fluvial sandstones in vertical sections sometimes exhibit inclined point bar surfaces which he termed epsilon cross-stratification and that they are approximately equal to the thickness of frequently observed fining upward cycles. He assumed that the thickness of fining upward cycles and the thickness of point bar surfaces was approximately equal to channel depth. Moody-Stuart (1966) arbitrarily assumed that channel width was equal to 1.5 times the horizontal extent of point bar surfaces; the length of a point bar as projected onto a horizontal plane. This value of 1.5 was used in subsequent publications (Allen, 1970; Cotter, 1971; Elliot, 1976; Nami; Padgett, 1966). However, these relationships between point bar surfaces and channel dimensions have not been tested in modern environments, in part because of the obvious lack of vertical exposures. Therefore, a valid question to ask is, do these outcrop parameters accurately reflect the channel dimension they are trying to measure. What is the error in such estimates?

To make matters even more complicated, point var surfaces and fining upward cycles are not fully developed in many fluvial sandstones. In this case Allen (1969) used a relationship between preserved bedform thickness and water depth to estimate channel depth. Later, Leeder (1973) developed a relationship between channel depth and channel width that was based on data from recent fluvial environments. This relationship was used to estimate channel width if point bar surfaces were not present in outcrop. Both relationships were presented as regression equations that contained large error of estimation. The large error is a result of the scatter of data points.

During the time that Allen was studying ancient fluvial sandstones in England, S.A. Schumm was studying the morphology of recent fluvial environments in North America and Pleistocene to Recent fluvial channels in Australia. He published a number of regression equations (Table VII) relating various morphologic and hydrologic characteristics of recent fluvial systems. He measured channel width, channel depth, the ratio of channel width to channel depth F, discharge and the sediment load parameter M, which is a measure of the silt-clay content of channel bank and alluvium. He then related those parameters to each other and to other morphologic characteristics, namely, channel sinuosity, meander wavelength and channel slope. He concluded that F, M and discharge were significant variables in determining channel morphology. Unfortunately, parameters that can be easily measured

from modern fluvial environments are not always measurable in ancient fluvial sandstones and vice-versa. Schumm's data could not be used to support or deny the relationships of point bar surfaces that Allen and others were developing for ancient fluvial sandstones. However, if the channel width, channel depth, width-depth ratio and the sediment load parameter could be measured from outcrops of ancient fluvial sandstones, then a methodology was available to estimate discharge. With discharge measured, meander wavelength slope, stream length and drainage basin area could then be estimated (Figure 64).

Two problems are apparent in this procedure. The first problem has to do with the accumulation of error as the calculations proceed from the initial determination of channel width and depth to the final calculation of drainage basin area and stream length. Channel width and depth still had to be estimated from the methods of Allen or Leeder. The error in estimating channel width and depth from point bar surfaces was unknown. Thus, unknown error was frequently introduced in the first step of the calculation. This error was compounded in the estimation of discharge. The error in estimating discharge had to be included in the subsequent calculation of meander wavelength, slope, drainage basin area and stream length. Error expanded so rapidly that the final calculations were only "ball park" figures. BeMent (1976), Figure 31) showed that overestimating the depth by a factor of three resulted in discharge and drainage basin area being off by a minimum factor of 8 and 12 respectively.

In this study channel width and depth are directly measured from abandoned channel meanders. Therefore the error can be significantly

reduced in the initial computation. More importantly, the relationships among point bar surfaces, thickness of preserved bedforms, thickness of fining upward cycles and channel width and depth can be critically evaluated with data from abandoned meanders.

The second problem with the methodology illustrated in the flow chart has to do with the calculation of discharge. It is obvious from an inspection of the flow chart that discharge is an important parameter in paleomorphologic calculations. It is the "spoke of the wheel". Most methods (Cotter, 1971; Leeder, 1973; Elliot, 1976; Miall, 1976; Nami, 1976; Padgett, 1976) that are used to calculate discharge are based on the empiric relationships developed by Schumm (1960, 1968) from streams in Australia and the Great Plains of the United States. These empiric equations relate discharge to various combinations of channel width, channel depth, width-depth ratio and the sediment load parameter M (Table VIII).

There are several potential problems with this approach. First, empiric equations based on recent fluvial environments may not be applicable to ancient fluvial systems from different climates, tectonic or geologic settings. Second, the sediment load parameter M can be easily determined for recent channels by sieve analysis but diagenesis often obscures or alters the silt-clay matrix in ancient fluvial sandstones. This introduces an unknown error when M is estimated for ancient fluvial sandstones (Leeder, 1973).

To improve this aspect of the methodology it is therefore necessary to develop additional techniques for calculating discharge; techniques

that are independent of those already established. The continuity equation, $\bar{Q} = \bar{V}A$ where $\bar{Q}$ is average discharge, $\bar{V}$ is average velocity and A is cross-sectional area, is an obvious possibility. This simple equation is seldom used in paleohydraulic calculations for two reasons. First, in all previous paleohydraulic studies it has not been possible to measure channel cross-sectional area accurately, because of the nature of fluvial outcrops. Complete fluvial channels were not observed in outcrop. The shape of fluvial channels was assumed to be rectangular (BeMent, 1976, Padgett, 1976) which is rarely an accurate assumption. Most recent fluvial channels are not rectangular in cross-section. The dimensions of the rectangle were channel width and depth as determined from the methods of Allen or Leeder. However, in this study, channel cross-sectional shape and area can be directly and accurately measured from well exposed, abandoned meander channels. Thus, the first problem with using the continuity equation can be overcome. Second, it is difficult to estimate velocity of flow in ancient fluvial channels. The few estimates that have been made are based on 1) diagrams of Guy, et.al., (1966) that give only a very general velocity range for particular bedforms and median grain size or 2) initiation of sediment motion curves (Shields, 1936; Sundborg, 1956). The velocity determined from these curves is the critical erosion velocity and does not necessarily reflect the velocity of flow during deposition. Therefore, if a method can be developed that accurately measures paleovelocity, then the continuity equation can be used in paleohydraulic calculations to estimate discharge.

Theoretical Background for Velocity Calculations

The primary objective of this section is to develop a more accurate technique for estimating velocity of flow in ancient fluvial channels. The question to be asked is what outcrop data can one measure that could be quantitatively related to flow velocity. It is generally agreed that grain size can be related to velocity and grain size of ancient fluvial sandstones can be measured with known degree of accuracy. A detailed review of hydraulic theory (Sundborg, 1956; Albertson, et.al., 1960; Briggs and Middleton, 1965; Allen, 1969; Gessler, 1971; Koloseus, 1971; Pettijohn, et.al., 1972; Jackson, 1975; Sagoe and Visher, 1977; Middleton, 1977) indicated that the parameter T_o, bottom shear stress, appears in one form or another in nearly every equation that relates flow velocity and conditions for sediment motion to grain size of the transported sediment. Therefore, to accurately estimate velocity a quantitative relationship must be developed among velocity, bottom shear stress and grain size or at least some attribute of the grain size distribution curve.

To develop such a relationship consideration must be given to the basic forces that govern flow in open channels. The basic forces are derived from parameters depicted in figure 65. It is assumed that the average depth does not vary with distance down channel (uniform flow), that the flow conditions do not change with time (steady flow) and that the slope, S, is constant and small so that the sine of the angle of slope is approximately equal to the slope itself ($S = h/L$). The third assumption is true of natural rivers on delta plains. The

FIGURE 65. Schematic diagram explaining symbols used in deriving velocity equation.

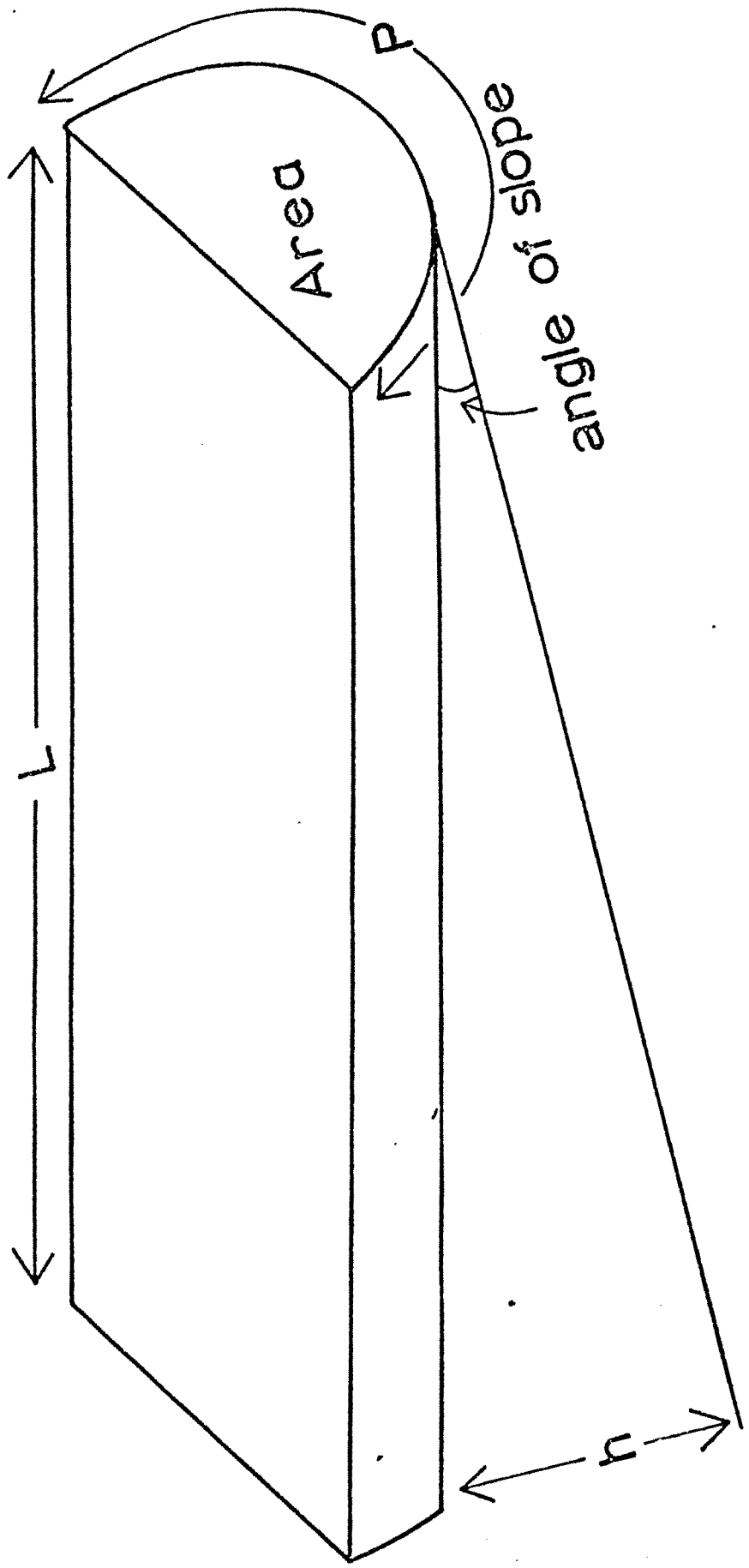

first two are only true for short distances and short periods of time. A quantitative analysis of the basic forces in open channel flow could not be made without those simplifying assumptions.

Given these assumptions, the gravity force G acting on a volume of water in a channel of length L and average cross-sectional area A is $G = \rho gAL$ where ρ = density of water and g = acceleration of gravity. The downslope component is $\rho gALS$. In equilibrium this force is balanced by the resistance of the boundary which is equal to the product of the average shear stress at the boundary T_o (bottom shear stress) and the area of the boundary in contact with the volume of water. This area is the product of the length L and the "wetted perimeter" P. Therefore,

$$\rho gALS = T_o LP \qquad \text{(Blatt, et.al, 1972)}$$

rearranging gives

$$T_o/\rho g = (A/P)S$$

By definition, A/P is the hydraulic radius R, thus,

$$T_o/\rho g = RS \qquad (1)$$

The resistance of the boundary to the flow in circular pipes is measured by the well established Darcy-Weisbach equwtion (Albertson, et.al., 1960) that relates the difference in head h at two points separated by a distance L on a pipe of diameter D to the average velocity $\bar{V}$ in a vertical section of pipe. This useful equation is

$$h = f\, L\bar{V}^2/D2g \qquad (2)$$

where g = the acceleration of gravity, f = Darcy-Weisbach friction coefficient.

For circular pipes,

$$R = A/P = \frac{D^2/4}{D} = D/4$$

Substituting 4R for D and S for h/L in equation (2) and rearranging gives

$$RS = f/4\ \bar{V}^2/2g$$

Substituting into equation (1) gives

$$T_o/\rho g = f/4\ \bar{V}^2/2g$$

or

$$T_o/\rho = f/4\ \bar{V}^2/2 \qquad (3)$$

By definition V^{*2}, the shear velocity squared, is equal to T_o/ρ . Substituting into equation (3) and rearranging, gives the useful equation

$$\bar{V} = V^*\sqrt{8/f} \qquad (4)$$

Equation (4) states that the average velocity of flow is a function of the Darcy-Weisbach friction coefficient f and the shear velocity V*. Values of f can be obtained from tables (Simon, et.al., 1971) where f is calculated for various types of natural rivers. This is half way to the goal of developing a quantitative relationship among velocity bottom shear stress and grain size.

To estimate the average velocity of flow for ancient fluvial channels it is now necessary to find some grain size parameter that can be quantitatively related to V*. Middleton (1976, 1977) has developed a method for calculating V* using log-probability plots of grain size distribution. The method is based on two assumptions. It is assumed that log-probability plots of grain size distribution show marked discontinuities that can be represented by a limited number of straight line segments. This assumption is generally accepted and is supported by studies of grain size distributions

from modern and ancient environments (Douglas, 1946; Inman, 1949; Sindowski, 1957; Visher, 1969, 1972).

Secondly, it is assumed that these straight line segments identify subpopulations of grains moved by different mechanisms of sediment transport, namely, traction, saltation and suspension (Figure 66) and that the breaks between two adjacent segments identify the size where one mechanism of transport changes to another. Gilbert (1914) in his classic flume experiments recognized that grains moved as a traction carpet (subpopulation C) by rolling and sliding along the bottom and as suspended load (subpopulation B) where grains are moved in turbulent suspension in the fluid. Bagnold (1941) and Moss (1962) recognized an intermediate saltation load (subpopulation A) where grains are lifted sufficiently clear of the bed (usually on the order of 10 to 100 grain diameters) to be carried in turbulent suspension, but generally fall back to the bed after a short period of time. Thus, Middleton (1976, 1977) assumed that the population of the "break" between the traction population and the saltation population, defined as the T-Junction, indicates the size of the coarsest particles that can be taken into suspension.

This statement is supported by data from a detailed analysis of the grain size of the crevasse splay in the Allen Sandstone. If deposits in the crevasse splay represent sediment carried in suspension in the main channel, a reasonable assumption, then the size of the coarsest grains in the crevasse splay should correspond to the T-Junction value at the elevation of the breach in the main channel.

FIGURE 66. Generalized log-probability plot of grain size distributions showing the relationship between straight line segments, breaks and mode of transport.

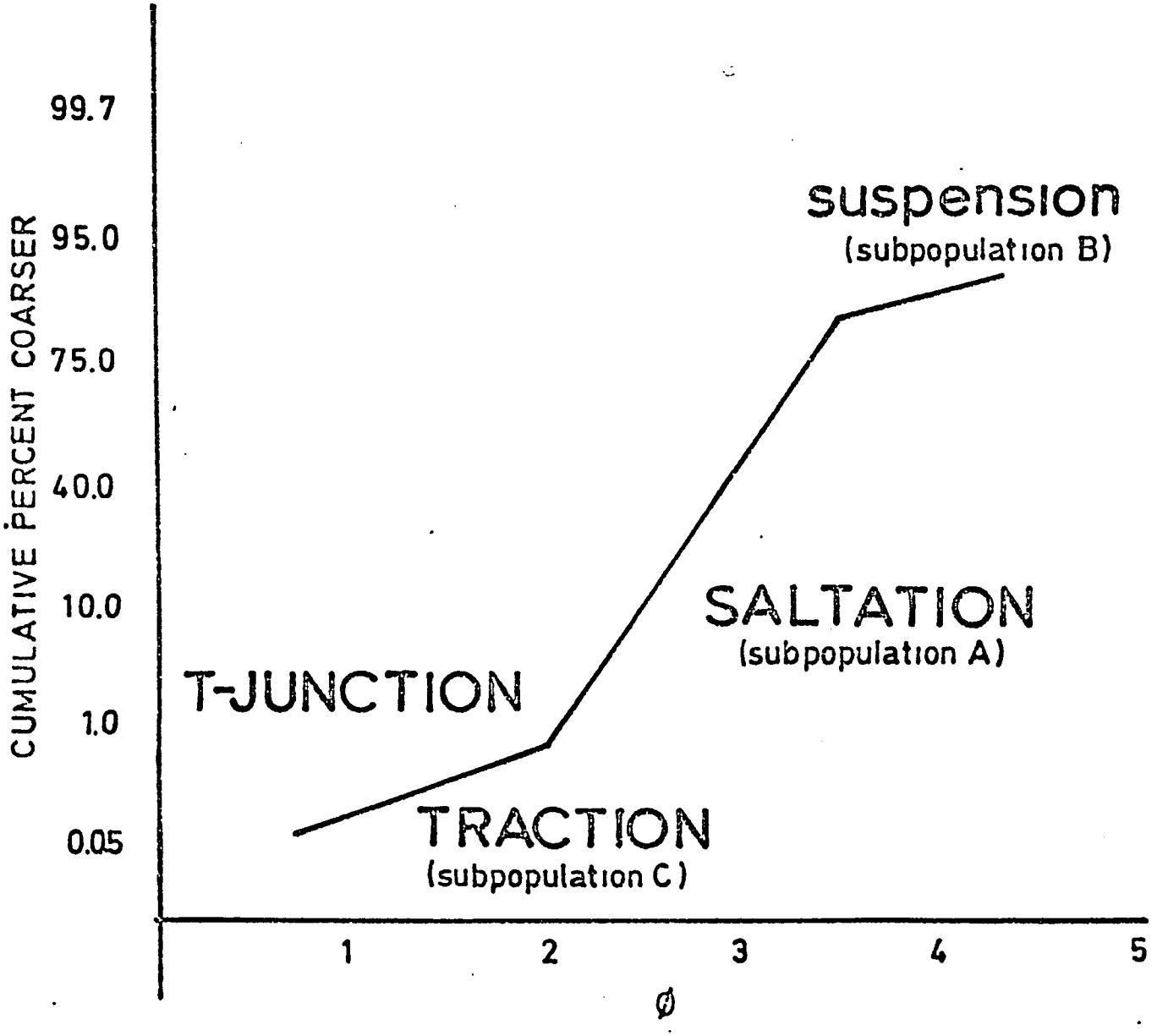

The crevasse splay is 5-6 meters thick and the fluvial channel sandstone is approximately 10 meters thick. If it is assumed that the crevasse splay deposits attained an elevation equal to the top of the main channel, then the size of the coarsest grains in the crevasse splay should equal the T-Junction value 4-5 meters above the base of the main channel. In fact, the maximum grain size of the crevasse splay, 1.7ϕ, agrees closely with the T-Junction value, 1.8ϕ, 5 meters above the base of the Allen Sandstone.

From experimental studies and theoretical considerations, Moss (1962) and Middleton (1977) related the T-Junction value to bottom shear stress. Allen (1970) and Sagoe and Visher (1972) concluded that bottom shear stress decreases with decreasing water depth, all else being equal. This conclusion is supported by data from this study (Figure 67). Samples had decreasing values of the T-Junction with increasing distance above the channel base, that is, decreasing water depth.

Not all authors agree that the "breaks" in the log-probability curves are related to the hydraulics of flow. In a study of 11,000 samples from various depositional environments, Shea (1974) concluded that the "breaks" on log-probability plots are controlled more by the size distribution of parent material and the way that material responds to the long term wearing down in the sedimentary mill than to the hydraulics of flow during deposition. If this were the case, one would expect the position of "breaks" on log-probability plots to be constant. However, a systematic and consistent variation in the

FIGURE 67. Plot of T-Junction versus distance above base. Data from table IV. The regression equation for the line is Y = 1.67 + 0.061X.
std. dev. = 0.34
where Y = T-Junction
X = distance above base
Data from table IV.

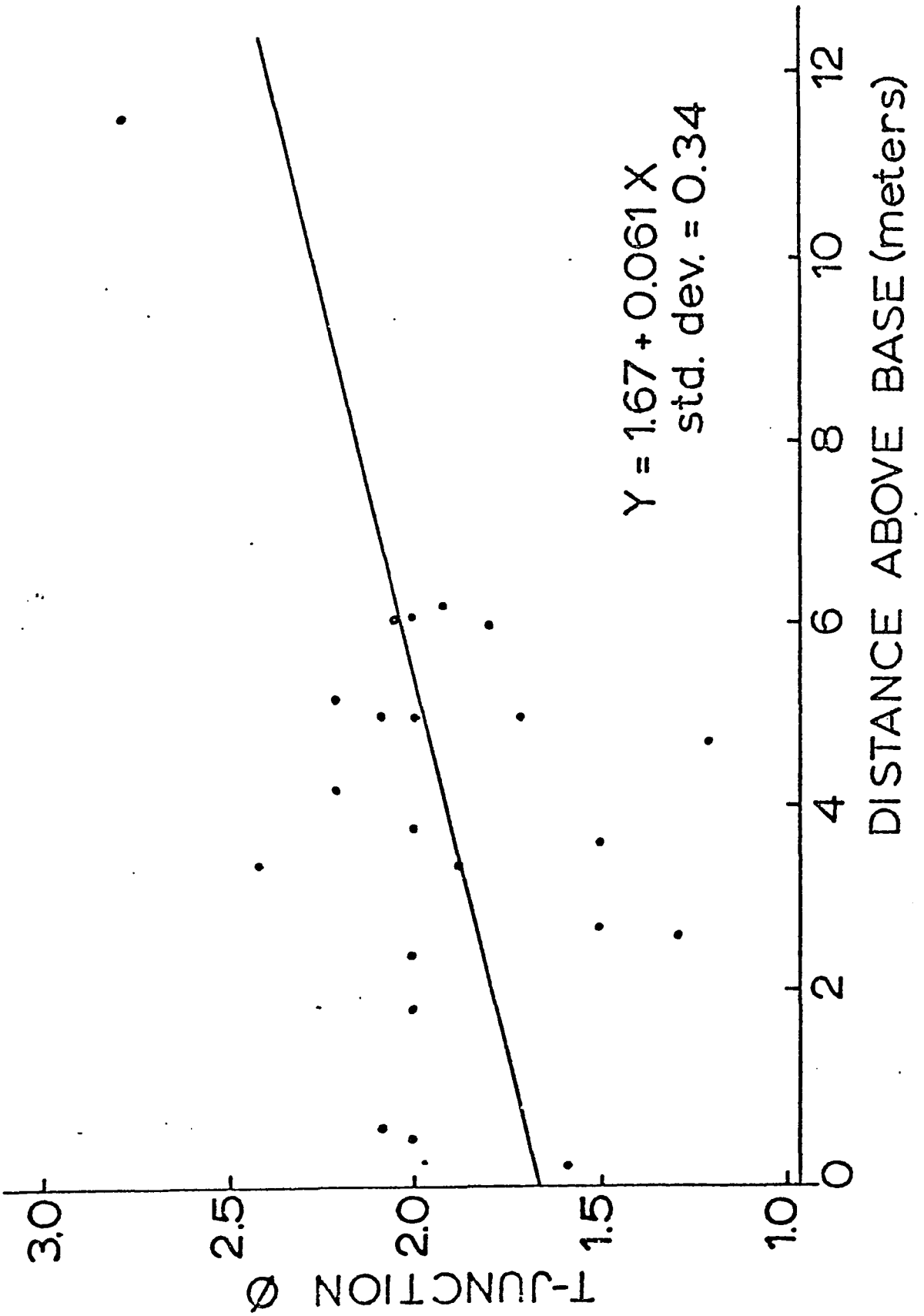

position of the "breaks" from sample to sample in this study indicates that hydraulic sorting is locally more important.

Based on these assumptions of grain size distribution curves, Middleton (1976, 1977) developed a quantitative relationship between V* and T-Junction values taken from log-probability plots of grain size distribution. He assumed that the coarsest particles that can be taken into suspension, as indicated by the T-Junction, will be those particles that have settling velocities, ω, equal to the upward vertical velocity fluctuations close to the boundary. The magnitude of these vertical velocity fluctuations is equal to the root mean square (rms) of the vertical velocity fluctuation. Thus,

$$\omega = \sqrt{(\bar{v}')^2} \qquad (5)$$

where $\bar{v}'$ is the instantaneous (turbulent) component of velocity in the vertical direction.

Observations of turbulence intensity show that the vertical (rms) velocity fluctuation are proportional to the shear velocity (Blinco and Parthenides, 1971). Data from Bowden (1962), McQuivey and Richardson (1969), Antonia and Luxton (1971) and Bagnold (1973) show that this proportionality is approximately unity. Thus,

$$\sqrt{(\bar{v}')^2} = V^* \qquad (6)$$

and substituting into equation (5) gives

$$\omega/V^* = 1 \qquad (7)$$

Equation (7) is Middleton's criterion for suspension and is extremely important because it provides a quantitative method for estimating shear velocity from the fall velocity of grain size at the T-Junction. Middleton (1977) has argued that this criterion for

suspension, $\omega/V^* = 1$, is supported by a comparison of hydraulic measurements with the settling velocity of the largest grain sizes present in the suspended load of several midwestern rivers. Francis (1973) produced a diagram (Figure 68) based on experimental data that clearly shows the transition from traction to saltation and suspension. This transition occurs when the value of ω approaches the value of V^*.

With a method established for estimating shear velocity from grain size, a parameter that can be measured from outcrop data, it is now possible to estimate velocity of flow of ancient fluvial channels. By substituting Middleton's criterion for suspension, equation (7) into equation (4), the important equation

$$\bar{V} = \omega\sqrt{8/f} \qquad (8)$$

is produced.

A review of the theoretical velocity calculations is necessary at this point. Equation (4), $\bar{V} = V^*\sqrt{8/f}$, was developed from basic hydraulic theory. It relates average flow velocity to shear velocity and Darcy-Weisbach friction coefficient. The criterion for suspension developed by Middleton that depicts the relationship between shear velocity and the fall velocity of grain size at the T-Junction on a log-probability curve, $\omega/V^* = 1$, was presented and supported by experimental work. Finally, a new equation, $\bar{V} = \omega\sqrt{8/f}$, was formulated that permits an estimation of the average flow velocity in a given river section from a parameter that can be measured from outcrop data.

This new method for calculating average velocity of flow of ancient fluvial sandstones was tested and verified by using available

FIGURE 68. Plot of dimensionless grain, velocity V_G/V against dimensionless shear velocity V^*/w .
V_G = velocity of grain movement
V = velocity of water
w = settling velocity of grains in motion
V^* = shear velocity
As grain velocity approaches flow velocity of water (V_G/V approaches 1), the mode of grain transport changes from traction to saltation and suspension. As a traction carpet, grains move at speeds less than one and is greater than V^*. When grains are moved by saltation or in suspension their velocity approaches that of the flowing water and values of V^* approach the value of w for the moving grains. Thus, V^*/w approaches 1. (After Francis, Figure 2, 1973).

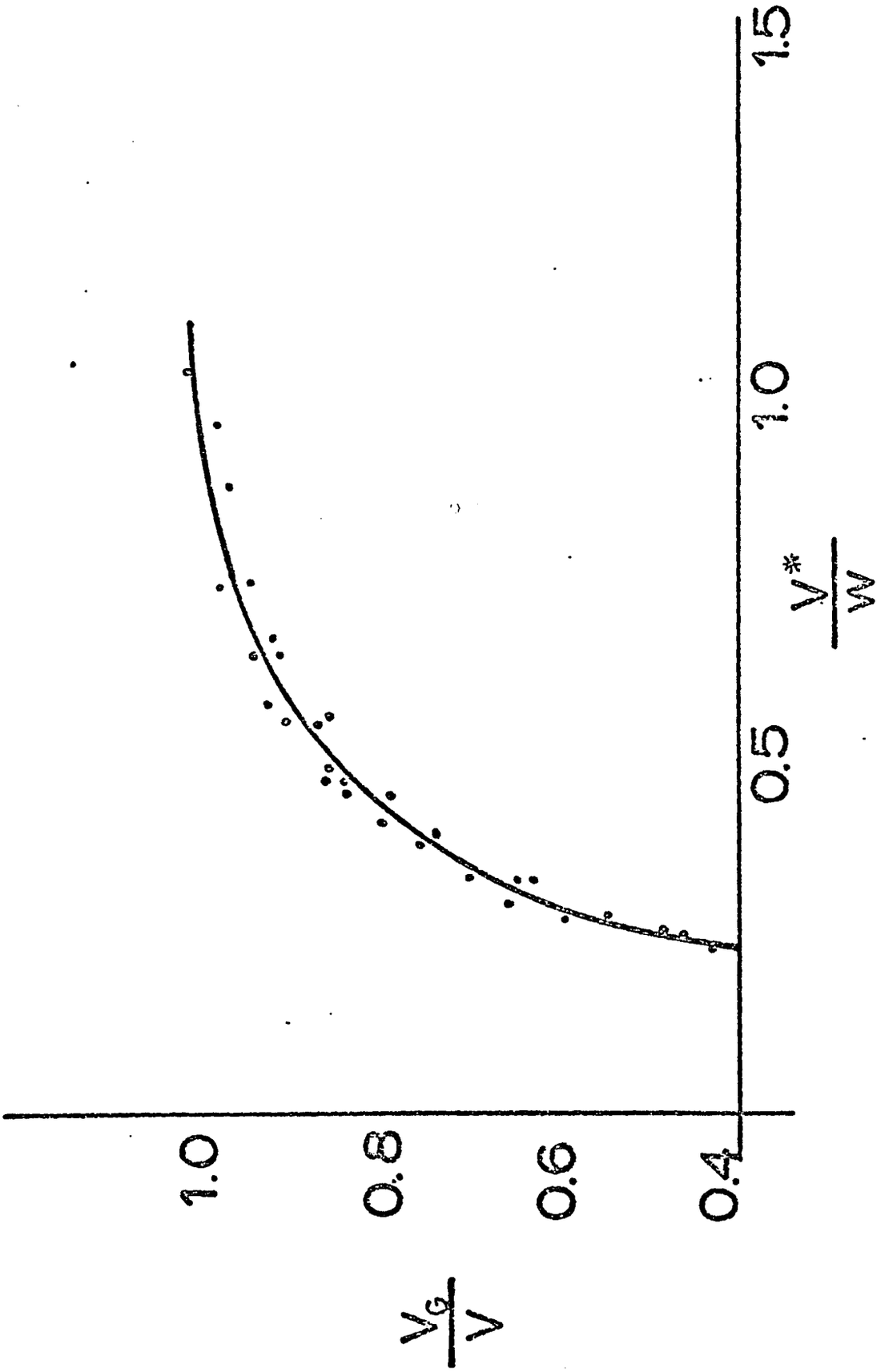

hydraulic data from modern fluvio-deltaic environments (Table IX). Data on grain size distribution, average velocity of flow and shear velocity are available from modern environments. Values calculated for ω/V^* were consistently close to one, in agreement with Middleton's criterion for suspension. At present, there is insufficient data from experimental studies or modern environments to statistically determine a confidence interval for the criterion for suspension. Predicted velocity values, using equation (8), $\bar{V} = \omega\sqrt{8/f}$, agree with observed velocities for rivers carrying fine grained sand. Predicted values show significant departure from observed velocity values for rivers with coarse sand and pebbles, as in Jackson's (1976) data from the Wabash River, indicating that this method may not be applicable to coarse grained fluvial systems.

Calculation of Paleohydraulic and Paleomorphologic Parameters

A detailed flow chart (Figure 69) illustrates the methodology used to calculate paleohydraulic and paleomorphologic parameters in this study. Empiric equations represented by lines that connect the various boxes are listed in table VIII. An 80 percent confidence interval was used in all calculations where confidence intervals for regression equations were available. A 5 percent error was introduced from the pace and Brunton method of measuring outcrop dimensions and a 10 percent error was assumed in estimating channel area.

Channel Dimensions: The first step in the paleohydraulic calculations is to determine the fluvial channel dimensions. Table X compares the values from different methods of estimation. The cross-

TABLE IX

ESTIMATES OF MIDDLETON'S CRITERION FOR SUSPENSION
AND COMPARISON OF OBSERVED VELOCITY AND CALCULATED VELOCITY[I]

Location	Fall Velocity ω Observed	Shear Velocity V^* Observed	Criterion for Suspension ω / V^*	Average Flow Velocity $\bar{V}$ Observed	Average Flow Velocity $\bar{V}$ Calculated From $\bar{V} = \omega\sqrt{8/f}$ [4]
Mississippi River at St. Louis, Mo., Jordan (1965)[1]					
Dec. 27, 1955	0.16	0.21	0.76	2.3	1.7
Feb. 21, 1956	0.23	0.21	1.09	2.2	2.4
April 24, 1956	0.32	0.27	1.18	3.7	3.5
May 9, 1956	0.29	0.27	1.07	3.3	3.2
July 9, 1956	0.24	0.25	0.96	2.7	3.5
May 13, 1959	0.24	0.30	0.80	4.4	2.6
Klaralven River, Sweden, Sundborg (1956)[1]	9.0			80.0	85.0
Wabash River, Illinois, Jackson (1975)[2]					
Fig. 18A Crest	8.0	7.0	1.14	100.0	86.0
Trough	19.0	18.0	1.05	82.0	200.0
Fig. 18C Trough	15.0	16.0	0.94	100.0	160.0
Fig. 18D Crest	11.0	6.3	1.74	66.0	118.0
Fig. 18F Trough	15.0	16.0	0.94	135.0	160.0

Location	Fall Velocity ω Observed	Shear Velocity V^* Observed	Criterion for Suspension ω/V^*	Average Flow Velocity $\bar{V}$ Observed	Average Flow Velocity $\bar{V}$ Calculated From $\bar{V} = \omega\sqrt{8f}$ [4]
South Esk River, Scotland, Bridge & Jarvis (1976) (f = 0.06 from his data)					
Feb. 2, 1976		6.8		79.0	78.0
		5.9		70.0	84.0
		5.9		68.0	83.0
		5.6		64.0	68.0
		5.7		66.0	66.0
Feb. 3, 1976		5.0		57.0	65.0
		2.5		30.0	50.0
		2.3		26.0	37.0
Feb. 11, 1976		5.4		62.0	65.0
		4.3		50.0	56.0
		2.3		27.0	22.0
Guadalupe River Delta, Texas, Donaldson, et al., (1970)[1]	4.2			40.0[3]	45.0
Rhone River Delta, France, Oomkens (1970)	9.0			100.0	96.3
Ebro River Delta, Spain, Maldonado (1975)	6.0			67.0[3]	64.0
Po River Delta, Italy, Nelson (1976)	6.8			73.0	80.0

I Where appropriate, all units in cm./sec. except Jordan (1965) in feet/sec.

1 Fall velocity calculated from coarsest particle in suspended load.

2 Fall velocity calculated from T-junction of log-probability plot of sediment composing bed of stream.

3 Average velocity equals mean annual discharge divided by the product of bankfull channel width and depth.

4 f = 0.07 unless otherwise stated. This is an average value for sandwaves and dunes, the bedforms at all sample locations.

FIGURE 69. Detail flow chart of paleohydraulic and paleomorphologic calculations showing the methodology used in this study. Numbers beside lines refer to numbered equations in table VIII. It is important to note that 1) the geometry of abandoned meanders permits calculation of channel width, channel depth and cross-sectional area directly from outcrop, 2) velocity and cross-sectional area are used in the calculation of discharge and 3) all parameters can be calculated from several independent methods.

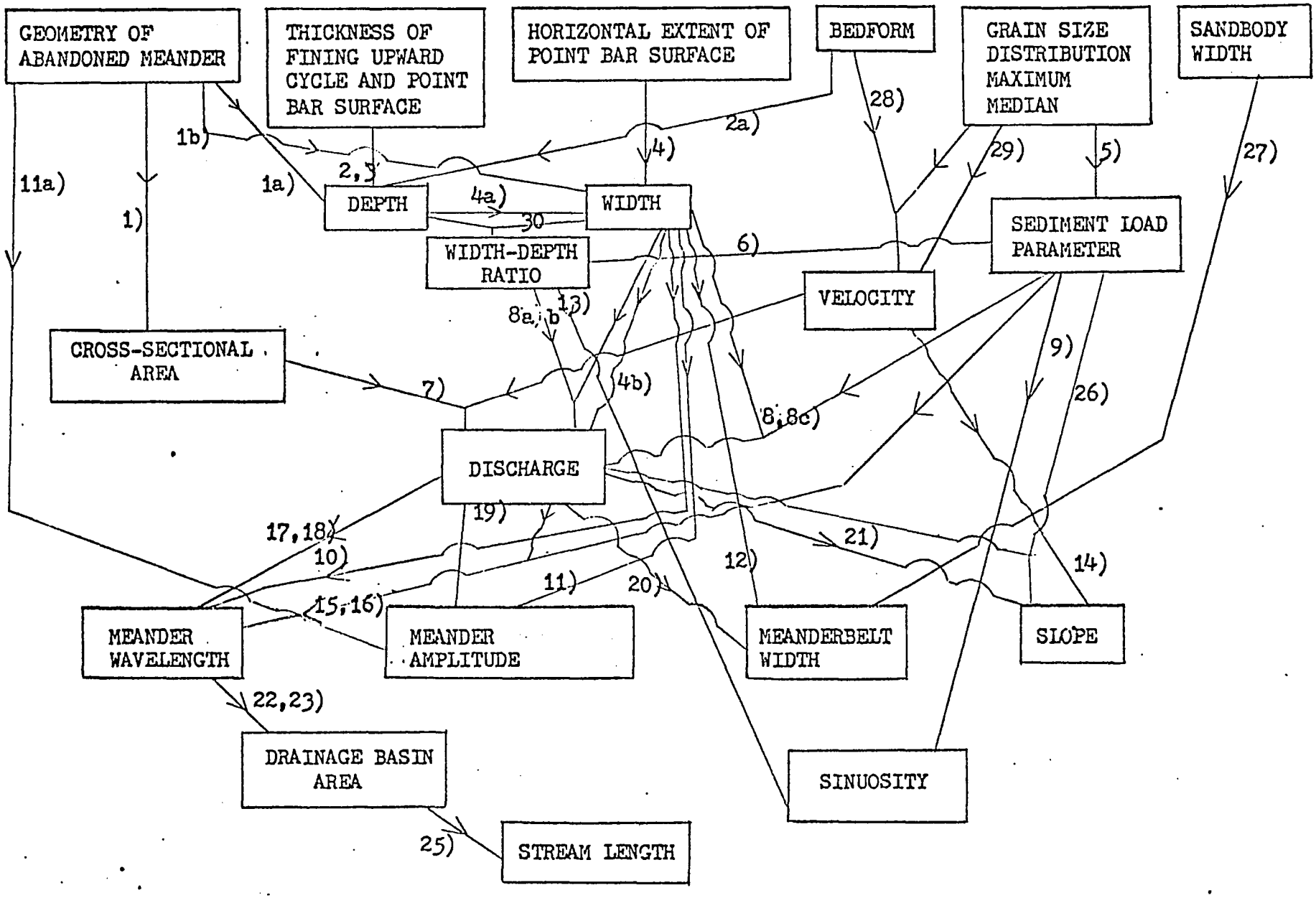

TABLE X

COMPARISON OF CHANNEL DIMENSIONS COMPUTED BY DIFFERENT TECHNIQUES

Channel Depth (Meters)

	Abandoned Meander	Fining Upward Cycle[1]	Point Bar Surface[2]	Preserved Bedform[3]
Harold Sandstone	10 ± 0.5	10 ± 2	10 ± 2	7.7
Allen Sandstone	10 ± 0.5	10 ± 2	10 ± 2	7.7

Channel Width (Meters)

	Abandoned Meander	Horizontal Extent of Point Bar Surfaces[4]	Depth[5]
Harold Sandstone	140 ± 7	130 - 155	210 - 250
Allen Sandstone	130 ± 6	125 - 155	210 - 250

Cross-Sectional Area (Square Meters)

	Abandoned Meander	Rectangular Shape[6]	Trapezoidal Shape[7]
Harold Sandstone	960 ± 100	1400 ± 140	900
Allen Sandstone	710 ± 70	1300 ± 130	800

1 Average thickness of fluvial vertical profiles; BB-2, HA-1, HA-2 for Harold Sandstone and HA-23, HA-27, HA-29, LA-3 and PR-7 for Allen Sandstone.

2 Average thickness of point bar surfaces; BB-2 and HA-1 for Harold Sandstone and HA-29, HA-30 and LA-1 for Allen Sandstone.

3 From equation 2a, Table VIII. Thickness of preserved bedforms in channel base is approximately one meter.

4 Calculated as 1.4 times horizontal extent of point bar surfaces.

5 From equation 4a, Table .

6 Area equals width times depth.

7 Area equals $\frac{1}{2}$ depth X (2 width - horizontal extent of point bar surfaces).

sectional area can be directly determined from outcrops of abandoned meanders that have been graphically oriented perpendicular to channel trend (Harold Sandstone, Figure 70, Allen Sandstone, Figure 71). Channel cross-sectional area does not approximate a rectangular shape. A trapazoid is a better approximation of channel shape. Area can then be estimated as $A = \frac{1}{2}d(2w - PB)$ where w = channel width, d = channel depth, PB = horizontal extent of point bar surface.

Maximum channel depth determined directly from abandoned meanders is 10 meters $\pm$ 0.5 meters, neglecting the effects of compaction. This corresponds to the thickness of preserved point bar deposits and to the thickness of fining upward cycles as measured from the bottom of the channel to the base of the overlying coal. Channel width estimated directly from abandoned meanders is 140 meters and 130 meters for the Harold and Allen Sandstones, respectively. Channel width is 1.4 times the horizontal extent of point bar surfaces (Table XI), slightly less than the arbitrary value of 1.5 used by other authors (Allen, 1965; Moody-Stuart, 1966 and Cotter, 1971).

Sediment Load: The sediment load parameter M appears in several paleohydraulic equations (Table VIII). It is the weighted percent silt and clay in the channel banks and alluvium. As defined by Schumm (1963).

$$M = \frac{(S_c \times w) + (S_b + d)}{w + 2d}$$

where w = channel width, d - channel depth, S_c = percent silt-clay in channel alluvium, S_b = percent silt-clay in channel banks.

Two methods have been employed to estimate M, but both are unreliable (Leeder, 1973). M can be estimated from point counts of

FIGURE 70. Construction of abandoned meander channel perpendicular to orientation of paleocurrent data for Harold Sandstone. Outcrop orientation is 40° and paleocurrent orientation is 10°. Lower left portion reproduces shape and cross-sectional area of abandoned channel that is perpendicular to flow. The abandoned channel is divided into five sections that are separated into equal elevations as measured along the channel bottom: section one from 0 - 2m. above the channel base, section two from 2 - 4m above the channel base, section three from 4 - 6m above the channel base, section four from 6 - 8m above the channel base and section five from 8 - 10m above the channel base. Velocity and discharge are calculated for each section in Appendix V. Note vertical exaggeration.

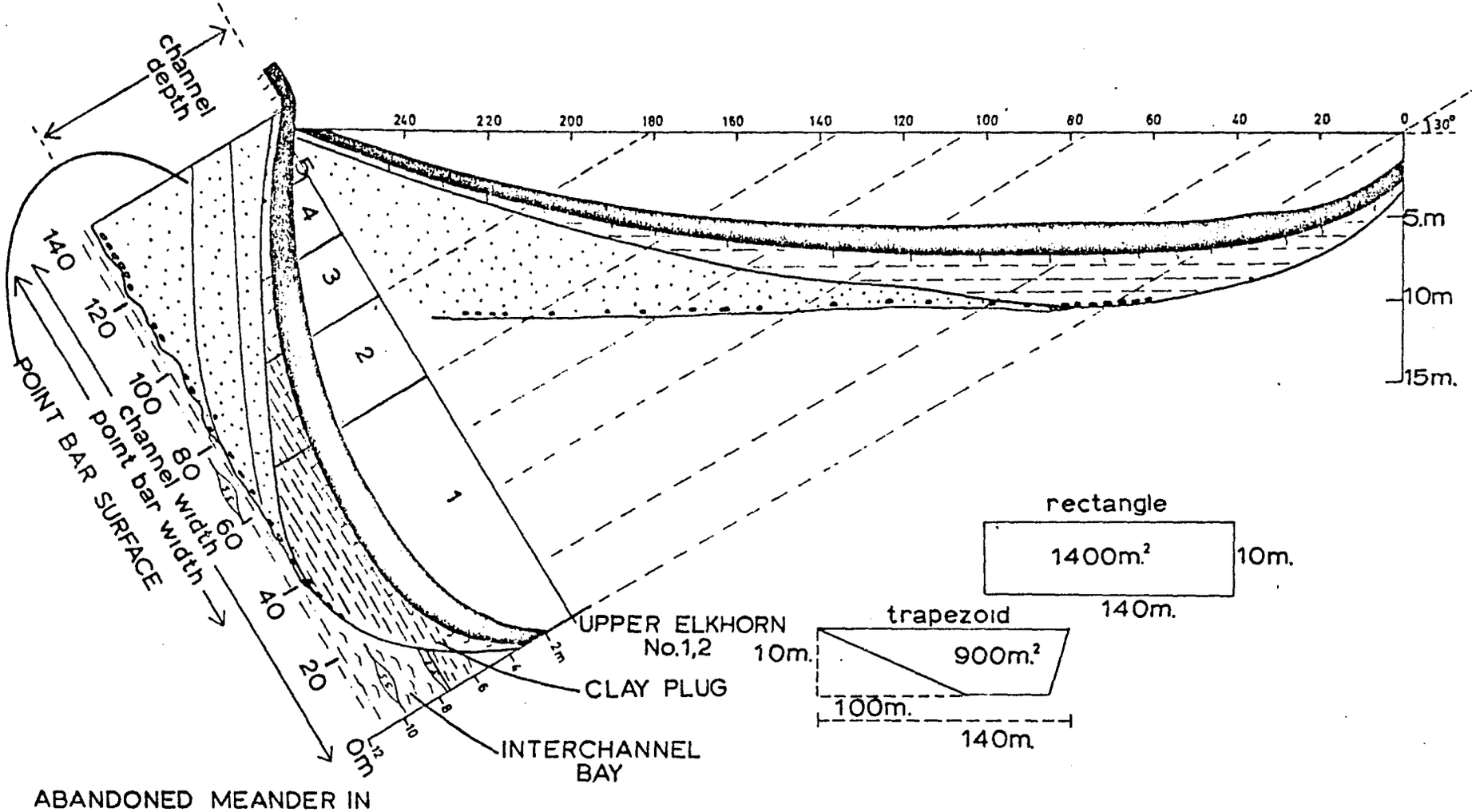

ABANDONED MEANDER IN HAROLD SANDSTONE AT BB-2